NASA Scientific Forum on Climate Variability and Global Change

UNISPACE III

Robert A. Schiffer
Sushel Unninayar

NASA/CP-1999-209240

THIRD UNITED NATIONS CONFERENCE
ON THE EXPLORATION AND PEACEFUL
USES OF OUTER SPACE
19 - 30 JULY 1999

Front cover: Image of Western Hemisphere as taken by GOES 8 meteorological satellite in September 1994.

Published by
National Aeronautics and Space Administration
as a contribution to
United Nations Office of Outer Space Affairs
for UNISPACE III

Design and Production by: Michele Meyett (Center of Excellence in Space Data and Information Sciences at NASA/GSFC)

P 96 388364

NASA Scientific Forum on Climate Variability and Global Change

20 July 1999

UNISPACE III

Robert A. Schiffer
Sushel Unninayar

THIRD UNITED NATIONS CONFERENCE ON THE EXPLORATION AND PEACEFUL USES OF OUTER SPACE
19 - 30 JULY 1999

Contents

Forum Program Plan: see inside back cover

Abbreviations

COLA .....Center for Ocean-Land-Atmosphere Studies
IRI ..... International Reserach Institute for Climate Prediction
NASA/GSFC .....National Aeronautics Space Administration/Goddard Space Flight Center
NCAR .....National Center for Atmospheric Research
NRL .....Naval Research Laboratory
SIO .....Scripps Institution of Oceanography
WMO/WCRP .....World Meteorological Organization/World Climate Research Programme

Foreword

The Forum on Climate Variability and Global Change is intended to provide a glimpse into some of the advances made in our understanding of key scientific and environmental issues resulting primarily from improved observations and modeling on a global basis. The climate of the Earth system is a consequence of a complex interplay of external solar forcing and internal interactions among the atmosphere, the oceans, the land surface, the biosphere and the cryosphere. Surface climate generally defines thresholds for the sustainability of water resources, agriculture, human shelter, transportation and health among others. Variability within the climate system has significant impact on natural and managed resources on all space and time scales, posing a particularly acute challenge to better observe the Earth system, understand interactive processes, and improve conceptual Earth system models. Inter-annual variability in the coupled ocean-atmosphere system is best exemplified by the well known El-Nino/Southern Oscillation event and its counterpart cold phase, the La-Nina; impacts are generally world wide. We now know that human activities are increasingly recognized as a potential factor forcing change in the global system by altering the chemical composition of the atmosphere and the oceans as well as the character of the land surface and vegetation cover. Increasing atmospheric concentrations of powerful greenhouse gases such as CO2 and CH4 are predicted to lead to accelerated global climate change, a central environmental issue of concern to Governments around the world. Of particular interest are the potential regional impacts of such changes on coastal areas, fresh water resources, food production systems, and natural ecosystems.

Space-based technology has advanced to a point that we are able to accurately observe and sense globally the entire Earth system and to understand Earth system processes that are central to Earth's climate. We need to document and understand the Sun-Earth connection as an external forcing of the Earth's climate, and also need to better understand the Earth's intricately linked internal processes such as the global water, energy and carbon cycles. Space-based platforms with their unique capacity to observe the Earth on a global basis, complement surface-based and in-situ measurements. Together with advances in computing and information system technology, modern data assimilation techniques, diagnostic and prediction models, they provide a powerful combination of tools for understanding of the Earth system and applying the knowledge and tools to the management of natural resources and the mitigation of natural hazards.

NASA's Earth Science Enterprise (ESE) is dedicated to using this unique combination of space-based information system technologies and scientific expertise to support the study of the Earth system and its environment. Active and passive remote sensing systems spanning a wide range of spatial, spectral and temporal coverage will contribute to capturing and documenting the state of the Earth's atmosphere, continents, oceans and life. The variety of high precision and well calibrated remotely sensed Earth observations that will be obtained by these missions will be unprecedented. We view this as a U.S. contribution to the international efforts to cooperatively develop a comprehensive international Earth

observing strategy to benefit humankind. The NASA Earth Observing System (EOS) is a program of multiple spacecraft (30 satellites to be launched into low Earth orbit between 1999 and 2005) and interdisciplinary science investigations to provide a 15-year data set of key parameters/processes needed to gain a better understanding of global climate processes. The first series of EOS satellite launches in 1999 include, Landsat-7, QuikScat, and Terra missions that will comprehensively monitor the Earth system. Preceding EOS, a number of individual satellite and the Space Shuttle-based missions are helping reveal the basic processes of atmospheric chemistry (Upper Atmosphere Research Satellite-UARS/ 1991), ozone distribution (Total Ozone Mapping Spectrometer-TOMS/1978, 1991, 1996, and 2000), ocean topography and circulation (TOPEX/Poseidon/1992), ocean winds (NASA Scatterometer-NSCAT/1996), ocean color (SeaWifs/1997), and global tropical energy and precipitation (Tropical Rainfall Measuring Mission-TRMM/1997), among others. These provide the scientific foundation on which EOS builds. For example, TRMM is providing unprecedented data on energy and precipitation processes and distribution in the tropics that will contribute substantially to the understanding of the global hydrological cycle. Landsat-7 was successfully launched in 1999 to continue and improve the data series provided by previous Landsat missions for 26 years since 1972. Later this year ESE will conduct the Shuttle Radar Topography Mission to use interferometric synthetic aperture radar to produce the first globally consistent and high precision digital-elevation model. We also plan to launch the Active Cavity Radiometer Irradiance Monitor (ACRIM) mission in 1999 to consolidate and extend over 20 years of observations of total solar irradiance.

EOS-PM, to be launched in year 2000 will provide unprecedented capability to monitor the Earth system, particularly: atmospheric temperature and humidity/water vapor profiles, radiation budget, clouds and aerosols, precipitation, sea surface winds, sea surface temperature, ice, snow, soil moisture, ocean color/biomass, vegetation cover/land productivity, among others. The SeaWinds scatterometer on Japan's ADEOS II mission to continue the measurements of sea surface wind vectors, and the US/France Jason-1—a follow-on to the highly successful TOPEX/Poseidon mission to capture sea surface topography which is also an indicator of upper ocean heat content; both are scheduled to be launched in the year 2000. In addition, we will launch the New Millennium Program Earth Observer-1 technology demonstration mission, designed to make future Landsat-type missions possible at vastly reduced size and cost. The New Millennium Program provides for the infusion of innovative new technologies with an initial focus on continuation of the systematic measurements, and will emphasize fast-track development and low-cost demonstration missions. These technologies, will lead to the development of smaller and lighter-weight instruments in order to be responsive to new and emerging scientific challenges requiring space-based observations.

Complementing EOS will be a series of small, rapid-development Earth System Science Pathfinder (ESSP) missions to study emerging science questions and make innovative measurements in parallel with the 15-year mission of EOS. ESSP will feature low life-cycle costs, and missions based on best science value. The first two ESSP missions, Vegetation Canopy Lidar (VCL), and Gravity Recovery and Climate Experiment (GRACE), a joint endeavor with Germany, are scheduled for launch in 2000 and 2001, respectively.

PICASSO-CENA, a joint endeavor with France, is planned to be launched in 2003 to study for the first time the three dimensional structures of the atmosphere, in particular, clouds, aerosols and volcanic plumes, and their role in the Earth's climate. CloudSat, a joint effort with Canada, will be launched in 2003 to provide significantly better data on vertical structure of thick clouds and their role in the Earth's radiation budget.

NASA's Earth Science Enterprise has adopted an evolutionary approach to fulfill its missions and goals. Future missions needed to achieve continuity for systematic measurements, together with those in the exploratory mode of ESSP, will be implemented according to the "better/faster/cheaper" paradigm. NASA will invest up-front in technology development, and base its mission selection on both scientific need and technology readiness. This will enable NASA to respond to emerging scientific observational needs in a timely fashion. The goal is to develop and launch the next generation of Earth observing satellites in 2 to 3 years instead of 7 to 10 years which is normal practice today.

Overall, it is an exciting era for space-based Earth observing systems, with significant research and operational applications benefits. With the advances being made in all countries, we hope to meet the needs for global Earth and environmental observations through a coordinated, cooperative strategy, firmly based on our scientific understanding of climate variability, environmental and global change issues of importance to nations around the world. The knowledge gained from these efforts will benefit equally natural resource managers, city planners, cartographers, and policy makers. Earth is the only planet in the solar system that supports carbon based life. Indeed it is the prime real estate of our solar system to support the current and future generations. It is time for the nations around the world to position themselves such that we benefit collectively from these wonderful technological innovations, and to foster establishment of sound environmental policy decisions for management and preservation of the Earth's unique conditions.

Ghassem R. Asrar
Associate Administrator
Office of Earth Science
NASA Headquarters
Washington, D.C.

OZONE DEPLETION, UVB AND ATMOSPHERIC CHEMISTRY

Richard S. Stolarski

NASA Goddard Space Flight Center
Laboratory for Atmospheres
(stolar@polska.gsfc.nasa.gov)

Background

Chapman's Pure Oxygen Model

The primary constituents of the Earth's atmosphere are molecular nitrogen and molecular oxygen. Ozone is created when ultraviolet light from the sun photodissociates molecular oxygen into two oxygen atoms. The oxygen atoms undergo many collisions but eventually combine with a molecular oxygen to form ozone (O_3). The ozone molecules absorb ultraviolet solar radiation, primarily in the wavelength region between 200 and 300 nanometers, resulting in the dissociation of ozone back into atomic oxygen and molecular oxygen. The oxygen atom reattaches to an O_2 molecule, reforming ozone which can then absorb another ultraviolet photon. This sequence goes back and forth between atomic oxygen and ozone, each time absorbing a uv photon, until the oxygen atom collides with and ozone molecule to reform two oxygen molecules. This sequence can be summarized by the following equations:

Production:

$$h\nu + O_2 \cdots\rightarrow O + O$$

Cycling:

$$O + O_2 + M \cdots\rightarrow O_3 + M$$

$$h\nu + O_3 \cdots\rightarrow O_2 + O$$

Destruction:

$$O + O_3 \cdots\rightarrow O_2 + O_2$$

This sequence of reactions is called the Chapman mechanism after Sidney Chapman who first proposed it in 1930. At high altitudes, the concentration of O_2 necessary for the production of O and O_3 decreases so that the concentration of ozone decreases with increasing altitude. At lower altitudes the solar ultraviolet radiation responsible for the production of ozone is absorbed by O_2 and by O_3. Thus the concentration decreases with decreasing altitude. This leads to a peak in the ozone at an altitude between these extremes. This peak occurs in the stratosphere where the ozone reaches concentrations of 5-10 parts per million by volume (ppmv).

Ozone Destruction by Catalysis

In the 1960s and early 1970s it was realized that the destruction reaction can be enhanced by catalytic reactions involving the oxides of hydrogen, nitrogen, chlorine, and bromine. For instance, chlorine atoms can act as a catalyst for ozone destruction through the simple two-step sequence:

$$Cl + O_3 \cdots\rightarrow ClO + O_2$$
$$ClO + O \cdots\rightarrow Cl + O_2$$

The net result of these two reactions is the recombination of an O and an O_3 to reform to O_2 molecules, exactly duplicating the destruction reaction in the Chapman mechanism. The chlorine atom has survived the reactions to participate in further cycles. Similar cycles occur with the chlorine atom replaced by NO, OH, or Br.

The existence of these catalytic compounds in the stratosphere depends on a source. The compounds themselves, such as chlorine atoms, ClO molecules, NO molecules, etc. cannot be readily transported from the ground to the stratosphere. During the slow journey of ground-level air up into the stratosphere, the molecules undergo many reactions forming compounds such as the acids HCl and HNO_3. These are soluble in water and will be removed during rain, adding to the acidity of that rain. Instead, unreactive and insoluble forms of chlorine and nitrogen can carry these atoms into the stratosphere. Nitrous oxide (laughing gas, N_2O) is a product of the nitrogen cycle in soils. It is insoluble and unreactive. Upon reaching the stratosphere it will react with excited oxygen atoms produced during the photolysis of ozone. This reaction produces two nitric oxide (NO) molecules.

The primary source of chlorine in today's stratosphere is the photodissociation of industrially-produced chlorofluorocarbons (CFCs). These insoluble, unreactive compounds include CFC-11 ($CFCl_3$) and CFC-12 (CF_2Cl_2). Because the time to transport these sources of catalytic compounds to the stratosphere is long, small sources can lead to significant accumulation over time. The reactions are catalytic and small amounts of catalysts can affect much larger concentrations of ozone. Thus, parts per billion of the catalysts can have a significant effect on the parts per million of ozone.

Meteorological Effects

The description of the photochemistry of stratospheric ozone given above does not explain all of the observed features of the concentration of ozone in the atmosphere. The photochemical theory would predict a peak in ozone at the equator where the solar radiation received is a maximum. Observations show a minimum in the ozone amount at the equator and a seasonally-varying maximum at high latitudes. The high-latitude maximum occurs in the spring and is located near the pole in the northern hemisphere and about 30 degrees off the pole in the southern hemisphere.

This lead Dobson and Brewer in the late 1940s to postulate a slow circulation in which rising air entered the stratosphere from below in the tropics and then proceeded poleward and eventually downward at mid and high latitudes. Thus air enters the stratosphere in the tropics with relatively low amounts of ozone characteristic of the troposphere. As that air is lofted to higher altitudes and latitudes, ozone is created by the ultraviolet photodissociation of O_2 in a region where the photochemistry is fast. This air is transported downward and poleward where ozone accumulates. There, enough ozone accumulates that it absorbs the ultraviolet radiation which leads to its own destruction. Ozone destruction slows down in the lower stratosphere because little uv radiation is available to produce atomic oxygen. The lifetime of ozone in the midlatitude lower stratosphere becomes as long as a year or more.

The picture that we now have of stratospheric ozone is one of photochemical production and loss plus dynamical redistribution of that ozone. The dynamical redistribution leads to the springtime seasonal high latitude peaks in the ozone amount. It also leads to the very different distribution of ozone in the southern and northern high latitudes. Dynamical redistribution leads to daily variations in ozone as weather systems pass through the midlatitudes. The total column amount of ozone exhibits time-varying patterns that look very much like the weather maps seen on the television news.

Penetration of UV Radiation

One of the primary properties of ozone is its strong absorption of ultraviolet radiation. The total column amount of ozone in the atmosphere is approximately 10^{19} molecules per cm^2. At a wavelength of 250 nm, the ozone absorption cross section is 10^{-17} cm^2. This means that radiation of 250 nm from the sun will be absorbed such that its intensity is reduced by e^{-100} from that which impinges on the top of the atmosphere. Thus, no radiation at wavelengths near 250 nm reaches the ground.

Of more concern are the wavelengths near 300 nm. These wavelengths still possess enough energy in a photon to break important bonds in biological molecules and their cross sections are small enough that some of the radiation from the sun can reach the ground. At 320 nm the cross section is about 2.5×10^{-20}. Thus the radiation from the sun is reduced by $e^{-0.25}$ when the sun is overhead. When the sun is lower in the sky, the reduction in the radiation is greater because of the greater path length of ozone through which the radiation must pass. When the column amount of ozone overhead varies, so too does the amount of uv radiation at wavelengths near 300 nm which is received at the ground. This radiation at the ground is affected by other factors. These include clouds, haze or aerosols, and the reflectivity of the surface.

Ozone Depletion

Ozone depletion is usually defined as a change in ozone brought about by a change in the chemicals which lead to ozone loss. This can be brought about either by direct injection or

by a change in the source gases. Thus there exists a "normal" amount of nitrogen oxides in the stratosphere due to production from nitrous oxide as a part of the natural cycle of nitrogen fixation and denitrification. This cycle can be changed by the addition of fertilizer nitrogen which enhances nitrogen cycling and produces more N_2O. A more direct way to enhance stratospheric nitrogen oxides is the direct injection by aircraft flying in the stratosphere.

Aircraft Effects

Aircraft engines burn fuel at high temperatures (~3000°C). At these temperatures the nitrogen and oxygen in the air passing through the engine are broken down and a portion of nitrogen oxides are produced. The current fleet of subsonic aircraft fly in both the troposphere and lowest part of the stratosphere. In this region, the primary effect of the added NO_x is the enhancement of the smog-like chemistry of the oxidation of methane. The result is an enhancement of ozone. In the early 1970s, a great deal of research was done on the possibility of a fleet of commercial supersonic transports which would fly in the stratosphere near 20 km altitude. At 20 km altitude, the effectiveness of the smog chemistry has decreased and the catalytic effects of the added nitrogen oxides begins to dominate.

Over the last 10 years, the idea of a commercial fleet of supersonic planes, now called the high-speed civil transport (HSCT) has been revived. Studies now reveal that reactions on the background sulfate aerosols in the stratosphere affect the balance of the nitrogen and chlorine chemistry. Thus added NO_x increases the rate of ozone loss through the NO_x catalytic cycle. At the same time, added NO_x ties up more chlorine as chlorine nitrate ($ClONO_2$) and decreases the rate of ozone loss through the chlorine cycle. The net effect on ozone is a combination of the direct catalytic effect of NO_x and of its interference with the chlorine cycle. This leads to a calculated net ozone loss at 20 km from this hypothetical fleet which is small (fraction of a percent). One unsolved problem is the determination of what fraction of the exhaust, from a fleet flying primarily at midlatitudes, would reach the tropics and be lofted to higher altitudes where aerosol concentrations are small. A small fraction of the exhaust reaching 30 km altitude could dominate the loss from the NO_x catalytic cycle.

Airplanes exhaust also contains water vapor and sulfur compounds. The water vapor leads to an increase in atmospheric hydrogen oxides which catalytically destroy ozone. Sulfur leads to the formation of small particles which increase the surface area of aerosols in the stratosphere. Increased surface area converts more chlorine to the active form ClO, and thus increases the ozone loss due to chlorine catalytic cycles.

Chlorofluorocarbons

Chlorofluorocarbons are source gases for stratospheric chlorine. They are long-lived compounds which are not reactive, nor soluble in water. The most common of the CFCs are CFC-11 ($CFCl_3$) and CFC-12 (CF_2Cl_2). These, and numerous other CFCs, are industri-

ally-produced compounds which did not exist in the atmosphere before their invention in a DuPont laboratory by Midgley in the 1930s.

Despite their atomic weights of approximately 100, CFCs are thoroughly mixed throughout the troposphere by small-scale motions, and are lofted to high altitudes by the slow transport circulation of the atmosphere. In the stratosphere, with much of the ozone layer below them, CFCs are destroyed by the absorption of uv photons which free a chlorine atom leaving a fast-reacting fragment. Subsequent rapid chemistry releases the rest of the fluorine and chlorine atoms from the CFC molecule.

Production of CFCs began in the 1930s and grew exponentially into the 1970s. Their growth became an issue in the mid 1970s and in 1977 the United States passed a ban on their use as a propellant in aerosol spray cans. Figure 1 illustrates the release rate for one specific chlorofluorocarbon, CFC-11. The release rate grew rapidly until about 1975 when it levelled off and even decreased a little. Then the release rate began to grow again until the Montreal Protocol was agreed upon in 1987. After that the release rate declined rapidly. The concentration of CFC-11 in the atmosphere responds only slowly to these changes in the production rate. The residence time of CFC-11 in the atmosphere is about 50 years. The loss rate is proportional to the amount in the atmosphere which continues to increase even as the production rate is decreasing. Eventually the production rate becomes small enough that the loss rate is greater and the concentration begins to decrease. Figure 1 shows that we are about at that level in the late 1990s for CFC-11.

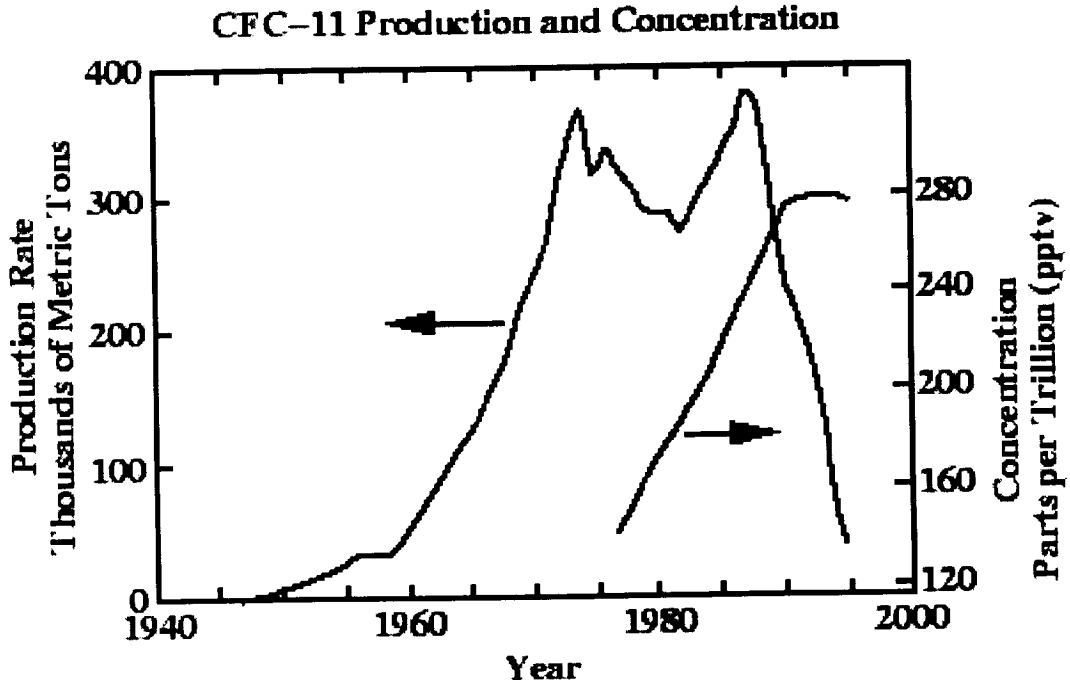

Figure 1: Time history of the production rate of CFC-11 and its atmospheric concentration. Production rate is given on the left scale while concentration in parts per trillion by volume is given on the right scale.

Other chlorine containing compounds are at different stages in this evolution. The rate of increase of the CFC-12 concentration has slowed but not ceased. The concentration of methyl chloroform (CH_3CCl_3) in the atmosphere is clearly decreasing. The concentration of some of the replacement HCFCs (e.g. HCFC-141b or CH_3CCl_2F) are increasing rapidly. The concentrations of all of these compounds can be taken together to indicate the amount of chlorine which will be available to the stratosphere as a function of time. This compilation shows that the available chlorine peaked in about 1994 and has decreased slightly since that time. There is a time delay of about 5 years between the peak in chlorine potentially available at the ground and chlorine available in the stratosphere. Thus, the peak in stratospheric chlorine should be occurring about now.

Once the chlorine is freed from the CFCs by ultraviolet absorption in the stratosphere, it undergoes a set of reactions which convert it from one molecular form to another. These reactions result in a quasi-steady-state in which the proportion of chlorine in each compound is determined by local factors such as the amount of solar ultraviolet radiation, the temperature, the concentration of ozone, and the concentration of other radicals such as OH and NO_2. In the midlatitude lower stratosphere, where the ozone concentration is a maximum, most of the chlorine available is converted into the temporary reservoir molecules HCl and $ClONO_2$. This is accomplished via the reactions:

$$Cl + CH_4 \dashrightarrow HCl + CH_3$$
$$ClO + NO_2 + M \dashrightarrow ClONO_2 + M$$

Chlorine is returned to the catalytically active Cl/ClO cycle by the reactions:

$$HCl + OH \dashrightarrow Cl + H_2O$$
$$ClONO_2 + h\nu \dashrightarrow ClO + NO_2$$

These reactions come to a balance in which a relatively small fraction of the chlorine is in the catalytically active Cl and ClO.

Thus, CFCs carry chlorine to the stratosphere. Once there, the chlorine begins to catalytically destroy ozone. The chlorine is converted to reservoir molecules such as HCl and $ClONO_2$. The reservoirs are converted back to active chlorine which continues to destroy ozone. This continues during the entire time that the chlorine is in the stratosphere. The chlorine is eventually transported out of the stratosphere on the downward-moving branch of the circulation at midlatitudes. During its residence time in the stratosphere, a typical chlorine atom can destroy as many as 10^4 to 10^5 molecules of ozone.

Bromine and halons

Bromine is an even more effective catalyst for ozone loss than is chlorine. Bromine monoxide (BrO) can react with itself to reform bromine atoms or it can react with ClO to reform bromine and chlorine atoms. This generates a catalytic cycle which does not need

atomic oxygen for its completion. Since atomic oxygen is in short supply in the lower stratosphere, these bromine cycles are much more effective there than the cycles requiring atomic oxygen.

Bromine is supplied to the atmosphere mainly as methyl bromide (CH_3Br). Methyl bromide has both natural and anthropogenic sources. It arises naturally from oceans where bromine atoms replace iodine in methyl iodide produced by seaweed. It is also destroyed in oceans where chlorine atoms can displace the bromine, forming methyl chloride. There is also a major anthropogenic source of CH_3Br. It is used as a fumigant for crops like strawberries. A field is covered with a plastic and CH_3Br is injected underneath this cover to kill the various pests which can ruin the fruit. The plastic is removed and the crops are grown. Inevitably a fraction of this CH_3Br is not destroyed during this process and is released to the atmosphere. Uncertainties remain in the quantitative effect of anthropogenic bromine on the bromine budget of the stratosphere.

Other important sources of bromine to the stratosphere are the halons, particularly halon-1211 ($CBrClF_2$) and halon 1301 ($CBrF_3$). The concentration of these compounds is only a few parts per trillion, but the rate of increase of all of the halons together is a little over 2%/year.

The Ozone Hole

By the early 1980s, predictions had been made of ozone changes which should occur due to enhanced ozone loss from reactions of chlorine from CFCs. These changes were predicted to occur in the upper stratosphere and have a relatively small effect on the total column amount of ozone. The predicted effect was small enough that it could not have been deduced from the data available. In 1985, Farman and colleagues published a paper on their data taken from the Antarctic station at Halley Bay beginning in 1957. They found that the average amount of ozone in the month of October had decreased from about 300 Dobson units (DU) to 180 DU. This observation was quickly confirmed using data from the Total Ozone Mapping Spectrometer (TOMS) and Solar Backscatter Ultraviolet (SBUV) instruments on the Nimbus 7 satellite. These instruments provided maps of the entire Antarctic region which showed that the springtime ozone loss was occurring over an area larger than the continent. It was clear that something was going on over Antarctica that was very different from what was occurring over the rest of the globe.

The difference at high latitudes is the formation of the winter polar vortices. Strong west to east winds circulate around the pole with a maximum velocity about 20 to 40 degrees off of the pole. The circulation is such that little exchange of air takes place between the polar region and the midlatitudes during the winter. This isolated pole is in the dark through most of the winter. The air radiates to space and cools to temperatures low enough that polar stratospheric clouds form despite the extremely dry nature of the stratosphere. The southern hemisphere polar region becomes more isolated and cold than does the northern hemisphere polar region. The distribution of mountains and land masses in the northern hemisphere causes the upward propagation of waves which distort and erode the northern hemisphere vortex causing it to weaken and disappear before the spring in most years.

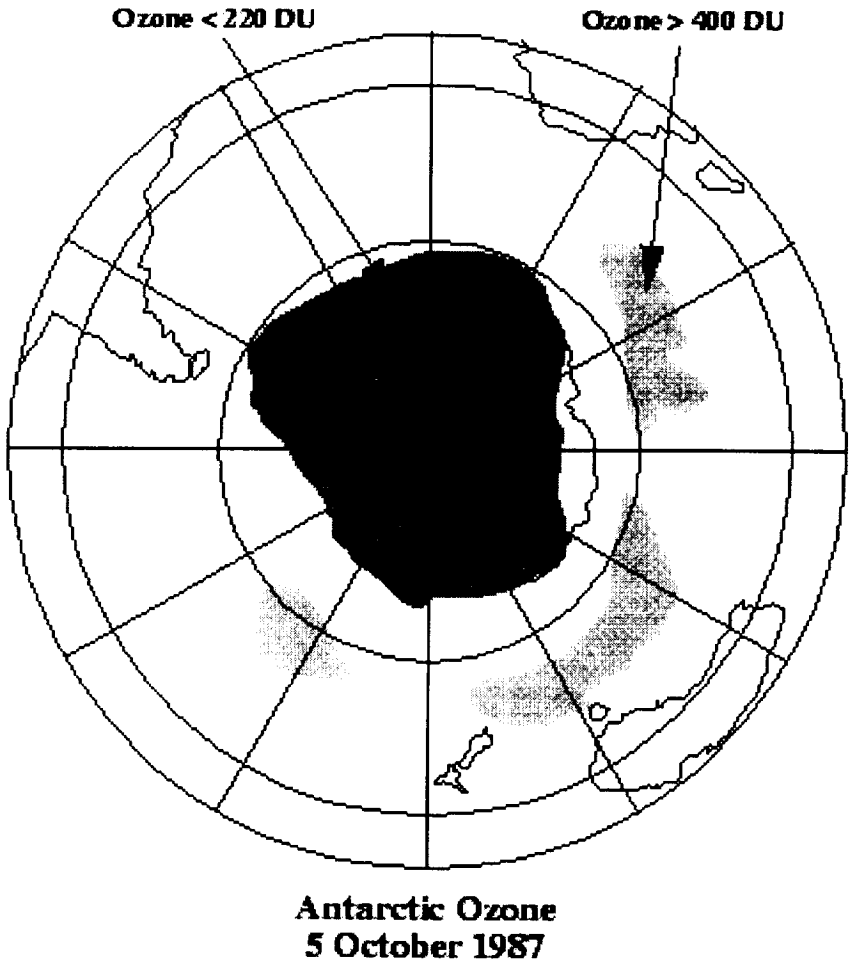

Figure 2: Schematic showing the extent of the ozone hole region for October 5, 1987. The area where ozone is less than 220 DU is shaded. Also in lighter shading is the area where the ozone amount is greater than 400 DU.

Air containing CFCs is well mixed in the troposphere. It enters the stratosphere in the tropics and is spread toward the poles. Air finally reaching the poles has been in the stratosphere an average of more than 5 years and has had much of its CFCs converted into active or reservoir chlorine. In the polar night reactions occur on the surfaces of polar stratospheric cloud particles which convert chlorine from the reservoir form to chlorine gas Cl_2. The most important of these reactions is:

$$HCl + ClONO_2 \cdots\rightarrow HNO_3 + Cl_2$$

The nitric acid sticks to the particle and the Cl_2 comes off as a gas. When the air sees sunlight in the early spring, Cl_2 is rapidly photodissociated to Cl atoms which react with ozone to form ClO. ClO reacts with itself to form a dimmer Cl_2O_2 which absorbs sunlight and photodissociates to Cl atoms and ClOO. These reactions form a catalytic cycle which

destroys ozone without the use of atomic oxygen. The result is a rapid springtime decrease in the ozone concentration of the lower stratosphere. This decrease is particularly pronounced in the southern hemisphere where a minimum is reached during October. Figure 3 shows the October monthly mean ozone amounts each year beginning in the late 1950s. During the 1950s, 1960s, and early 1970s, the October mean ozone amount over the Halley Bay Station on the Antarctic continent was about 300 DU. This decreased throughout the 1980s until the typical October mean amount was barely over 100 DU. This situation has continued throughout the 1990s.

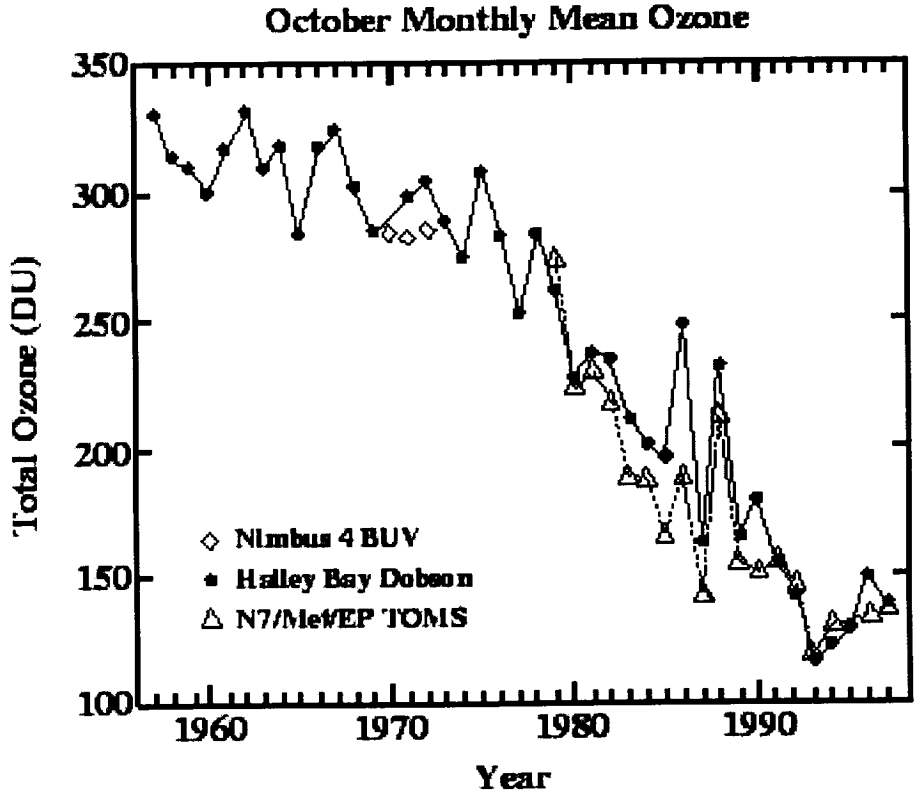

Figure 3: October monthly mean ozone amounts over Antarctica. The filled circles are the monthly mean amounts measured over the Halley Bay Station by the Dobson instrument located there (data courtesy J. Shanklin, British Antarctic Survey). The triangles are the minimum monthly mean from the TOMS maps of total ozone over the Antarctic. The diamonds are the similar data from the Nimbus 4 BUV instrument.

Another measure of the Antarctic ozone hole is its size. We saw in figure 2 an example of a day when the region of ozone amounts less than 220 DU was larger than the size of the continent of Antarctica. Figure 4 shows the average size of the ozone hole, as measured by the various TOMS instruments, for each year since 1979. The size is defined as the area where the ozone amount is less than 220 DU averaged between September 7 and October 13.

Measurements by balloon-borne sondes indicate that the ozone loss is occurring in the lower stratosphere between about 12 and 22 km altitude. This is the region of the maximum in the ozone concentration. In recent years the loss has become nearly complete over this region and the minimum amount of total columne ozone measured is just that at altitudes above and below the primary depletion region. Thus, the minimum amounts of total ozone reached in October as shown in Figure 3 have not continued to decline as there is no more ozone to be lost unless the depletion extends to either higher or lower altitudes than before.

Long-term Global Trends

The Antarctic ozone hole provides the most spectacular example of changes in stratospheric ozone. Changes of a much smaller magnitude are also evident over large portions of the globe. The deduction of long-term trends must be made by accounting for various known natural variations of ozone. Ozone amounts vary on a seasonal cycle. At midlatitudes, this seasonal cycle is the dominant variation seen in the data. When an average seasonal cycle is removed from the data, other variations become apparent. These include the 11-year solar cycle and the 27 month quasi-biennial oscillation (QBO). Finally, if all of these variations are removed, the residual should show the trend, if any. Typically, these analyses are done by fitting to a statistical model which contains terms for all of the variations including the trend and the residual noise.

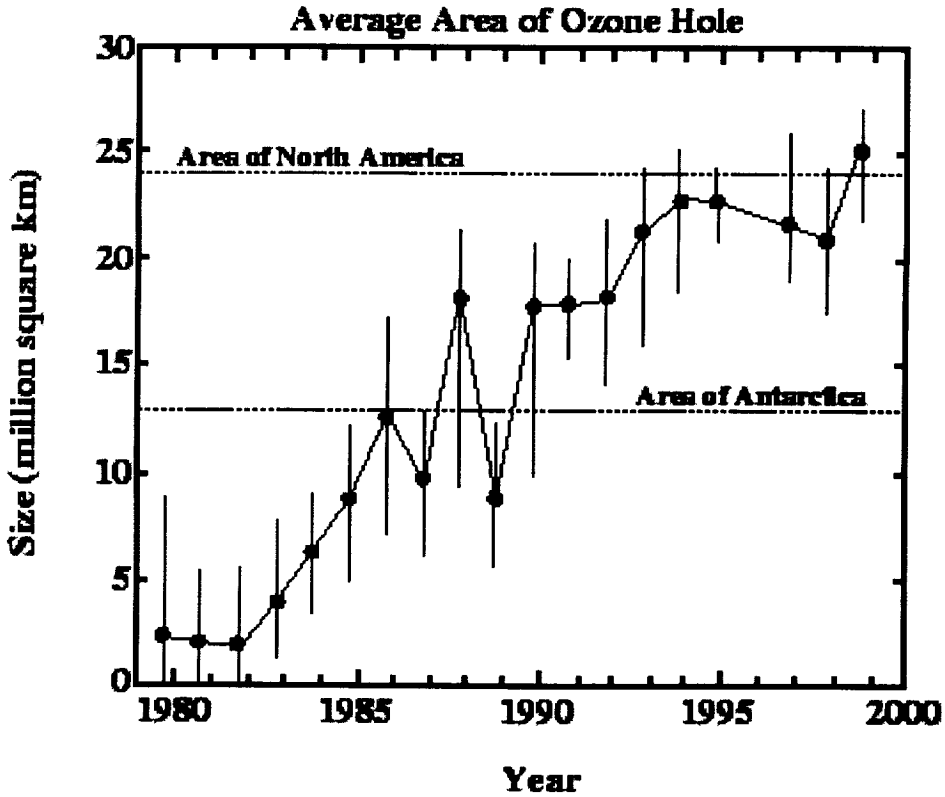

Figure 4: Area of Antarctic ozone hole as defined by ozone amounts less than 220 DU. Filled circles indicate the area averaged from September 7 to October 13 of each year. Vertical bars indicate the daily range of the area over this time period.

The resulting trends from one such calculation are shown in Figure 5 as a function of latitude and season. Small, insignificant trends are deduced for the equatorial region. Trends in the southern hemisphere springtime are large as the region of the Antarctic ozone hole is approached. Northern hemispheric trends show a strong seasonal variation with a maximum negative trend in the winter and early spring.

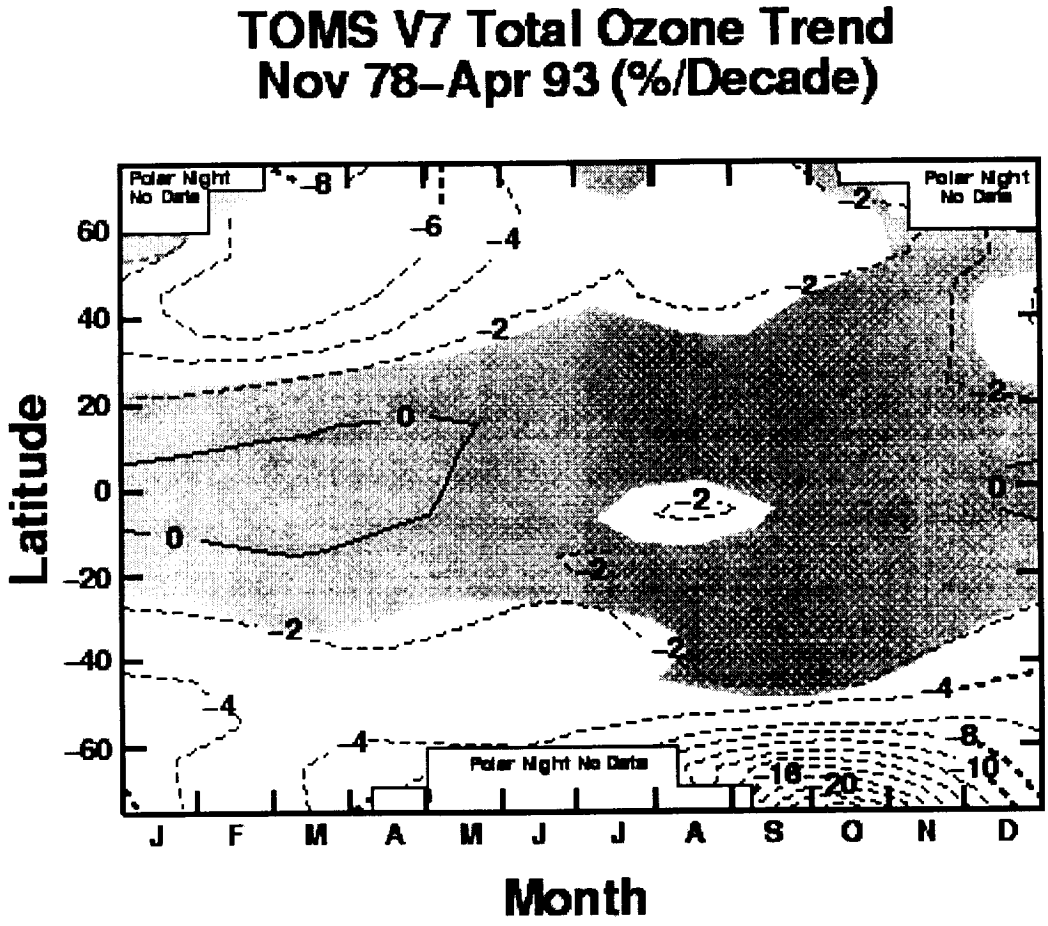

Figure 5: Trends in total ozone deduced from the data of the Nimbus 7 TOMS instrument for the time period from late 1978 through May of 1993.

Prospects for recovery

We saw above that the provisions of the Montreal Protocol have already resulted in a marked decrease in the production of some important CFCs. At the same time, production of replacement compounds has increased. The total amount of tropospheric organic chlorine compounds determines the amount of chlorine which is available for transport to the stratosphere. The sum of the chlorine in these compounds was determined to have peaked sometime in 1994. About a 5-year delay is expected before that turnaround would be seen in stratospheric chlorine available for ozone depletion. Satellite measurements of the reservoir gas, HCl indicate that a leveling off in the available chlorine is beginning to take place in the stratosphere. Thus, the driving term for stratospheric ozone loss should be now leveling off.

How soon will it be before we can see the result in the ozone data itself? The time variations of the CFCs and of HCl were dominated by the trend term. It was thus relatively easy to observe the flattening out of these time series. The same is not true of ozone. Its variations are dominated by natural causes and the trend terms are not dominant.

One method for testing for early evidence of a flattening out of the trend was used recently by Lane Bishop in the recent UNEP/WMO Ozone Assessment Report. He used the globally-integrated ozone amount because that record averages out much of the strong seasonal and interannual variation. He then fit the data from 1979 through mid 1991 (pre-Pinatubo) to a standard statistical model with terms for seasonal variation, trend, QBO, solar cycle, and noise. That calculation is reproduced below in Figure 6 for the TOMS data from three satellites; Nimbus 7, Meteor 3, and Earth Probe.

Figure 6 shows only two terms from the statistical model fit; the annual mean trend term and the residual noise. Put another way, Figure 6 shows the data minus the model fit for the annual cycle, the solar cycle, the QBO, and the annual component of the trend term. The upper panel shows the data in the same form as analyzed by Bishop, using the calibrations given with each satellite data set. The lower panel shows the same calculation using satellite data which has been renormalized to the overpasses of the ground-based network of ozone-measuring stations.

The top panel of Figure 6 shows the Earth Probe TOMS data from 1996-1998 to be well above the extrapolated trend line (~2%). This would provide some indication of the beginning of recovery except for the uncertainty in the establishment of the Earth Probe TOMS calibration with respect to the calibration of the Nimbus 7 and Meteor 3 TOMS instruments. It is also worth noting that the estimated uncertainty on global trends is greater than 1%/decade (2σ) which would place the Earth Probe data on the edge of significance even if the calibration were to be believed.

The bottom panel, where the ground-based adjustment has been used, shows the recent Earth Probe TOMS data to be only marginally above the extrapolated trend line. This is well within the uncertainty of the determination of that trend line. This data set thus provides no indication yet of any recovery. Note that the trend deduced from this data is smaller than that deduced from the unadjusted TOMS data in the upper panel (-1.7%/decade vs. 2.0%/decade).

We are currently working on producing an internally-consistent satellite data set which is independent of the ground based network. This relies on using the data from the NOAA-9 SBUV/2 to establish the relative calibration of Earth Probe and the other TOMS instruments. This has proved difficult because of the drift in the orbit of NOAA-9.

UVB Radiation

There is a large and growing literature on the effects of UVB radiation and on the measurement of the amount reaching the ground. Here we will only be able to make a brief statement of some of the main issues.

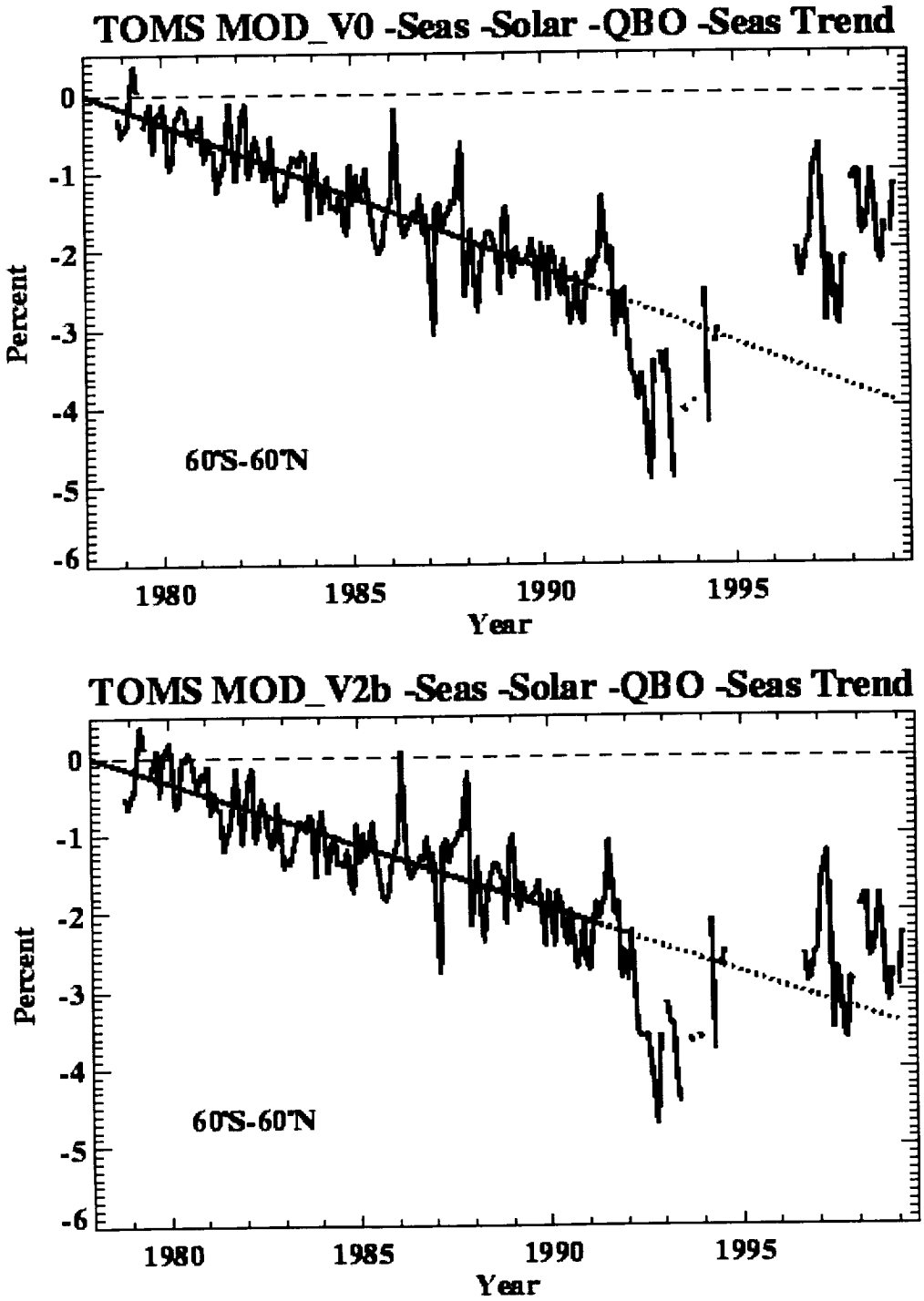

Figure 6: TOMS global average total ozone data. Shown is the residual from a statistical model fit which includes seasonal variation, an 11-year solar cycle, a quasi-biennial oscillation, and a seasonal trend term. The residual is the annual mean trend plus the noise term. The top panel shows data from three TOMS instruments using their original calibrations. The bottom panel shows the same data using calibrations that have been adjusted by a smoothed time-dependent offset determined from overpasses of a set of 38 ground-based stations.

UVB is defined as the radiation between wavelengths of 285 nm and 315 nm. UVB radiation at 285 nm is strongly absorbed by ozone while that at 315 nm is much more weakly absorbed by ozone. Thus, more radiation at 315 nm penetrates the ozone layer than does radiation at 285.

The UVB radiation which reaches the surface is affected by many factors in addition to ozone absorption. Rayleigh scattering by atmospheric molecules reduces the amount of direct-beam UVB but increases the diffuse component of UVB. Aerosols and haze cause scattering which adds to the diffuse component of the UVB. Clouds affect UVB by both reflection and scattering. Finally, surface reflectivity affects the UVB received near the surface. For instance, snow or water surfaces increases the UVB dosage which leads to sunburn.

Determination of the trend in UVB requires an absolute calibration in a given wavelength region which must be maintained to high precision over a long period of time. UVB at the surface is highly variable, both because ozone is variable and because of the cloudiness and haze factors described above. In general, the best way to determine a trend in UVB would be to measure it relative to some other wavelength of UV which is not expected to show a trend in time. In fact, this is how ozone is measured; by the ratio of UVB to UVA ($\lambda > 320$ nm). These measurements show a clear decrease in UVB relative to UVA.

With the provisions of the Montreal Protocol, we hope to be able to observe the slow decrease in the net amount of UVB reaching the ground over the coming decades as the ozone layer slowly recovers with the decrease in the atmosphere's chlorine content.

GLOBAL CLIMATE SYSTEM CHANGE AND OBSERVATIONS

Kevin E. Trenberth

National Center for Atmospheric Research
sponsored by the National Science Foundation
(trenberth@near.ucar.edu)

Abstract

Following a brief introduction to the climate system, a discussion is given of the natural greenhouse effect and the enhancements arising from human activities and other agents of change. The atmosphere is the most volatile component of the climate system and large weather variability confounds the detection of small climate signals. The ocean is also fluid and plays an active role. The atmosphere and oceans together can give rise to phenomena that would not occur without interactions between them, with the best example being El-Niño. Feedback processes are briefly discussed, including the critical role of clouds. Observations of global climate change are summarized along with the need to be able to assemble all the understanding into global climate models, which can then be used to make better sense of the observations and to carry out numerical experiments. The important role of changes in the hydrological cycle as well as temperatures is emphasized.

Even for instrumental observations, the long time-series of high quality observations needed to discern small changes are often compromised by non-physical effects, and special care is required in interpretation. From space, similar problems arise from the orbital decay and drift in equator crossing times of individual satellites, the finite life time of instruments and satellites which result in different platforms for instruments (even if the same) and electronic noise from nearby instruments, calibration of instruments, and conversion of radiances into geophysically meaningful quantities. Yet both systems have substantial advantages. A call is made for a true sustained climate observing system composed of both space-based and in situ components that capitalizes on the advantages of each.

The Climate System

The internal interactive components in the climate system include the atmosphere, the oceans, sea ice, the land, snow cover, land ice, and fresh water reservoirs (Figure 1). The greatest variations in the composition of the atmosphere involve water in various phases in the atmosphere, as water vapor, clouds of liquid water, ice crystal clouds, and hail. However, other constituents of the atmosphere and the oceans can also change and humans are having a discernible influence, so this brings considerations of atmospheric chemistry, marine biogeochemistry, and land surface exchanges into climate change. The main focus in this article is on the atmosphere as the most variable component of the Earth system; it is afterall where we live and makes up the air we breathe.

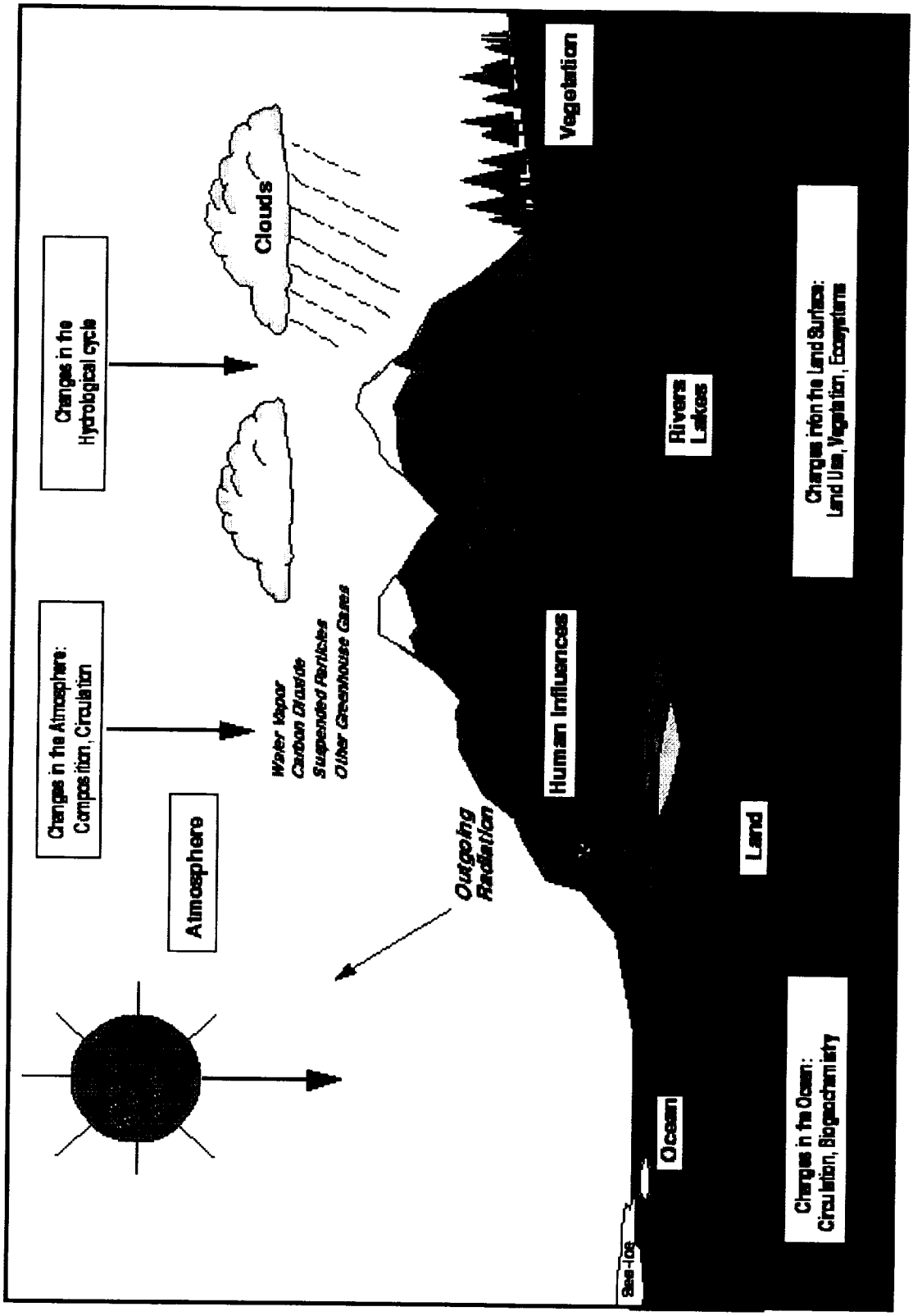

Figure 1: Schematic view of the components of the global climate system (bold), their processes and interactions (thin arrows) and some aspects that may change (bold arrows).

The source of energy which drives the climate is the "short wave" radiation from the sun and much of this energy is in the visible. Because of the roughly spherical shape of the Earth, at any one time half the Earth is in night and the average amount of energy incident on a level surface outside the atmosphere is one quarter of the total solar irradiance or 342 Wm^{-2}. About 31% of this energy is scattered or reflected back to space by molecules, tiny airborne particles (known as aerosols) and clouds in the atmosphere, or by the Earth's surface, which leaves about 240 Wm^{-2} on average to warm the Earth's surface and atmosphere (Figure 2), see Kiehl and Trenberth (1997) for details.

To balance the incoming energy, the Earth itself must radiate on average the same amount of energy back to space (Figure 2). It does this by emitting thermal "long-wave" radiation in the infrared part of the spectrum. For a completely absorbing surface to emit 240 Wm^{-2} of thermal radiation, it would have a temperature of about -19°C. This is much colder than the conditions that actually exist near the Earth's surface where the annual average global mean temperature is about 15°C. However, because the temperature in the troposphere falls off quite rapidly with height, a temperature of -19°C is reached typically at an altitude of 5 km above the surface in mid-latitudes. This provides a clue about the role of the atmosphere in making the surface climate hospitable.

The Greenhouse Effect

Some of the infrared radiation leaving the atmosphere originates near the Earth's surface and is transmitted relatively unimpeded through the atmosphere; this is the radiation from areas where there is no cloud and which is present in the part of the spectrum known as the atmospheric "window". The bulk of the radiation, however, is intercepted and re-emitted both up and down. The emissions to space occur either from the tops of clouds at different atmospheric levels (which are almost always colder than the surface), or by gases present in the atmosphere which absorb and emit infrared radiation. Most of the atmosphere consists of nitrogen and oxygen (99% of dry air) which are transparent to infrared radiation. It is the water vapor, which varies in amount from 0 to about 3%, carbon dioxide and some other minor gases present in the atmosphere in much smaller quantities which absorb some of the thermal radiation leaving the surface and re-emit radiation from much higher and colder levels out to space. These radiatively active gases are known as greenhouse gases because they act as a partial blanket for the thermal radiation from the surface and enable it to be substantially warmer than it would otherwise be, analogous to the effects of a greenhouse. This blanketing is known as the natural greenhouse effect. In the current climate, water vapor is estimated to account for about 60% of the greenhouse effect, carbon dioxide 26%, ozone 8% and other gases 6% for clear skies (Kiehl and Trenberth 1997).

Agents of Change and Feedbacks

The Earth System can be altered by effects or influences from outside the planet usually

regarded as "externally" imposed. Most important are the sun and its output, the Earth's rotation rate, sun-Earth geometry and the slowly changing orbit, the physical make up of the Earth system such as the distribution of land and ocean, the geographic features on the land, the ocean bottom topography and basin configurations, and the mass and basic composition of the atmosphere and ocean. These components determine the mean climate which may vary from natural causes. A change in the average net radiation at the top of the atmosphere due to perturbations in the incident solar radiation or the emergent infrared radiation leads to a change in heating. Changes in the net incident radiation energy at the Earth's surface might occur from the changes internal to the sun but may also occur from changes in atmospheric composition such as may arise from natural events like volcanoes, which can create a cloud of debris that blocks the sun. Other forcings that might be regarded as external include those arising as a result of human activities.

Evidence for human influences are all around. Most obvious are the changes in land use and building cities. Conversion of forest to cropland, in particular, has led to a higher albedo in places such as the eastern and central United States and changes in evapotranspiration, both of which have probably cooled the region, in summer by perhaps 1°C and especially in autumn by more than 2°C, although global effects are less clear (Bonan 1997). In addition, storage and use of water (dams, reservoirs, irrigation) is important. While there is substantial generation of heat by human activities for space heating, generation of electricity and so on, the amounts are small compared with the throughflows from natural systems. Locally, in cities, these effects are important and combine to produce the "urban heat island". However, the process of generating some of the heat through combustion of fossil fuels also generates particulate pollution, (e.g., soot, smoke) as well as gaseous pollution that can become particulates (e.g. sulfur dioxide, nitrogen dioxide; which get oxidized to form sulfate and nitrate particles), and carbon dioxide. Human activities also generate other gases: methane, nitrous oxide, the chlorofluorocarbons (CFCs) and tropospheric ozone (especially from biomass burning, landfills, rice paddies, agriculture, animal husbandry, fossil fuel use, leaky fuel lines, and industry). The result is changes the composition of the atmosphere.

Moreover, the gases mentioned are all greenhouse gases and thus are radiatively active in perturbing the heat flows on Earth, and many also have long lifetimes. The average lifetime of carbon dioxide is estimated to be over 100 years before it is taken out of the system. Consequently, continual emissions of these gases lead to increased concentrations which are clearly evident from measurements. Carbon dioxide has increased by over 30% over the past 200 years, and mostly after World War II. Atmospheric aerosols also change the composition of the atmosphere but typically have a lifetime of only a week or less mainly because they are washed out by precipitation processes. Consequently aerosols are mainly found relatively close to their sources and predominantly in the Northern Hemisphere or tropics (the latter from biomass burning), whereas the greenhouse gases become globally distributed and result in global forcings of climate.

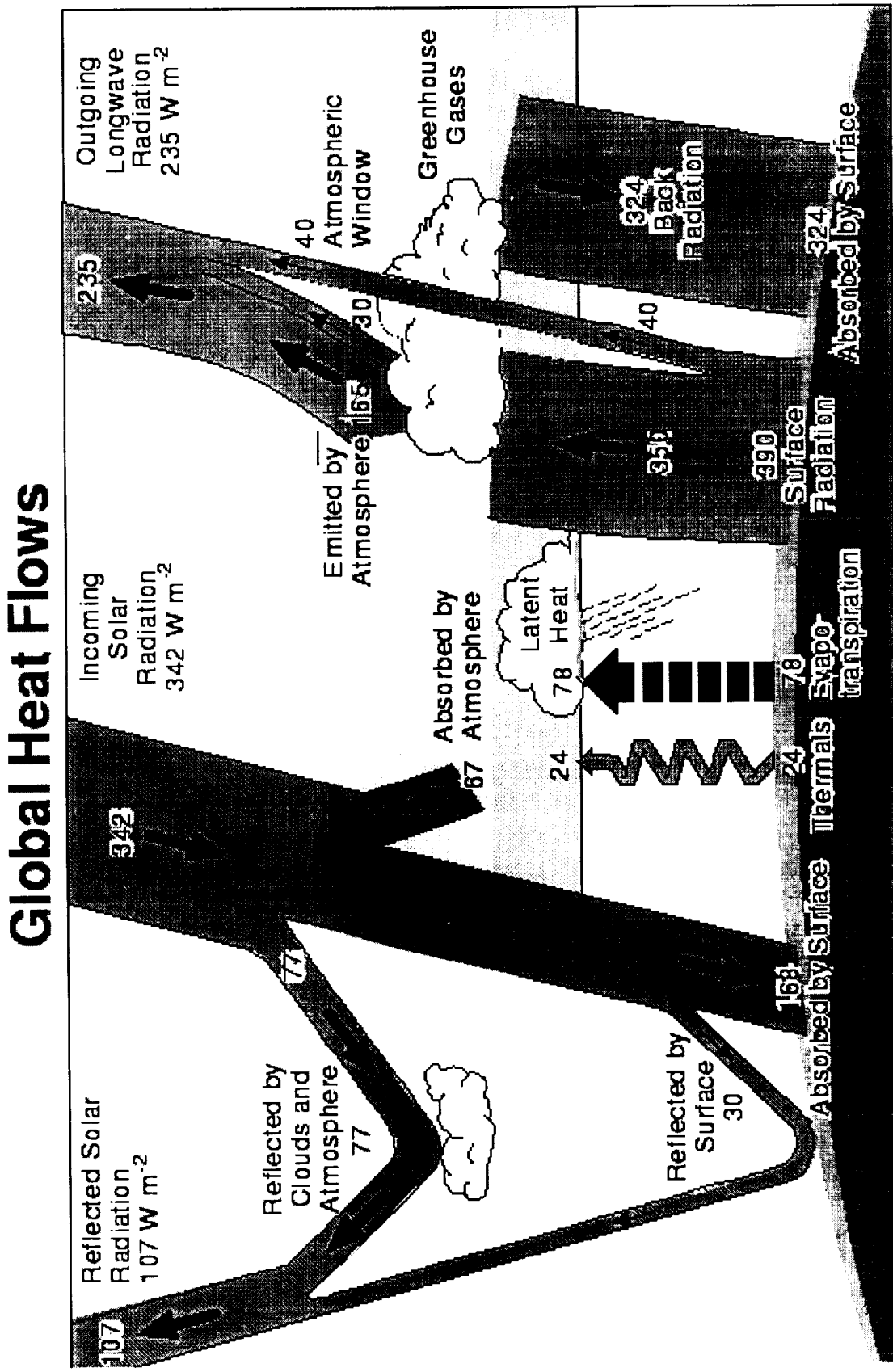

The Earth's radiation balance. The net incoming solar radiation of 342 Wm-2 is partially reflected by clouds and the atmosphere, or at the surface, but 45% is absorbed by the surface. Some of that heat is returned to the atmosphere as sensible heating and most as evapotranspiration that is realized as latent heat in precipitation. The rest is radiated as thermal infrared radiation and most of that is absorbed by the atmosphere and re-emitted both up and down, producing a greenhouse effect, as the radiation lost to space comes cloud tops and parts of the atmosphere much colder than the surface. From Kiehl and Trenberth (1997).

Increased heating leads naturally to expectations for increases in global mean temperatures (often mistakenly thought of as "global warming"), but other changes in weather are also important. Increases in greenhouse gases in the atmosphere produce global warming through an increase in downwelling infrared radiation, and thus not only increase surface temperatures but also enhance the hydrological cycle as much of the heating at the surface goes into evaporating surface moisture. Global temperature increases signify that the water-holding capacity of the atmosphere increases and, together with enhanced evaporation, this means that the actual atmospheric moisture increases, as is observed to be happening in many places (Trenberth 1998, 1989). It follows that naturally-occurring droughts are likely to be exacerbated by enhanced drying. Thus droughts, such as those set up by El-Niño, are likely to set in quicker, plants will wilt sooner, and the droughts may become more extensive and last longer with global warming. Once the land is dry then all the solar radiation goes into raising temperature, bringing on the sweltering heat waves.

Further, globally there must be an increase in precipitation to balance the enhanced evaporation. The presence of increased moisture in the atmosphere implies stronger moisture flow converging into all precipitating weather systems, whether they are thunderstorms, or extratropical rain or snow storms. This leads to the expectation of enhanced rainfall or snowfall events, which is also observed to be happening (Karl and Knight 1998, Trenberth 1998), see Figure 3.

The response of the climate system to the agents of change is complicated by feedbacks in the climate system, some of which amplify the original perturbation (positive feedback) and some of which diminish it (negative feedback). If, for instance, the amount of carbon dioxide in the atmosphere were suddenly doubled, but with other things remaining the same, the outgoing long-wave radiation would be reduced by about 4 Wm^{-2} and instead trapped in the atmosphere. To restore the radiative balance, the atmosphere must warm up and, in the absence of other changes, the warming at the surface and throughout the troposphere would be about 1.2°C. In reality, many other factors will change, and various feedbacks come into play, so that the best estimate of the average global warming for doubled carbon dioxide is 2.5°C (IPCC, 1990, 1995). In other words the net effect of the feedbacks is positive and roughly doubles the response otherwise expected.

The main positive feedback comes from water vapor as the amount of water vapor in the atmosphere increases as the Earth warms and, because water vapor is an important greenhouse gas, it amplifies the warming. However, increases in cloud may act either to amplify the warming through the greenhouse effect of clouds or reduce it by the increase in albedo; which effect dominates depends on the height and type of clouds and varies greatly with geographic location and time of year. Ice-albedo feedback probably leads to amplification of temperature changes in high latitudes. It arises because decreases in sea ice and snow cover, which have high albedo, decrease the radiation reflected back to space and thus produces warming which may further decrease the sea-ice and snow cover extent. However, increased open water may lead to more evaporation and atmospheric water vapor, thereby increasing fog and low cloud amount, offsetting the change in surface albedo.

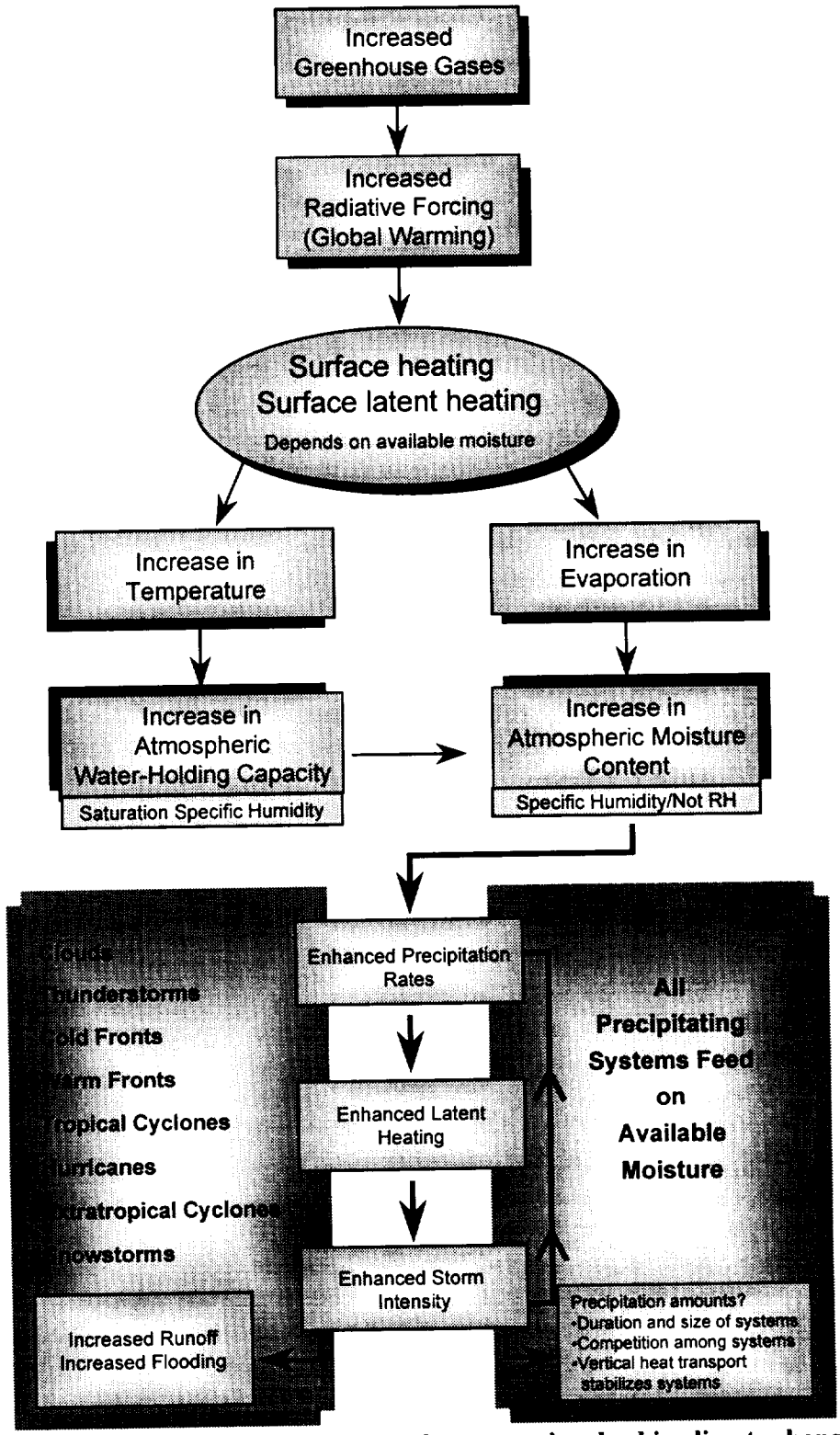

Figure 3: Schematic outline of the sequence of processes involved in climate change and how they alter moisture content of the atmosphere, evaporation, and precipitation rates. All precipitating systems feed on the available moisture leading to increases in precipitation rates and feedbacks. From Trenberth (1999).

Other more complicated feedbacks may involve the atmosphere and ocean, and the main example is the set of processes that give rise to the El-Niño-Southern Oscillation (ENSO) phenomenon in the tropical Pacific Ocean. The surface winds drive the ocean currents and patterns of upwelling, determine the sea surface temperatures, which in turn determine the preferred locations of atmospheric convection and tropical rainfall. These dominate the tropical atmospheric heating and thus determine the local and even global atmospheric circulation, through teleconnections, which include the surface winds. As this system is perturbed it sets up a positive feedback loop as an El-Niño or La Niña event, and certain negative feedbacks, including slow ocean adjustments to atmospheric effects from a year or two previously, and changes in heat content within the ocean lead to the demise of the events. Another example is the cold waters off of the western coasts of continents (such as California or Peru) that encourage development of extensive low stratocumulus cloud decks which block the sun and this helps keep the ocean cold. A warming of the waters, such as during El-Niño, eliminates the cloud deck and leads to further sea surface warming through solar radiation. Warming of the oceans from increased carbon dioxide may diminish the ability of the oceans to continue to take up carbon dioxide, thereby enhancing the rate of change, as more remains in the atmosphere.

A number of feedbacks involve the biosphere and are especially important when considering details of the carbon cycle and the impacts of climate change. For example, in wetland soils rich in organic matter, such as peat, the presence of water limits oxygen access and creates anaerobic microbial decay which releases methane into the atmosphere. If climate change acts to dry the soils, aerobic microbial activity develops and produces enhanced rates of decay which releases large amounts of carbon dioxide into the atmosphere.

Much remains to be learned about these feedbacks and their possible influences on predictions of future carbon dioxide concentrations and climate. Adequate observations to better understand these processes are needed as well as the ability to observe changes in the relevant variables to allow these effects to be determined.

Observed Climate Change

Analysis of observations of surface temperature show that there has been a global mean warming of about 0.7°C over the past one hundred years; see Figure 4 for the instrumental record of global mean temperatures. The warming became noticeable from the 1920s to the 1940s, leveled off from the 1950s to the 1970s and took off again in the late 1970s. The warmest year on record, by far, is 1998. The previous record was for 1997. The last ten years are the warmest decade on record. Moreover, recent information from paleodata further indicates that these years are the warmest in at least the past 1,000 years, which is as far back as a near-global estimate of temperatures can be made (Mann et al. 1998, 1999). The melting of glaciers over most of the world and rising sea level confirms the reality of the global temperature increases. The observed trend for a larger increase in minimum than maximum temperatures is linked to associated increases in low cloud amount and aerosol as well as the enhanced greenhouse effect (Dai et al. 1999).

There is firm evidence that moisture in the atmosphere is increasing. In the Western Hemisphere north of the equator, annual mean precipitable water amounts below 500 mb are increasing over the United States, Caribbean and the North Pacific by about 5% per decade as a statistically significant trend from 1973 to 1993 (Ross and Elliott 1996), and these correspond to significant increases in relative humidities of 2 to 3% per decade over the Southeast, Caribbean and subtropical Pacific. Precipitable water and relative humidities are not increasing significantly over much of Canada, however, and are decreasing slightly in some areas. In China, recent analysis by Zhai and Eskridge (1997) also reveals upward trends in precipitable water in all seasons and for the annual mean from 1970 to 1990. A claim for recent drying in the tropics by Schroeder and McGuirk (1998) using TOVS data is questionable owing to the changes in instruments and satellites. Clearly, there is a need to obtain more reliable atmospheric moisture trends over the entire globe.

Moreover, there is clear evidence that rainfall rates have changed in the United States. This has been shown by an analysis of the percentage of the U.S. area with much above normal proportion of total annual precipitation from 1 day extreme events, where the latter are defined to be more than 2 inches (50.8 mm) amounts (Karl et al. 1996). The "much above normal proportion" is defined to be the upper 10%. This quantity can be reliably calculated from 1910, and the percentage has increased steadily from less than 9 to over 11%, a 20% change. Karl and Knight (1998) have provided further analysis of U.S. precipitation increases and show how it occurs mostly in the upper tenth percentile of the distribution and that the portion of total precipitation derived from extreme and heavy events is increasing at the expense of more moderate events. Other evidence for increasing precipitation rates occurs in Japan and Australia.

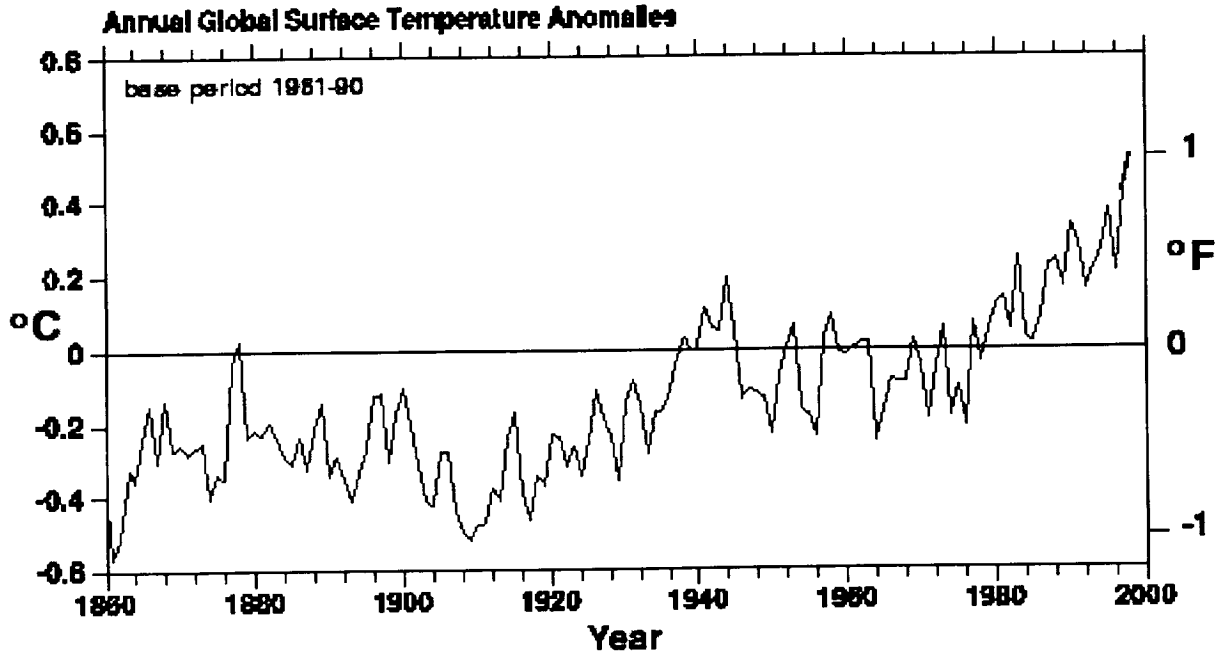

Figure 4: Global annual mean temperatures from 1860 to 1998 as departures from the 1961 to 1990 means. (Courtesy Jim Hurrell, adapted from data provided by Hadley Center, UKMO, and Climate Research Unit, Univ. East Anglia).

Modeling the Climate System

A full climate system model should deal with all the physical, chemical and biological processes that occur in nature and the interactions among the components of the climate system, the atmosphere, ocean, land surface, sea ice, surface hydrology, and biosphere (Figure 1). The models and their components are based upon physical laws represented by mathematical equations which are solved using a three dimensional grid over the globe. A major component of climate models are so-called atmospheric general circulation models (AGCMs) which are designed to simulate the detailed evolution of weather systems and weather phenomena, as well as the physical and dynamical processes involved. For AGCMs, typical resolutions for climate simulations are about 250 km (156 miles) in the horizontal direction and 1 km in the vertical.

It is well established that there is a limit to the predictability of weather of about two weeks owing to the mathematical phenomenon now known as "chaos" in which small uncertainties in the analysis of current weather conditions rapidly grow and eventually become large enough to render the forecast worthless. This essentially random error component is overcome in climate forecasts by predicting only the statistics of the weather, i.e., the climate. Accordingly, systematic influences of changing conditions in the ocean, sea ice, land surface, solar radiation, or other factors are reflected in atmospheric variations on various time scales. The most obvious example is the climate change with the seasons.

Climate models can be used in four-dimensional data assimilation (4DDA) to produce global analyses of variables in a multivariate analysis that uses the model to help define inter-relationships in a physically and dynamically consistent way. Once the models have been adequately tested and validated (see Trenberth 1997), they can be used in numerical experiments to make projections of possible future outcomes or to determine the climate response to various forcings.

An ensemble of several climatic simulations, each of which begins from somewhat different starting conditions, can be used to clearly establish which climatic features are reproducible in the simulations and thus are predictable with the model. These features constitute the "climate signal", while those which are not reproducible can be considered weather-related "climate noise". Climate predictability is a function of spatial scales. Natural atmospheric variability is enormous on small scales and most climate forcings, such as from increases in greenhouse gases, are predominantly global. Hence the noise level of natural variability will increasingly mask a climate signal as smaller regions are considered. Production of multiple repetitions of each experiment with small variations requires enormous computer resources.

Top-of-the-atmosphere Radiation and Clouds

Clouds absorb and emit thermal radiation and have a blanketing effect similar to that of the greenhouse gases. But clouds are also bright reflectors of solar radiation and thus also

act to cool the surface. Consequently, the effects of clouds can be clearly seen on the Absorbed Solar Radiation (ASR) and the Outgoing Longwave Radiation (OLR)(Figure 5). However, on average there is strong cancellation between the two opposing effects of short-wave and long-wave cloud heating (Figure 5), and the net global effect of clouds in our current climate, as determined by space-based measurements, is a small cooling of the surface. A key issue is how clouds will change as climate changes. This issue is complicated by the fact that clouds are also strongly influenced by particulate pollution, which tends to make more smaller cloud droplets, and thus makes clouds brighter and more reflective of solar radiation. These effects may also influence precipitation. If cloud tops get higher, the radiation to space from clouds is at a colder temperature and so this produces a warming. If low clouds become more extensive, then this is more likely to produce cooling because of the greater influence on solar radiation. Observational evidence indicates that increases in cloud amounts have been occurring (Dai et al. 1999).

The geometry of the Earth-sun system and the orbit of the Earth around the sun largely determines the distribution of net radiation, although with important structure associated with clouds, as noted above. However, the equator-to-pole and land-sea differences that exist drive atmospheric and oceanic circulations that transport moisture, heat and energy around the globe. Overall, the vertically-integrated divergence of the total atmospheric transport of energy, which consists of dry static energy, latent energy and kinetic energy, is balanced by the net radiative flux through the top of the atmosphere plus the flow into the oceans. In turn, the latter is balanced by the redistribution of heat within the oceans by ocean currents. Any small imbalances contribute to such things as changes in temperature. With the observations in Figure 5, and others from space and from the ground, we are able to compute the heat, moisture and energy budgets in detail and provide more and more information on the workings of our climate system, improve models, and increase the challenges for improved and new observations.

Observing the Earth and Monitoring Climate Change

We usually view the climate system from our perspective as individuals on the surface of the Earth. Just a few decades ago, the only way a global perspective could be obtained was by collecting observations of the atmosphere and the Earth's surface made at points over the globe and analyzing them to form maps of various fields, such as temperatures. The observational coverage has increased over time, but even today is not truly global because of the sparse observations over the southern oceans and the polar regions. Earth observing satellites have changed this, as two polar-orbiting sun-synchronous satellites can provide global coverage in about 6 hours, and geostationary satellites provide images of huge portions of the Earth almost continuously. However, it is difficult to see below the ocean surface, and observations in the ocean domain remain few and far between.

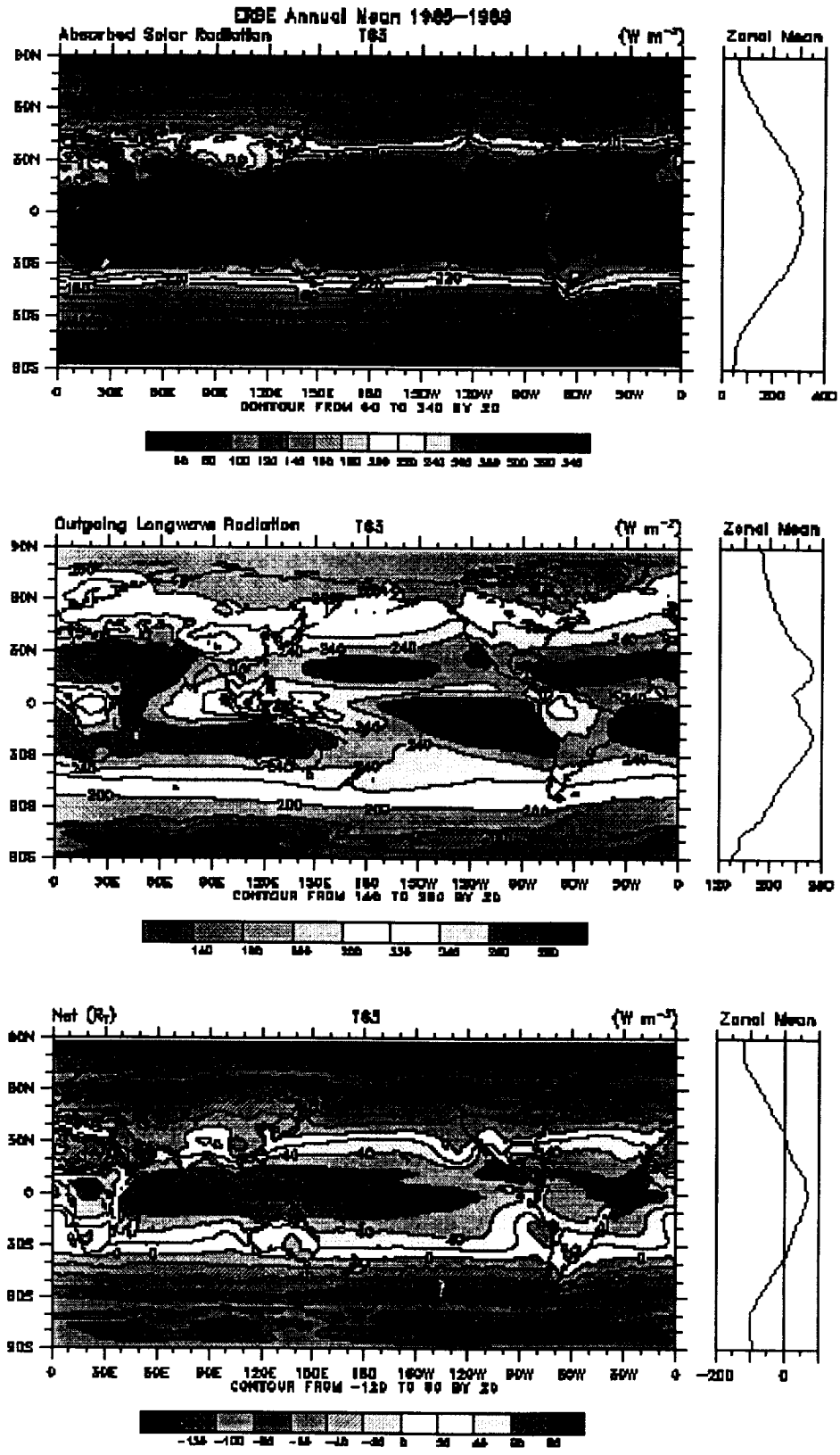

Figure 5: Net, ASR and OLR annual means from the Earth Radiation Budget Experiment (ERBE) based on the period February 1985 to April 1989, as reprocessed by Trenberth (1997b).

Even for instrumental observations, the long time-series of high quality observations needed to discern small changes are often compromised by non-physical effects, and special care is required in interpretation. Most observations have been made for other purposes, such as weather forecasting, and therefore typically suffer from changes in instrumentation, instrument exposure, measurement techniques, station location and observation times, and in the general environment (such as the building of a city around the measurement location) and there have been major changes in distribution and numbers of observations. Adjustments must be devised to take into account all these influences in estimating the real changes that have occurred.

From space, similar problems arise from the orbital decay and drift in equator crossing times of individual satellites, the finite life time of instruments and satellites which result in different platforms for instruments (even if the same) and electronic noise from nearby instruments, calibration of instruments, and conversion of radiances into geophysically meaningful quantities.

We need to know how the climate has changed and is changing. And because the future climate will be different from that today, we need to develop the capability to make reliable predictions of what it will be. Such predictions start from the initial observed state: not just for the atmosphere as in weather forecasting, but also for the oceans and every other active component of the climate system. In future, routine observations from a variety of networks could provide a much more comprehensive snapshot of the state of the environment: from space, from autonomous profiling floats at various depths the ocean, and from new sensors. The challenge is to ensure that we have in place a means not only to measure these variables, but to do so in a manner that enables us to understand whether multi-decadal observed changes reflect real changes in the environment versus different methods of observing.

In order to reduce our uncertainty about the sensitivity of the climate system to human alteration of the environment, it will be critical to evaluate our model simulations. We must be capable of adequately simulating the climate during pre-industrial times, and especially since that time, when humans have changed the composition of the atmosphere in a dramatic manner. To evaluate our models we require not only snapshot pictures of many physical, chemical, and biological quantities, but reliable long-term records. However, we are dependent on services of large operational networks that are presently being operated for purposes other than studying climate change. We currently do not have an adequate system for monitoring climate.

In addition to the standard atmospheric variables (temperatures, winds) much better fields are needed for clouds, water vapor and ozone, and probably other trace constituents, as well as precipitation. At the surface, surface winds (from scatterometry) and sea level (from altimetry), ocean color, soil moisture, as well as glacial ice volume will be important. Also important will be continuing measurements of any forcings of climate, such as the total solar irradiance, and the four dimensional distribution of aerosol loading from volcano and human sources and top-of-the-atmosphere radiation. Many of these fields can be obtained from space but information, such as vertical structure, is also needed from the

ground, and measurements within the ocean must come from in situ sources. Synthesis of all the measurements and generation of important products must come from global models, and four-dimensional assimilation must play a major role.

In the past, space-based systems measurements have been converted to geophysical variables using various algorithms. Increasingly, 4DDA makes direct use of radiances along with information on all other variables in a multivariate analysis. A new challenge, therefore, is to determine what are the requirements for radiances that should be measured to produce the required accuracy of geophysical variables? A related challenge is to include bias corrections for various observing systems (satellite and in situ) as they change with time.

A call is made for a true climate observing system composed of both space-based and in situ components that capitalizes on the advantages of each and which adheres to guiding principles that ensure long term integrity. The space-based component produces regular global coverage but is not stable. Multiple overlapping satellites can help transfer the record from one satellite to another, but all satellites suffer from orbital decay and drift that alter the time of day of measurements. While advanced station-keeping can help, there is also a need for a stable ground-based climate observing system. The in situ instruments can be changed as long as overlaps are included as part of the strategy and the space-based record can also help transfer the record across transitions. Methods of monitoring observing system performance and processing all the data with appropriate bias corrections must also be a part of this. Special efforts and institutional commitments are needed to design and sustain such a system.

References

Bonan, G. B. (1997). Effects of land use on the climate of the United States. *Clim. Change*, **37**, 449-486.

Dai, A., Trenberth, K. E. and Karl, T. R. (1999). Effects of clouds, soil moisture, precipitation and water vapor on diurnal temperature range. *J. Clim.*, (in press).

Houghton, J. T., Meira Filho, F. G., Callander, B. A., Harris, N., Kattenberg, A. and Maskell, K. (Eds.). (1996). IPCC (Intergovernmental Panel of Climate Change). *Climate Change 1995: The Science of Climate Change*. (pp. 572) Cambridge, U.K.: Cambridge Univ. Press.

Karl, T. R., and Knight, R. W. (1998). Secular trends of precipitation amount, frequency and intensity in the USA. *Bull. Am. Meteorol. Soc.*, **79**, 231-242.

Karl, T. R., Knight, R. W., Easterling, D. R. and Quayle, R. G. (1996). Indices of climate change for the United States. *Bull. Am. Meteorol. Soc.*, **77**, 279-292.

Karl, T. R., Knight, R. W. and Plummer, N. (1995). Trends in high frequency climate variability in the twentieth century. *Nature,* **377**, 217-220.

Kiehl, J. T., and Trenberth, K. E. (1997). Earth's annual global mean energy budget. *Bull. Am. Meteorol. Soc.*, **78**, 197-208.

Mann, M. E., Bradley, R. S. and Hughes, M. K. (1998). Global-scale temperature patterns and climate forcing over the past 6 centuries. *Nature*, **392**, 779-787.

Mann, M. E., Bradley, R. S. and Hughes, M. K. (1999). Northern hemisphere temperatures during the past millennium: Inferences, uncertainties, and limitations. *Geophys. Res. Lett.*, **26**, (in press).

Ross, R. J., and Elliot, W. P. (1996). Tropospheric water vapor climatology and trends over North America: 1973-93. *J. Clim.*, **9**, 3561-3574.

Schroeder, S. R., and McGuirk, J. P. (1998). Widespread tropical atmospheric drying from 1979 to 1995. *Geophys. Res. Lett.*, **25**, 1301-1304.

Trenberth, K. E. (1997). The use and abuse of climate models in climate change research. *Nature*, **386**, 131-133.

Trenberth, K. E. (1997b). Using atmospheric budgets as a constraint on surface fluxes. *J. Climate*, **10**, 2796-2809.

Trenberth, K. E. (1998) Atmospheric moisture residence times and cycling: Implications for rainfall rates with climate change. *Clim. Change*, **39**, 667-694.

Trenberth, K. E. (1999) Conceptual framework for changes of extremes of the hydrological cycle with climate change. *Clim. Change*, **40**, (in press).

Zhai, P., and Eskridge, R. E. (1997). Atmospheric water vapor over China. *J. Clim.*, **10**, 2643-2652.

PREDICTING DECADE-TO-CENTURY CLIMATE CHANGE: PROSPECTS FOR IMPROVING MODELS

Richard C. J. Somerville

University of California, San Diego
Scripps Institution of Oceanography
(rsomerville@ucsd.edu)

Abstract

Recent research has led to a greatly increased understanding of the uncertainties in today's climate models. In attempting to predict the climate of the 21st century, we must confront not only computer limitations on the affordable resolution of global models, but also a lack of physical realism in attempting to model key processes. Until we are able to incorporate adequate treatments of critical elements of the entire biogeophysical climate system, our models will remain subject to these uncertainties, and our scenarios of future climate change, both anthropogenic and natural, will not fully meet the requirements of either policymakers or the public. The areas of most-needed model improvements are thought to include air-sea exchanges, land surface processes, ice and snow physics, hydrologic cycle elements, and especially the role of aerosols and cloud-radiation interactions.

Of these areas, cloud-radiation interactions are known to be responsible for much of the inter-model differences in sensitivity to greenhouse gases. Recently, we have diagnostically evaluated several current and proposed model cloud-radiation treatments against extensive field observations. Satellite remote sensing provides an indispensable component of the observational resources. Cloud-radiation parameterizations display a strong sensitivity to vertical resolution, and we find that vertical resolutions typically used in global models are far from convergence. We also find that newly developed advanced parameterization schemes with explicit cloud water budgets and interactive cloud radiative properties are potentially capable of matching observational data closely. However, it is difficult to evaluate the realism of model-produced fields of cloud extinction, cloud emittance, cloud liquid water content and effective cloud droplet radius until high-quality measurements of these quantities become more widely available. Thus, further progress will require a combination of theoretical and modeling research, together with intensified emphasis on both in situ and space-based remote sensing observations.

Introduction

Seen from space, the Earth appears as a mainly blue ocean planet flecked with constantly changing intricate patterns of white clouds. The clouds, which cover about half the surface of the planet, are critical to climate. They cool the Earth by reflecting away sunlight. At the same time, they warm the Earth by trapping the Earth's heat, thus contributing to the natural greenhouse effect. Of course, clouds are also a source of water in the form of

rain and snow, critical to all aspects of life and central to agriculture and thus to the well-being of humankind. If climate changes, whether for natural or man-made reasons, clouds are likely to change as well and have important feedbacks on the climate.

In computer modeling of the global climate system, which is our main technique for forecasting future climate, we first have to understand climate science well enough to build crucial physical processes into our models realistically. Among the key science areas, treating clouds accurately is an especially critical issue, because clouds have such important effects on climate. However, clouds are much too small and short-lived to be modeled explicitly in a global simulation, and the physical processes involved in clouds are still imperfectly understood. Nevertheless, clouds and their consequences are much too important to be ignored, and so their effects are treated by simple rules.

Climate models are solved numerically on global grids with a typical resolution of a few hundred kilometers horizontally. When the model values of climate variables at this resolution are used to prescribe clouds, the resulting rules are often highly simplistic. For example, a typical rule might make the cloud amount in a model grid area proportional to relative humidity. However, the behavior of rules of this sort often bears little resemblance to the way clouds actually vary in space and time in the present atmosphere, let alone as to how they will change and feed back on any future climate which differs from the present one. These rules are rarely well-founded theoretically and have almost never been tested observationally in any thorough and satisfying way.

It is crucial that observational and modeling research be done to show how clouds behave in the actual atmosphere. Only recently have appropriate observations begun to be available to tackle this task. These observations provide invaluable information for the development of improved models. Space-based data have been critical to progress. Supporting the research to obtain and use these data optimally is a key to further progress in making future climate projections reliable, detailed and useful to policymakers.

Research strategy

Progress in attacking these questions depends on a multi-faceted research strategy. It is now well-recognized in the community that single-column models (SCMs) are tools which have a valuable role to play in testing and improving parameterizations by evaluating them empirically against field observations. E. g., see Randall et al. (1996). This paper features some representative examples of the ability of SCMs to aid in evaluating and improving global climate model (GCM) parameterizations.

Our SCM contains switch-selectable parameterizations based on current GCM practice. Our approach involves evaluating parameterizations directly against measurements from field programs, and using this validation to tune existing parameterizations and to guide the development of new ones. We use the single-column model (SCM) to make the link between observations and parameterizations. Surface and satellite measurements are both used to provide an initial evaluation of the performance of the different parameterizations. The results of this evaluation are then used to develop improved cloud-precipitation schemes, and finally these schemes are tested in GCM experiments (Lee et al., 1997).

Our single-column model has evolved from the one described by Iacobellis and Somerville (1991a,b). The SCM now is a versatile and economical one-dimensional model, resembling a single column of a general circulation model (GCM). The SCM contains the full set of parameterizations of subgrid physical processes that are normally found in a modern GCM. The SCM is applied at a specific site having a horizontal extent typical of a GCM grid cell. Since the model is one-dimensional, the advective terms in the budget equations are specified from observations. For a more complete discussion of SCMs, see Randall et al. (1996) and Iacobellis and Somerville (1991a,b).

The standard SCM uses the longwave radiation parameterization of Morcrette (1990) and the solar radiation parameterization of Fouquart and Bonnel (1980). A variety of parameterizations representing cumulus convection, cloud prognostication, cloud radiative properties, cloud water budgets and precipitation can be tested in this manner and used for intercomparison. The cumulus convection parameterizations which we have used include those of Kuo (1974) (as modified by Anthes, 1977) and of Arakawa and Schubert (1974) (with downdrafts as specified by Kao and Ogura, 1987), and of Emanuel (1991). The cloud prediction schemes are those of Slingo (1987), Smith (1990), Sundqvist et al. (1989) and Tiedtke (1993). The cloud radiative properties are specified from either McFarlane et al. (1992) or a combination of Stephens (1977) (water clouds) and Suzuki et al. (1993) (ice clouds). Cloud liquid water is a prognostic model variable when the Smith or Sundqvist or Tiedtke scheme is active, but not when the Slingo routine is being used. These parameterizations are switch-selectable in the present version of the model.

Model experiments

Long-term experiments in the TOGA-COARE region

As an example of the use of single-column models, we first present a series of seven "long-term" experiments from the 1992-93 tropical field experiment TOGA-COARE (Tropical Ocean Global Atmosphere – Combined Ocean-Atmosphere Response Experiment). The model configuration in each experiment differs only in the specification of the cumulus convection parameterization, the cloud prognostication scheme and/or the parameterization of cloud-radiative properties. The parameterizations used in each experiment are shown in Table 1.

In each experiment, the SCM was applied at 19 5°x 5° sites within the bounded region of the western tropical Pacific extending from 137.5°E-172.5°E and 7.5°N-7.5°S. The size and location of the individual sites was selected to coincide with the ECMWF Operational Analysis data which is used as model forcing in these experiments. Each experiment extends from 01 November 1992 to 28 February 1993 which corresponds to the IOP of TOGA-COARE. At each site the model was initialized at 01 Nov 1992 00LST and run for a period of four days. The model was then reinitialized and run again for the next four days. This process was repeated a total of 30 times with the last 4-day run extending from 25 February 1993 to 28 February 1993. These 30 runs were repeated at each of the 19 5°x 5° sites. Long-term regional means during the TOGA-COARE IOP are formed by averag-

ing results from the 570 (19 sites x 30 4-day periods) model runs for each configuration of model parameterizations.

Table 1: Model Configurations

Exp. No.	Cumulus Convection	Cloud Scheme	Cloud-Radiative Properties
1	Kuo-Anthes	Slingo	McFarlane
2	Emanuel	Slingo	McFarlane
3	Arakawa-Schubert	Slingo	McFarlane
4	Kuo-Anthes	Smith	Stephens+Suzuki
5	Emanuel	Smith	Stephens+Suzuki
6	Arakawa-Schubert	Smith	Stephens+Suzuki
7	Kuo-Anthes	Sundqvist	Stephens+Suzuki

The cloud radiative forcing terms (Ramanathan et al. 1989; Senior and Mitchell, 1993) and other cloud-radiation variables produced by the these SCM experiments can be examined to understand how the various parameterizations may affect the modeled climatological heat budget of the TOGA-COARE region. The cloud radiative forcing represents the extra amount of radiation that is either emitted to space or absorbed by the earth-atmosphere system due to the presence of clouds. The total cloud forcing (CF) is composed of a shortwave component (SWCF) and a longwave component (LWCF), or, in equation form:

$$CF = CF_{SW} + CF_{LW} = (Q - Q_c) - (F - F_c)$$

where Q is the net incoming solar radiation, F is the outgoing longwave radiation and the subscript c indicates clear-sky fluxes. If CF is positive then the clouds have a warming effect on the earth-atmosphere system. These terms averaged over all 19 sites and over the 4 month time period for each of the seven SCM experiments are shown in Table 2. The last row of Table 2 contains the observed values obtained from GMS-4 satellite measurements (Flament and Bernstein, 1993).

These results show that when the Slingo cloud scheme is used (experiments 1-3) model averages of CF_{SW}, CF_{LW}, OLR, albedo and insolation are less sensitive to the choice of cumulus parameterization than when the Smith cloud scheme is employed (experiments 4-6). The effect of the treatment of cloud liquid water can be seen by comparing the results from experiments 1, 4 and 7. Here the Kuo-Anthes convection was used in each case while the cloud prognostication scheme varied. The model results show large decreases in insolation and OLR and large increases (in magnitude) in albedo and both the shortwave and longwave cloud forcing terms for experiments 4 and 7 compared to experiment 1.

Table 2: Cloud Forcing and Radiative Results

Exp. No.	CF_{SW} (W m^{-2})	CF_{LW} (W m^{-2})	CF (W m^{-2})	Albedo	OLR (W m^{-2})	Insol. (W m^{-2})
1	-100	56	-44	0.33	236	200
2	-101	57	-44	0.33	229	199
3	-108	65	-43	0.35	224	191
4	-121	66	-55	0.38	225	176
5	-137	76	-61	0.42	210	159
6	-144	82	-62	0.44	207	151
7	-138	71	-67	0.42	220	154
GMS	-108	62	-46	0.37	228	---

The model results are much closer to the observed GMS-4 values when cloud liquid water is not an interactive variable (experiments 1-3). The larger absolute values of the cloud forcing terms, the increase in albedo, and the decrease in OLR and insolation in experiments 4-7, all indicate that the model is either over-estimating the cloud fraction and/or the cloud optical thickness when cloud liquid water is an interactive variable.

Short-term experiments in the IFA region

The SCM is now applied over the site of the Intensive Flux Array (IFA). In this series of experiments the horizontal advection terms necessary to force the SCM are derived from sounding measurements taken along the perimeter of the IFA. Thus, direct observations are used to force the model in these experiments as opposed to model assimilation products used in Section 3.1. The SCM was run for several 5-day periods within the TOGA-COARE IOP of 01Nov92 - 28Feb93 using model configuration #7 (see Table 1).

Figure 1 shows results that typify the SCM response during low precipitation conditions over the IFA. During these 'dry' events, the SCM typically reproduced the observed temperature and humidity evolution and produced diagnostic radiative quantities that compared very well to both surface and satellite measurements. SCM results from a 5-day period that experienced significant precipitation are shown in Figure 2. During these 'wet' events the SCM often underestimated the surface downwelling solar radiation and overestimated the planetary albedo while reproducing well the precipitation as measured by the satellite measurements of the Microwave Sounding Unit (MSU).

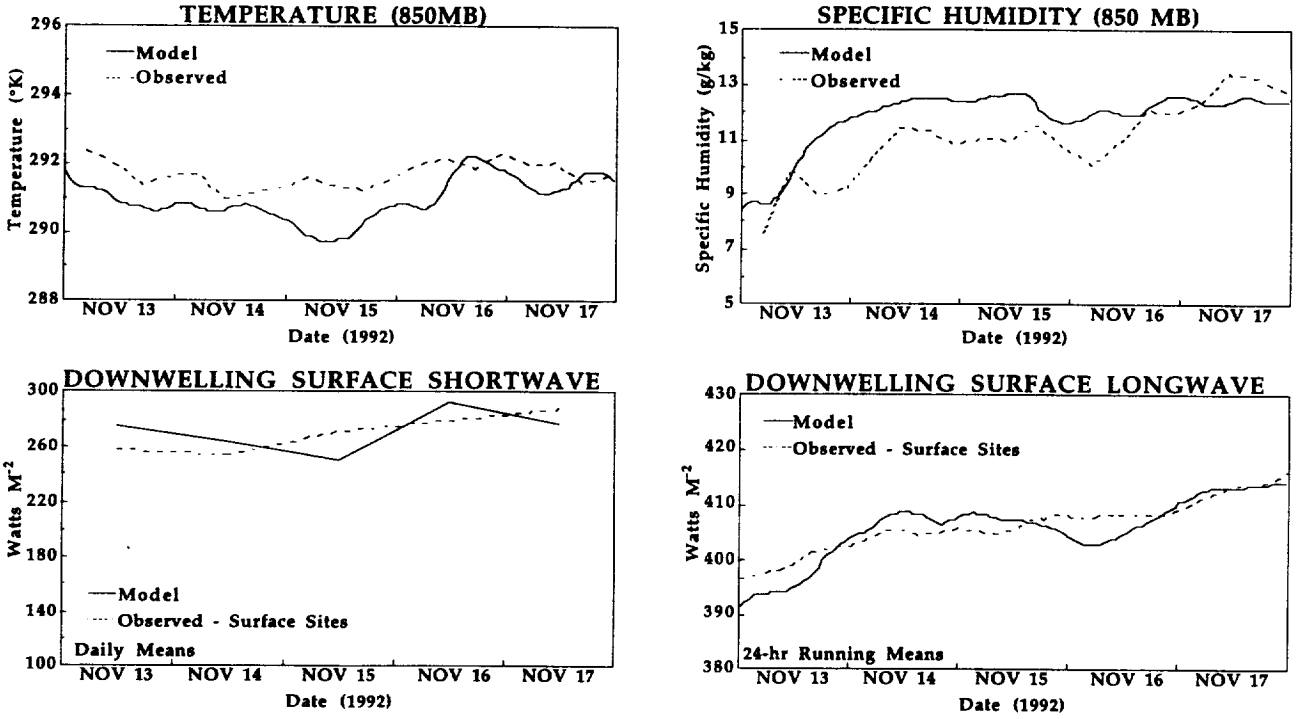

Figure 1: Model vs. observation comparisons for low-precipitation conditions

These model results from the IFA site are consistent with the long-term runs discussed above in that they both indicate the model parameterizations are over-estimating the cloudiness and/or cloud optical thickness. Further analysis of the model results indicates that very large errors in cloud optical thickness would be necessary solely to explain the model discrepancies in albedo and surface shortwave. Thus, overestimation of the fractional cloud coverage is more likely to be the cause of the majority of the errors in albedo and surface shortwave. The fractional cloud cover for convective clouds in the Sundqvist cloud scheme is given by:

$$\mathrm{CLD} = \xi\tau(1 + RH)(1 + (\sigma_b - \sigma_t)/A)/(1 + B\xi\tau)$$

where CLD is fractional cloud amount, RH is relative humidity, σ_b, σ_t are the sigma level of cloud base and cloud top, ξ is a quantity proportional to the moisture convergence, τ is a convective time scale and A, B are constants. In Sundqvist's scheme, the values of A and B are set to 0.3 and 2.5 respectively. We performed numerous SCM runs in the IFA region throughout the IOP period, each run with different values of A and B. A comparison of model albedo and surface shortwave to observations yielded "optimized" values of A and B of approximately 0.5 and 4.0.

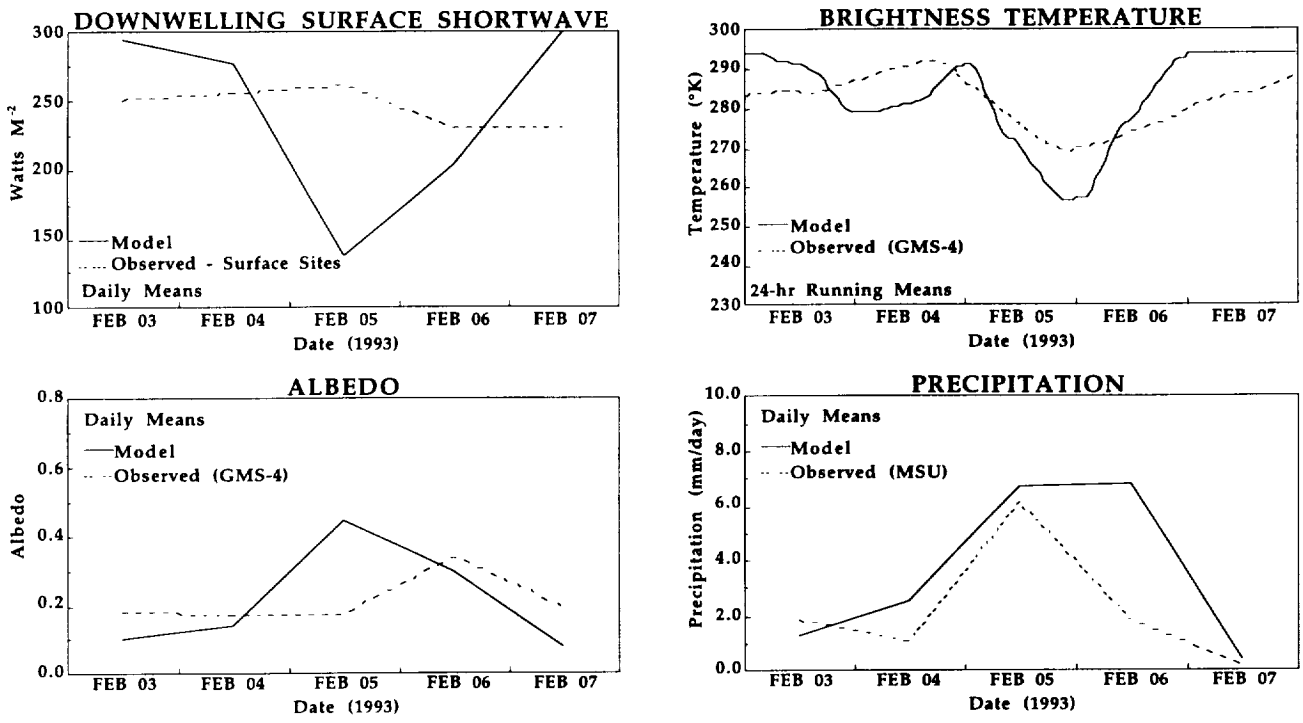

Figure 2: Model vs. observation comparisons for significant precipitation conditions

The use of these optimized values of A and B improves the SCM estimates of albedo and downwelling shortwave radiation during precipitation events in the IFA region. A further and more substantial test of this optimization was performed by rerunning the long-term runs (SCM in configuration 7) with the optimized values of A and B. The model results from the "optimized" run and the original run are shown below in Table 3, along with measured values from the GMS-4 satellite. The results from the SCM run using the optimized values of A and B show a clear improvement over the original run when compared to GMS-4 measurements taken during the TOGA-COARE IOP.

Table 3: Original vs. Optimized

	CF_{SW} (W m^{-2})	CF_{LW} (W m^{-2})	CF (W m^{-2})	Albedo	OLR (W m^{-2})	Insol. (W m^{-2})
Original	-138	71	-67	0.42	220	154
Optimized	-112	59	-53	0.36	232	183
GMS	-108	62	-46	0.37	228	---

Summary and outlook

The results of global climate models (GCMs) are sensitive to small-scale physical processes. Yet these processes are often treated simplistically and even crudely. For example, we have considered in particular the task of treating the role of clouds in affecting radiation, both solar and terrestrial, passing through the atmosphere. One needed quantity is the cloud amount, i. e., the fraction of a GCM grid area covered by cloud at different altitudes. Numerous observational studies demonstrate that cloud amount is not a simple function of relative humidity.

Today, GCM parameterizations are held to a higher standard than only a few years ago, because it has become recognized that the role of cloud feedbacks is crucial in determining the sensitivity of GCM climates to changes in the atmospheric concentration of carbon dioxide and other greenhouse gases, and to the direct and indirect effects of atmospheric aerosols. Early GCMs had fixed clouds and hence a low sensitivity to prescribed carbon dioxide changes. When cloud amounts are parameterized on relative humidity, several positive feedbacks come into play. One is the reduction of cloud amount in a warmer climate, a typical GCM result. This change produces an augmented warming, because GCM clouds, like global average real clouds, have a larger contribution to the planetary albedo than to the planetary greenhouse effect. In more precise terms, their shortwave forcing dominates their longwave forcing.

A separate class of positive feedbacks arises from an increase in average cloud altitude, which is also a characteristic GCM response to climatic warming. On average, higher clouds are less effective infrared emitters to space, because they are colder, and they are less effective reflectors of incoming solar photons, because they are optically thinner, than lower clouds. In combination with the reduction in cloud amount, the increase in cloud height has the effect of powerfully reinforcing the warming which gives rise to these changes in cloud amount. It is the GCMs which incorporate these effects most strongly, and which do not include compensating negative feedbacks, that produce the highest sensitivities to changes in greenhouse gas concentrations.

The GCMs which have the lowest sensitivities, on the other hand, are those which are dominated by negative cloud feedbacks. One such feedback is due to hypothetical cloud microphysical processes. Chief among these is a hypothesized increase in cloud water content accompanying a warmer climate. If in fact a warmer climate is characterized by wetter clouds, then, other things being equal, the wetter clouds may produce a negative feedback by increasing the optical thickness and hence the albedo of lower clouds, or a positive feedback by increasing the infrared emissivity of optically thin higher clouds.

Which of these conflicting effects will dominate? Is it scientifically justifiable to focus on global average cloud feedbacks to the neglect of regional ones? How do these cloud feedbacks depend on season, or synoptic regime, or geographical locale? What are the dynamical and thermodynamic consequences of the diabatic processes which depend on cloud feedbacks. These questions form much of the research agenda of the climate community. Even if anthropogenic climate change were not such an important policy issue, cloud pro-

cesses would play an important role in climate modeling, because they have such a pervasive influence on climate, as evidenced by recent GCM results (e. g., Lubin et al., 1998).

In this work, we have diagnostically evaluated several current and proposed model cloud-radiation treatments against extensive field observations. Satellite remote sensing provides an indispensable component of the observational resources. We find that newly developed advanced parameterization schemes with explicit cloud water budgets and interactive cloud radiative properties are potentially capable of matching observational data closely. However, it is difficult to evaluate the realism of model-produced fields of cloud extinction, cloud emittance, cloud liquid water content and effective cloud droplet radius until high-quality measurements of these quantities become more widely available. Thus, further progress will require a combination of theoretical and modeling research, together with emphasis on both in situ and space-based remote sensing observations.

We may draw several far-reaching conclusions from current climate research results:

1. Predicting the future of Earth's climate, which can change for both natural and human-related reasons, requires an improved understanding of key physical processes, such as those related to clouds. Satellite measurements have been essential to progress.

2. The research needed to achieve this understanding is now underway, and the needed measurements are beginning to be made, but much more effort is needed to make key observations and use them to improve computer simulations. Space-based measurements will continue to have a key role to play.

3. Even after the research has been advanced and the models have become more trustworthy, producing climate predictions with sufficient realism for policymakers will require vastly increased computer power, and continuing scientific and political leadership.

Acknowledgments

The research reported in this paper has been sponsored in part by the U. S. Department of Energy under Grant DE-FG03-90-ER61061, the National Science Foundation under Grant ATM91-14109, and the National Oceanic and Atmospheric Administration under Grant NA36GP0372, and the National Aeronautics and Space Administration under Grant No. NAG5-2238. I deeply appreciate the many essential contributions of my collaborators: Carolyn Baxter, Joannes Berque, Sam Iacobellis, Dana Lane, Wan-Ho Lee and Boris Shkoller.

References

Anthes, R. A. (1977). A cumulus parameterization scheme utilizing a one-dimensional cloud model. *Mon. Wea. Rev.*, **105**, 270-286.

Arakawa, A., and Schubert, W. H. (1974). Interaction of a cumulus cloud ensemble with the large-scale environment, Part I. *J. Atmos. Sci.*, **31**, 674-701.

Bower, K. N., Choularton, T. W., Latham, J., Nelson, J., Baker, M. B. and Jenson, J. (1994). A parameterization of warm clouds for use in atmospheric general circulation models. *J. Atmos. Sci.*, **51**, 2722-2732.

Emanuel, K. A. (1991). A scheme for representing cumulus convection in large-scale models. *J. Atmos. Sci.*, **48**, 2313-2335.

Flament, P. and Bernstein, R. (1993). *Images from the GMS-4 satellite during TOGA-COARE (November 1992 to February 1993).* (Technical report 93-06, 20pp, School of Ocean and Earth Science and Technology). University of Hawaii, Honolulu (with two CD-ROMs)

Fouquart, Y. and Bonnel, B. (1980). Computation of solar heating of the Earth's atmosphere: a new parameterization. *Beitr. Phys. Atmos.*, **53**, 35-62.

Iacobellis, S. F., and Somerville, R. C. J. (1991a). Diagnostic modeling of the Indian monsoon onset, I: Model description and validation. *J. Atmos. Sci.*, **48**, 1948-1959.

Iacobellis, S. F., and Somerville, R. C. J. (1991b). Diagnostic modeling of the Indian monsoon onset, II: Budget and sensitivity studies. *J. Atmos. Sci.*, **48**, 1960-1971.

Kao, J. C.-Y. and Ogura, Y. (1987). Response of cumulus clouds to large-scale forcing using the Arakawa-Schubert Cumulus Parameterization. *J. Atmos. Sci.*, **44**, 2437-2458.

Kuo, H. L. (1974). Further studies of the parameterization of the influence of cumulus convection on large-scale flow. *J. Atmos. Sci.*, **31**, 1232-1240.

Lee, W.-H., Iacobellis, S. F. and Somerville, R. C. J. (1997). Cloud radiation forcings and feedbacks: General circulation model tests and observational validation. *J. Climate*, **10**, 2479-2496.

Lubin, D., Chen, B., Bromwich, D. H., Somerville, R. C. J., Lee, W.-H. and Hines, K. M. (1998). The impact of cloud radiative properties on a GCM climate simulation. *J. Climate*, **11**, 447-462.

McFarlane, N. A., Boer, G. J., Blanchet, J.-P. and Lazare, M. (1992). The Canadian Climate Centre second-generation general circulation model and its equilibrium climate. *J. Climate*, **5**, 1013-1044.

Morcrette, J.-J. (1990). Impact of changes to the radiation transfer parameterizations plus cloud optical properties in the ECMWF model. *Mon. Wea. Rev.*, **118**, 847-873.

Price, J. F., Weller, R. A. and Pinkel, R. (1986). Diurnal Cycling: Observations and models of the upper ocean response to diurnal heating, cooling, and wind mixing. *J. Geophys. Res.*, **91**, 8411-8427.

Ramanathan, V., Barkstrom, B. R. and Harrison, E. F. (1989). Climate and the Earth's radiation budget. *Phys. Today*, May, 22-32.

Randall, D. A., Xu, K.-M., Somerville, R. C. J. and Iacobellis, S. (1996). Single-column models and cloud ensemble models as links between observations and climate models. *J. Climate*, **9**, 1683-1697.

Senior, C. A., and Mitchell, J. F. B. (1993). Carbon dioxide and climate: The impact of cloud parameterization. *J. of Climate*, **6**, 393-418.

Slingo, J. M. (1987). The development and verification of a cloud prediction scheme for the ECMWF model. *Q. J. R. Meteorol. Soc.*, **113**, 899-927.

Smith, R. N. B (1990). A scheme for predicting layer clouds and their water content in a general circulation model. *Q. J. R. Meteorol. Soc.*, **116**, 435-460.

Stephens, G. L. (1978). Radiation profiles in extended water clouds. II: Parameterization studies. *J. Atmos. Sci.*, **35**, 2123-2132.

Sundqvist, H., Berge, E. and Kristjánsson, J. E. (1989). Condensation and cloud parameterization studies with a mesoscale numerical weather prediction model. *Mon. Wea. Rev.*, **117**, 1641-1657.

Suzuki, T., Tanaka M. and Nakajima, T. (1993). The microphysical feedback of cirrus cloud in climate change. *J. Meteor. Soc. Japan*, **71**, 701-713.

Tiedtke, M. (1993). Representation of clouds in large-scale models. *Mon. Wea. Rev.*, **121**, 3040-3061.

Zhang, G. J., and McFarlane, N. A. (1995). Sensitivity of climate simulations to the parameterization of cumulus convection in the Canadian Climate Centre general circulation model. *Atmosphere-Ocean*, **33**, 407-446.

SUN-CLIMATE CONNECTIONS

Judith Lean

E.O. Hulburt Center for Space Research
Naval Research Laboratory, Washington, D.C.
lean@demeter.nrl.navy.mil

Abstract

Does the Sun influence climate? Solar radiation varies continuously; so too does Earth's global environment. But despite more than a century of debate, and the identification of numerous empirical relationships among assorted solar and climate parameters, the extent of Sun-climate connections remains to be reliably specified. To what extent is the 0.6°C surface warming of the past 130 years a result of increased concentrations of industrial greenhouse gases, or part of a longer term, solar-related warming, or some combination of these and other natural and forced processes? Only from space can solar monitoring instruments acquire data with sufficiently high precision to specify Sun-climate connections. With this goal, a suite of cavity-type radiometers on various spacecraft have tracked day-to-day and solar cycle fluctuations in the Sun's total irradiance during the past two decades. Space-based spectroradiometers have also measured concomitant changes in the shorter wavelength ultraviolet spectrum. Primary irradiance variability mechanisms -- dark sunspots and bright faculae -- have been identified, and models developed that replicate much of the observed variance in the extant irradiance database. When extended to centennial time scales, the models predict irradiance variability in the range 0.2 to 0.5%. General circulation model simulations are beginning to explore the physical pathways through which the climate systems responds to changes in total solar irradiance. Improved knowledge of Sun-climate connections requires future simulations that include an adequate representation of the spectral nature of the Sun's radiative output changes, and of the indirect pathways that solar UV irradiance variability may influence climate via its control of atmospheric ozone concentrations. Continued space-based solar monitoring with radiometers having improved stability and spectral coverage is critical for the detection of long term irradiance changes, and to characterize spectral irradiance variability at all wavelengths.

Climate Change

Climate change, manifest in the surface temperature of the Earth, occurs on time scales of years, decades, centuries and millennia. Earth's surface temperature, shown in Figure 1, increased 0.6°C during the past century. Fluctuations of a few tenths °C are evident, as well, in surface temperatures reconstructed over the past millennium.

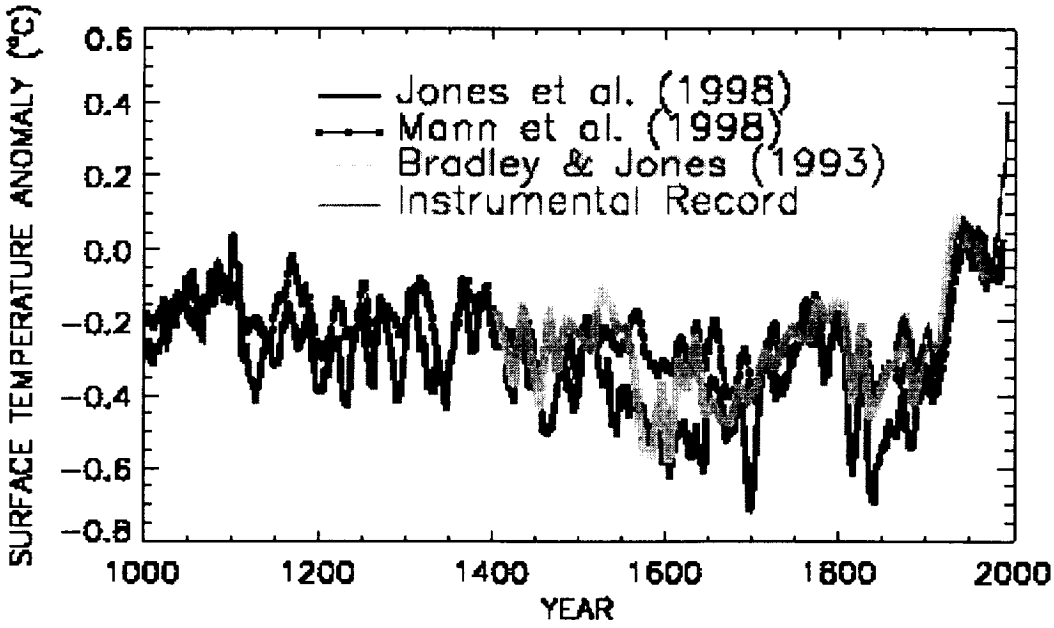

Figure 1: Surface temperature anomalies - last millennium

Potential causes of climate change are manifold, and include both anthropogenic and natural forcings, as well as unforced variability within the climate system itself. Since 1850, the largest climate forcings are those associated with the increasing concentrations of greenhouse gases (CO_2, CH_4, N_2O, CFCs) and industrial sulphate aerosols in the Earth's atmosphere. Changing ozone concentrations and land use patterns may contribute additional climate forcing, as may natural processes associated with solar variability and volcanic eruptions. As Figure 2 illustrates, knowledge of the amplitudes of climate forcings during the last 150 years, other than by greenhouse gases, is very uncertain. Also uncertain is the temporal profile of the forcings, examples of which are shown in Figure 3.

The extent of surface temperature change ΔT (°C) accruing from climate forcing ΔF (Wm^{-2}) depends on the sensitivity κ (°C per Wm^{-2}) of the climate system to each specific forcing. Climate sensitivity is estimated to be in the range 0.3 to 1°C per Wm^{-2}. When multiple forcings are present, $\Delta T = \sum \kappa_i \Delta F_i$ where κ_i for an individual forcing depends on the amplitude, spatial and altitudinal distribution and temporal history of that forcing. Assuming that climate responds similarly to various forcings, Figures 2 and 3 suggest that during the past century surface cooling by increasing industrial aerosols in the troposphere may have canceled a significant fraction of the warming expected from greenhouse gases. Likewise, cooling by CFC-induced decreases in stratospheric ozone counters part of the warming attributed to increases in tropospheric ozone. Canceling of anthropogenic climate forcings by each other may mean that variance exists in the climate change record from natural forcing by solar variability and volcanic aerosols, even though their forcing amplitudes are estimated to be less than that of greenhouse gases.

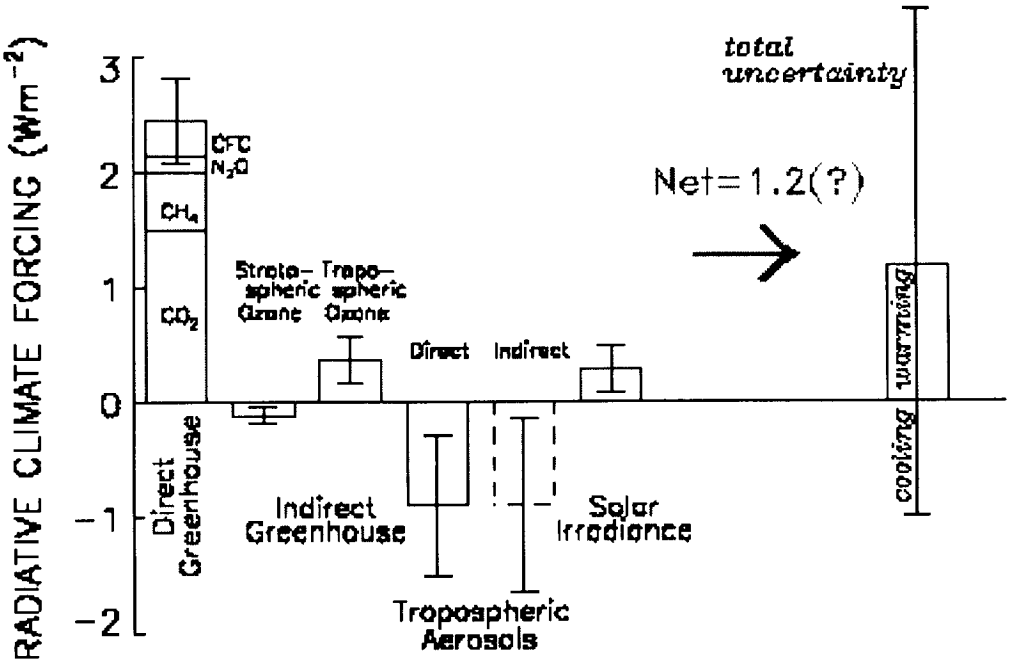

Figure 2: Global change forcing magnitude - IPCC95

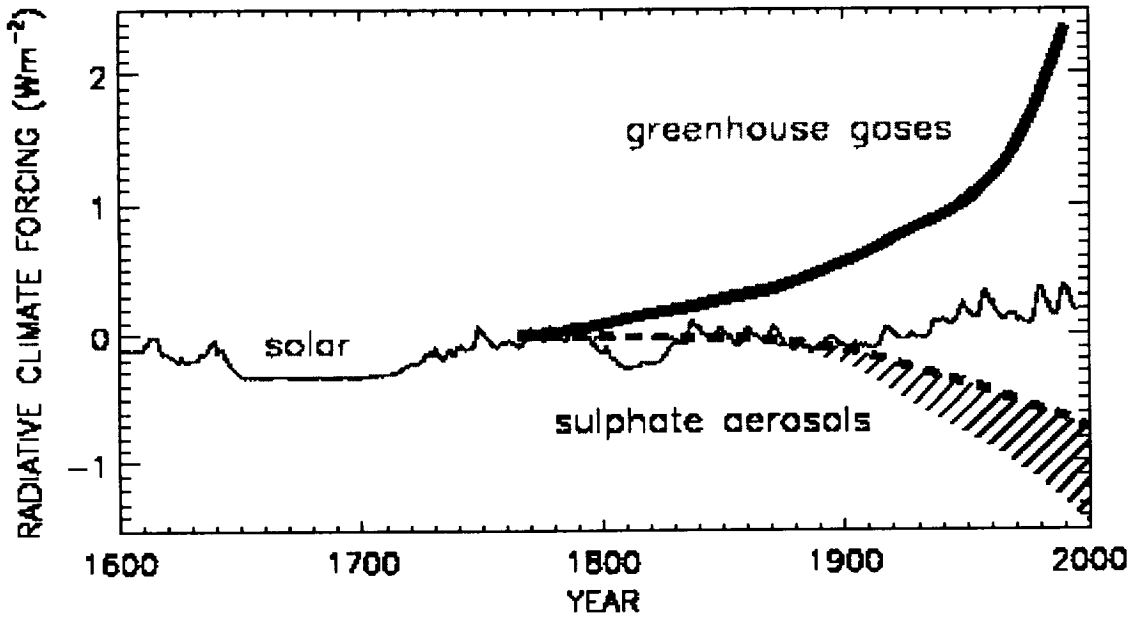

Figure 3: Comparison of solar vs. anthropogenic forcings on centennial time scales

Solar Activity and Radiative Climate Forcing

Solar Activity

The Sun has the potential to influence climate because the energy it provides to the Earth (primarily in the form of radiation) varies continuously. This variability occurs because the Sun, like other stars of comparable age, mass and evolution, is a magnetically active star. The most familiar evidence of the Sun's magnetic activity is the fluctuation in the number of small, compact dark features -- called sunspots – on its surface. Sunspots occur frequently during certain epochs (e.g., 1980 and 1990) but are much reduced at other times (e.g., 1986 and 1996). The approximate 11-year cycle in sunspot numbers, shown in Figure 4, is only one manifestation of solar magnetism. Accompanying the sunspot cycle are fluctuations in a wide range of other solar parameters, including the eruption of flares and coronal mass ejections, radiant energy from X-rays to radio fluxes, and particle energy outputs.

The Sun's activity cycle is constant neither in amplitude nor phase. In particular, the amplitudes of recent cycles of sunspot numbers are seen in Figure 4 to be some of the largest of the past 400 years. Solar activity is presently at a high overall level relative to the anomalously low levels from 1645 to 1715, when sunspots were absent entirely from the Sun's disk for years at a time. During this period of low solar activity, called the Maunder Minimum, levels of ^{14}C and ^{10}Be cosmogenic isotopes in, respectively, tree rings and ice cores are seen in Figure 4 to be elevated. Low solar activity weakens the magnetic coupling of the Sun and the Earth, permitting enhanced fluxes of galactic cosmic rays to enter the heliosphere where they produce isotopes of atmospheric gases. Contemporary solar activity is also at high overall levels in comparison with other stars of similar mass and age. This suggests that the overall level of solar activity is more likely to decrease, rather than increase, in the future.

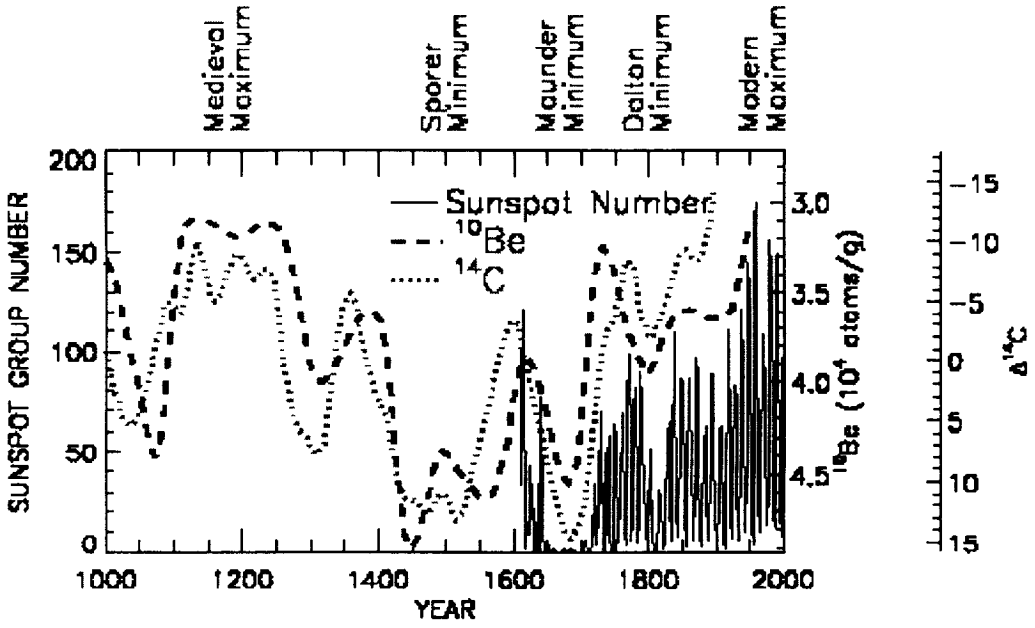

Figure 4: Sunspot numbers and cosmogenic isotopes

ObServed Solar Radiative Forcing

The Sun's radiation varies in concert with the 11-year "sunspot" activity cycle. Solar irradiance increases when solar activity is high, relative to times of solar minima. Evident in the composite space based record of the total (i.e., spectrally integrated) solar irradiance, shown in Figure 5, is an increase of ~0.1% during activity maxima in 1980 and 1990 relative to the 1986 and 1996 minima. This total irradiance change of 1.3 Wm^{-2} at the top of the Earth's atmosphere equals an equilibrium radiative climate forcing change of 0.22 Wm^{-2}. Prior to the space era, however, the Sun's total irradiance was thought to be invariant -- and termed the solar "constant" -- because a century of ground based monitoring had failed to detect its true variability.

Fluctuations in the spectrum of solar radiation, shown in Figure 6, have yet to be defined observationally at most wavelengths. The exception is in the UV spectrum where changes of 1.1% and 0.25%, respectively, in the 200-300 nm and 300-400 nm wavelength bands are estimated to contribute 13% and 18% (a total of 31%) of solar cycle total irradiance variations. Radiation in the visible and near infrared spectrum (400 to 1000 nm) is estimated to vary in the range 0.07% to 0.11%, which is comparable to the variability of total irradiance.

The epoch of direct measurements of solar irradiance from space is too short, by far, to permit unambiguous detection of solar forcing changes on climatically relevant multi-decadal and centennial time scales. Inaccuracies and sensitivity drifts in the solar radiometers preclude reliable detection of multi-decadal scale irradiance fluctuations in the space-based observations, which cover less than two 11-year cycles. Depending on the interpretation of solar versus instrumental components in the extant data records, long term irradiance fluctuations may be negligible over the decade from 1986 to 1996, or as much as 0.04%. That models of irradiance variability predict similar irradiance levels during the 1986 and 1996 minima suggests that claims of a 0.04% change may be spurious. The variability models, developed from magnetic features in the solar atmosphere -- dark sunspots and bright faculae and plages -- account for 88% of the variance in the composite total irradiance record in Figure 5.

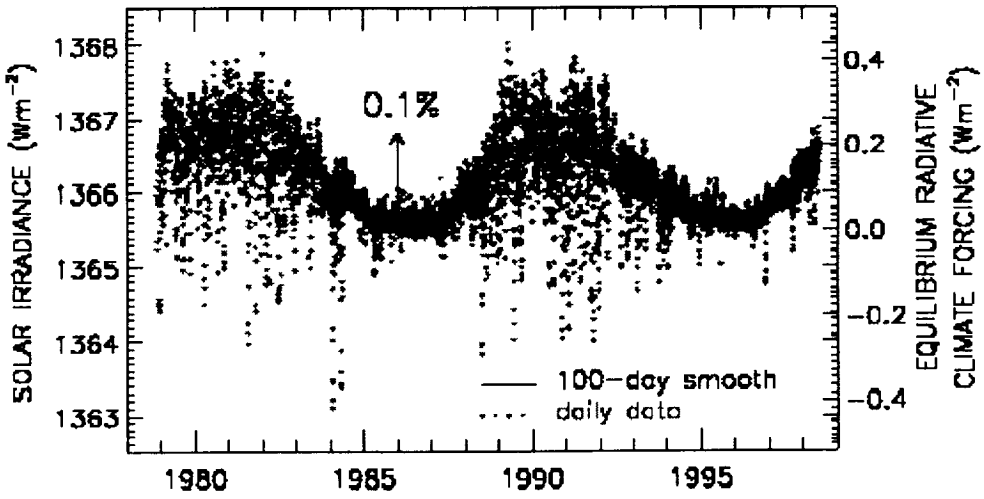

Figure 5: Solar irradiance observations - composite, with radiative forcing

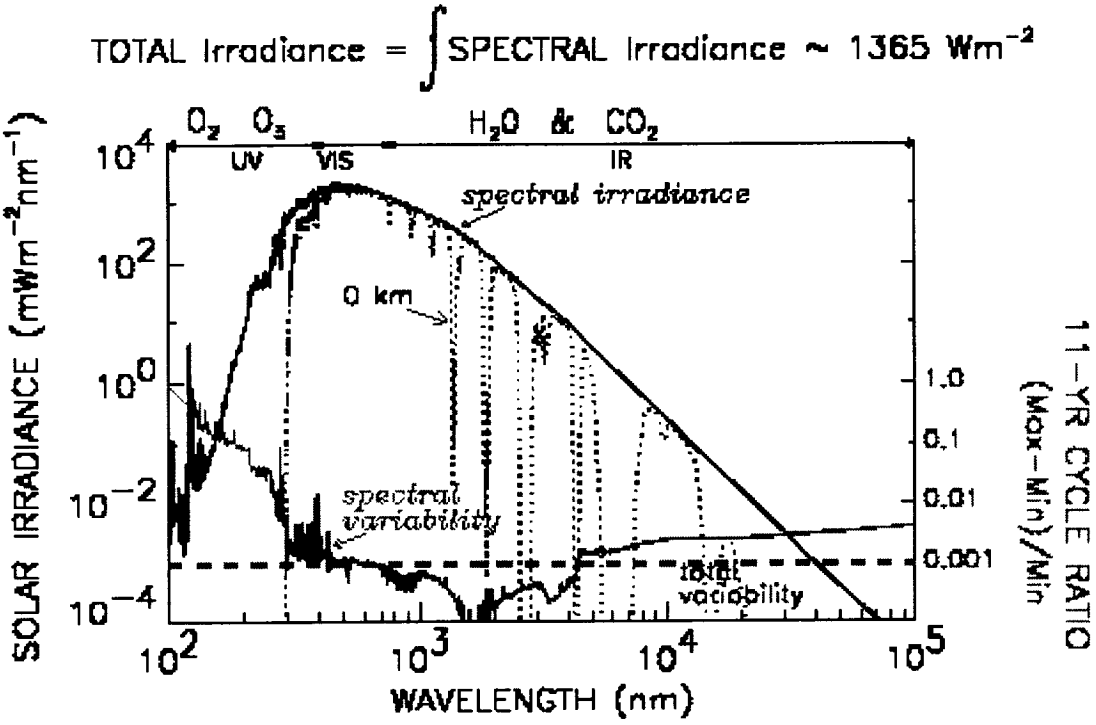

Figure 6: Solar spectrum and variability

Speculated Historical Solar Radiative Forcing

In lieu of direct space-based solar observations, historical data such as sunspots, geomagnetism and cosmogenic isotopes that pertain to various aspects of solar magnetism are utilized to infer the extent of long term solar irradiance variability. Relating these activity proxies to observed solar irradiance variability, and within the broader context afforded by monitoring of Sun-like stars, yields long term solar irradiance reconstructions such as depicted in Figure 7. Although explicit physical connections between solar irradiance and activity proxies have yet to be adequately deduced over longer time scales, the empirical historical reconstructions suggest that solar irradiance was reduced in the mid 1600s relative to the present period, analogous to the reduced overall flux levels present in non-cycling stars (like the Maunder Minimum Sun?) relative to their cycling counterparts (the Modern Sun?). Estimates of the total irradiance decrease are uncertain, and range from 0.2 to 0.5%. The temporal footprint of solar forcing change over this 350 year period is also uncertain because solar activity proxies exhibit somewhat different temporal fluctuations. For example, using the length of the 11-year sunspot cycle as an irradiance proxy predicts solar forcing fluctuations that are at times out of phase by as much as 20 years with a proxy based on sunspot cycle amplitude, as comparison of two different total irradiance reconstructions in Figure 7 shows. The present lack of understanding of the mechanisms for long term solar irradiance variability inhibits improved definition of historical solar forcing changes.

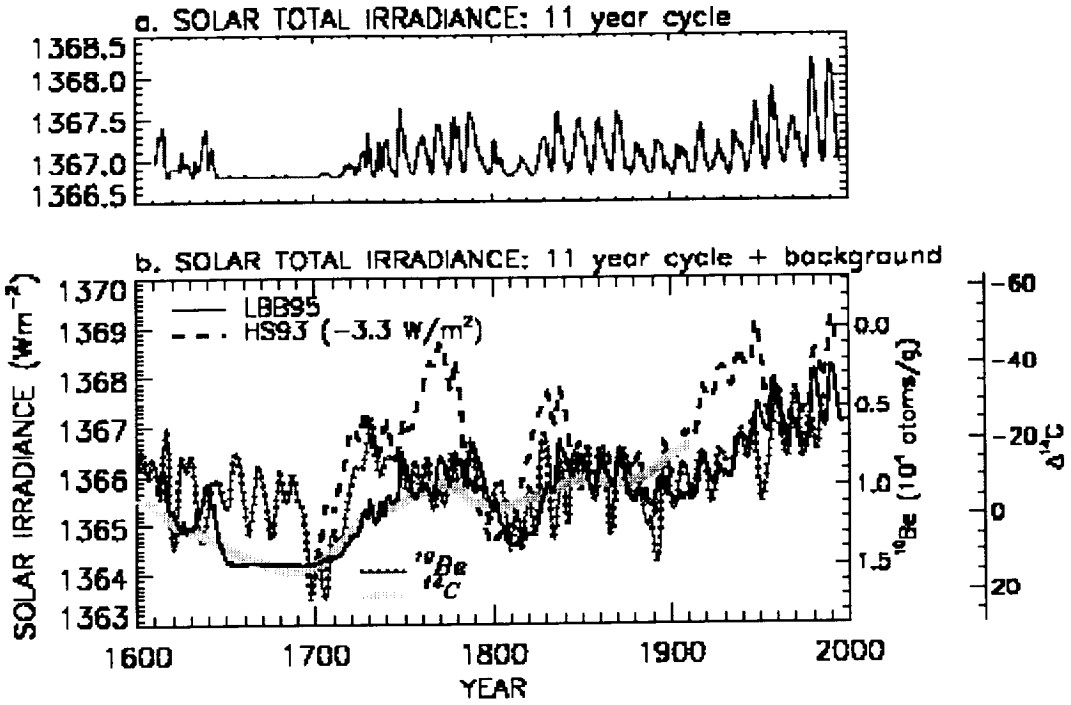

Figure 7: Long term solar variability- 11-year cycle and longer term

Empirical Sun-Climate Connections

Numerous empirical and statistical similarities exist between historical solar and climate data, on time scales that include 11-, 22-, 80- and 200- years, and longer. Land and ocean surface temperatures, US drought, rainfall, forest fires, cyclones, cloud cover, tropospheric temperatures, ice-core $\delta^{18}O$ and dust layer thickness, and tropical corals all exhibit various of these cycles during some portion of the recent past. Centennial changes in both the instrumental and proxy climate records have been correlated with long term solar activity changes during the recent Holocene. Many reported Sun-climate similarities occur in local geographical regions but, importantly, connections encompass global and NH surface temperatures as well.

The most recent of the centennial Sun-climate associations is the parallel increase in surface temperatures since the Little Ice Age with the increase in solar activity since the Maunder Minimum. From the mid seventeenth century to the present, Earth's surface temperature increased in the range of 0.6 to 1°C, coincident with a solar irradiance increase estimated to be in the range of 0.2 to 0.5%. This apparent Sun-climate connection exists separately in each of the three different ocean basins. However, the empirical relationship that connects common solar and climate variations in the pre industrial era differs from that in the twentieth century. From 1650 to 1790, Figure 8 shows a northern hemisphere surface temperature increase of $\Delta T=0.3^{o}C$, corresponding to $\Delta F_{sun}=0.35$ Wm^{-2}. Since 1850, however, $\Delta T=0.6^{o}C$ and $\Delta F_{sun}=0.38$ Wm^{-2}. Although the overall twentieth century

increase in both surface warming and solar activity has lead to claims that solar forcing can, alone, explain recent climate change, the pre-industrial Sun-climate relationship of 0.85°C per Wm^{-2} constrains this to only about half of the industrial warming. As Figure 8 depicts, a plausible interpretation of climate change in the past four hundred years includes a notable solar influence from 1600 to 1800, a period of cool temperatures as a result of significant volcanic activity in the nineteen century, followed by twentieth century warming attributable in part to solar activity, but primarily to anthropogenic influences, especially during the past three decades. From1976 to 1996, annual mean surface temperatures are seen in Figure 9 to increase 0.2 °C even though the levels of solar irradiance were similar in 1976 and 1996, according to the space-based record of total solar irradiance in Figure 5, whose annual means are shown in Figure 9.

While the overall climate warming from1976 to 1996 is apparently not the result of solar variability (based on the comparisons in Figure 9), adjusting the surface temperatures for volcanic cooling in 1982 and 1992, does reveal a decadal signal that may be solar-related. More generally, climate parameters frequently exhibit decadal variability. An example, in Figure 10, is the association of a decadal mode of surface temperature with solar activity during the three strong11-year cycles since the 1950s. The peak-to-peak amplitude of the decadal climate component is roughly ~0.1 °C, in phase with an 11-year solar cycle radiative forcing of ~0.2 Wm^{-2}. Like the centennial scale variability, this decadal climate change is present not only globally but separately in each of the three different ocean basins, and is detected, as well, from independent wavelet analysis of the surface temperature record.

The extent of climate change that is actually attributable to solar forcing remains uncertain in part because the common solar and climate cycles are typically neither stationary, nor deterministic, nor evident in all climate parameters at all times, nor always global, nor phase locked with each other. This lack of rigorous statistical associations leads climate researchers to often reject empirical evidence for solar effects on climate. Yet climate cycles in general (including the now ubiquitous ENSO), are neither stationary nor phase stable nor even linearly related to the assumed forcings, whatever their origins. The abundance of solar related cycles and correlations in numerous climate records cautions against premature dismissal of this large body of empirical evidence as coincidental instead of a real Sun climate connection, and motivates better specification of the possible physical processes.

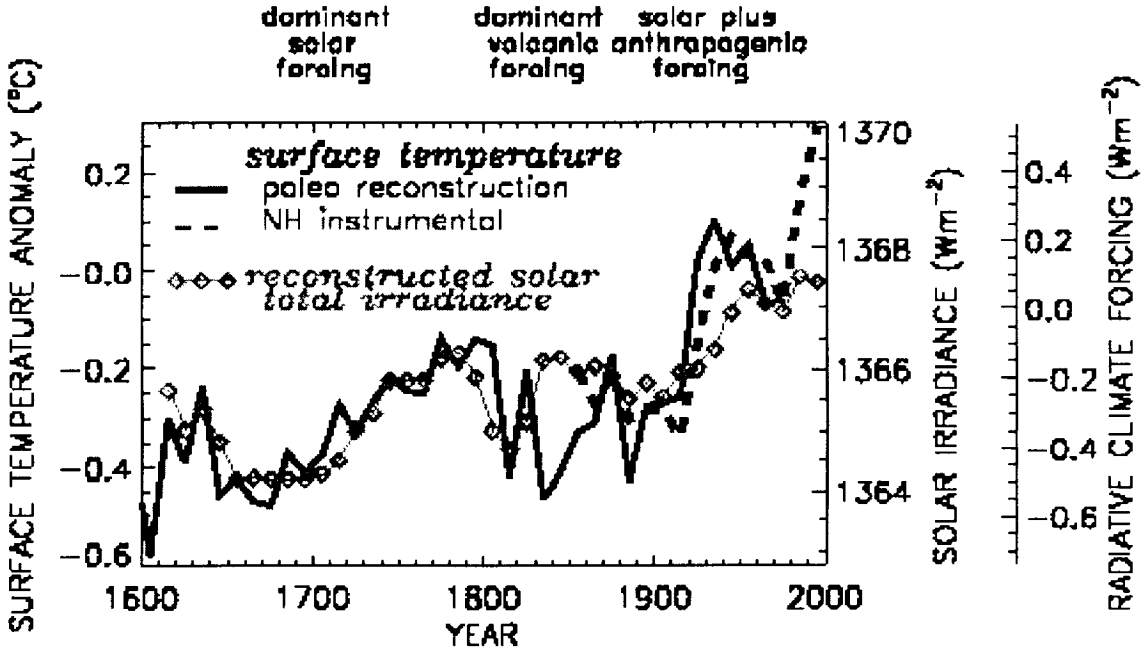

Figure 8: Sun-climate correlation since 1600

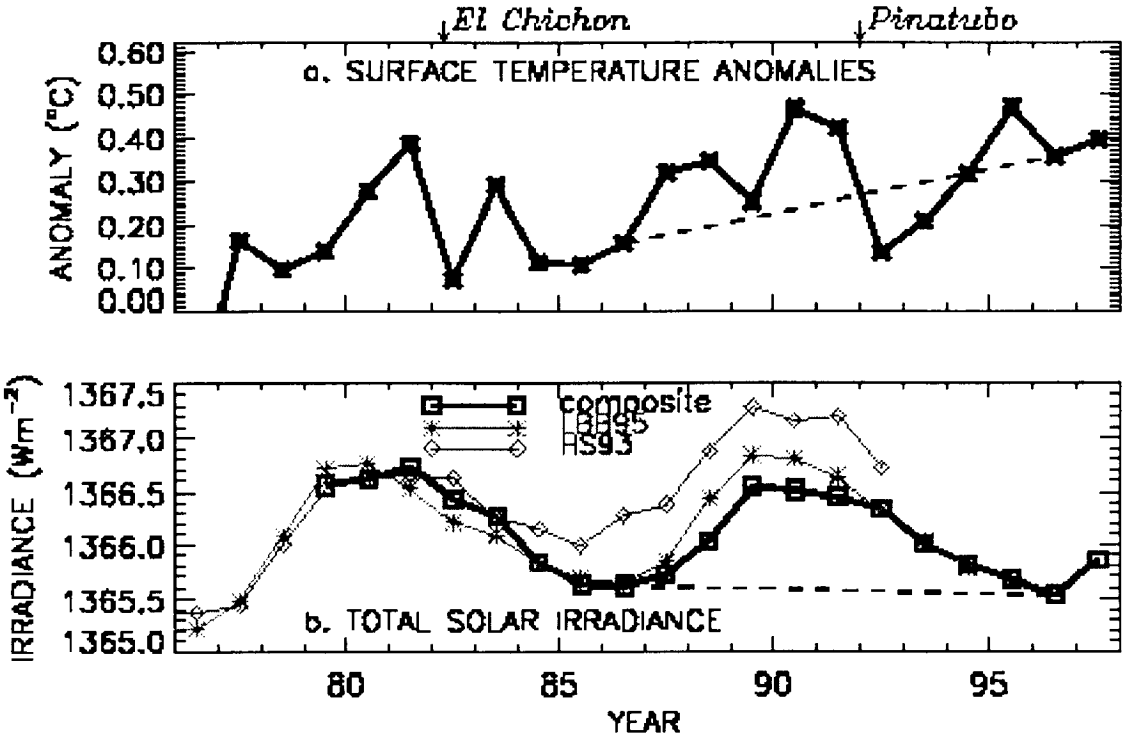

Figure 9: Solar irradiance and surface temps since 1976

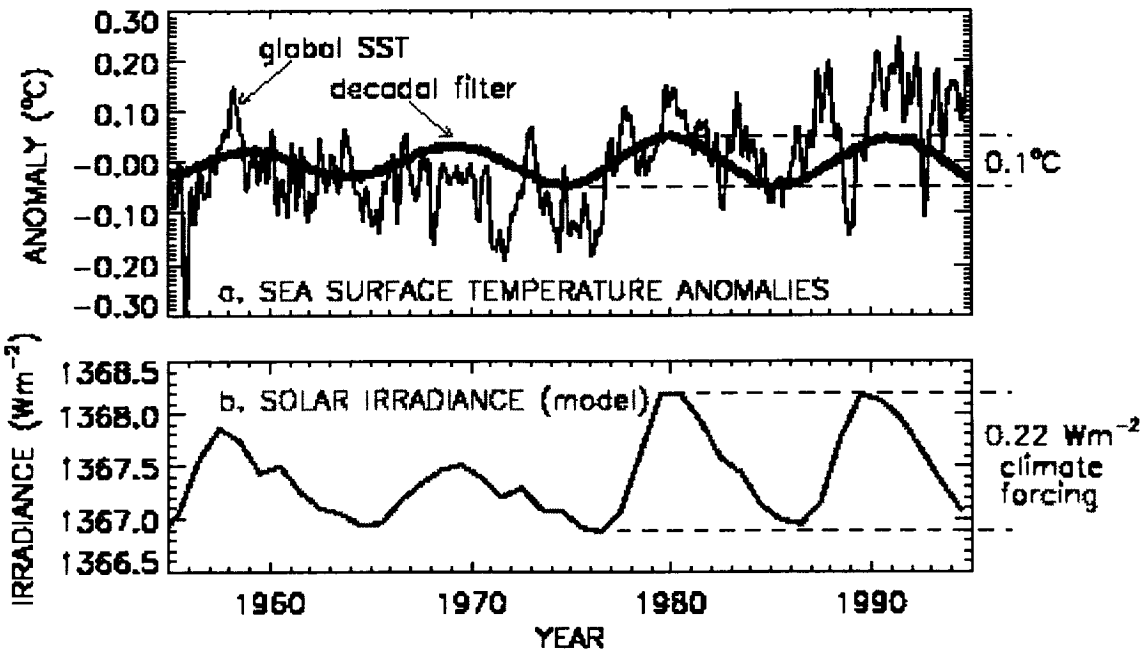

Figure 10: SST vs. solar irradiance

Simulated Climate Response to Solar Radiative Forcing

Predicting the climate system's response to natural and anthropogenic forcings such as those in Figure 2 requires simulations by models of physical processes that involve water vapor, sea ice and clouds. The models range in complexity from simple energy balance models to coupled atmosphere ocean general circulation models (AO-GCM), that have varying degrees of spatial and altitudinal resolution.

Time dependent simulations with the Goddard Institute for Space Studies (GISS) atmospheric GCM, shown in Figure 11, predict a global surface warming of ~0.45°C in response to an adopted 0.25% increase in the Sun's total irradiance since the Maunder Minimum (as indicated in Figure 7). The GISS model has 9 vertical atmospheric layers, 8°x10° horizontal resolution, and a mixed layer ocean of variable depth with heat transport by specified "Q" fluxes. Its sensitivity is in the range 0.8 to 1°C per Wm^{-2}, as a result of known climate feedbacks, whose response to solar irradiance forcing are shown in Figure 12. Feedbacks by water vapor, cloud cover and sea-ice/snow achieve their full equilibrium response on centennial time scales, and account for a total of 65% (respectively, 35%, 20% and 10%) of the 0.45°C surface warming simulated in response to solar radiative forcing since 1650. The average of four model simulations shown in Figure 11 supports the inferences from the pre-industrial empirical relationship in Figure 8 that solar variability potentially accounts for most of the surface temperature changes in the pre-industrial epoch from 1600-1800, about half of the warming from 1850 to 1970, but very little of the warming since then.

On decadal time scales climate model feedbacks are unable to achieve their full equilibrium response, in part because of the large thermal inertia of the oceans. As a result, the GCM surface temperature simulations do not show a clear response to solar forcing during the 11-year solar cycle, and they cannot replicate the empirical relationships between decadal solar and global ocean surface temperature fluctuations evident in Figure 10. One explanation for this disagreement is that an internal oscillation within the ocean-atmosphere system, rather than solar forcing, is the source of decadal climate variability. Another explanation may lie in the inability of present climate models to simulate rapid climate response to solar variability because of a lack of processes that amplify internal decadal oscillations by forcing of a similar period.

Climate models thus far have simulated only those processes that respond to direct forcing by changes in the bulk radiation of the Sun, without proper spectral differentiation of the variability. The models also lack interactive pathways through which solar variability may influence climate indirectly, such as by changing the middle atmosphere and ozone concentrations, and by modulation of energetic particles in the atmosphere. Solar cycle changes of a few percent occur in the total ozone column and significant 11-year cycles occur in upper troposphere and lower stratosphere temperatures and pressures. In modifying the heating and dynamics of the atmosphere, these solar-induced changes affect the propagation of planetary waves. The ozone changes, shown in Figure 13, may impact climate by modifying radiative forcing of the troposphere, changing the input energy and affecting the strength of the Hadley cell circulation. The extend of the indirect solar-induced climate change depends strongly on the altitudinal profile of the ozone changes which are as yet poorly specified. Simulations with middle atmosphere models have identified plausible pathways for this indirect climate effect of solar UV modulation of the atmosphere, although sensitivities in the models are smaller than the observational relationships infer.

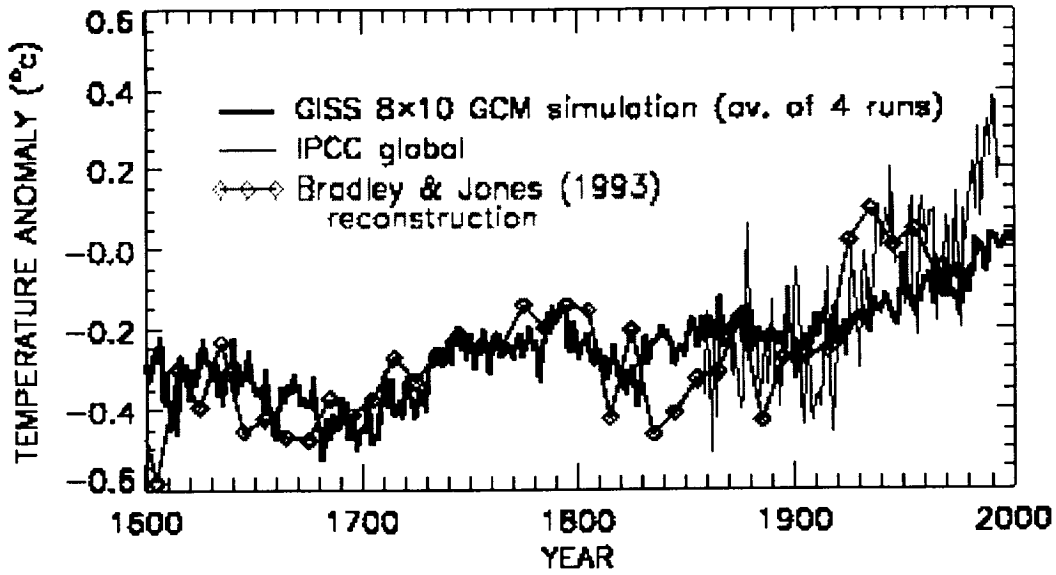

Figure 11: GCM response - average of 4. with power spectra (but not solar forcing)

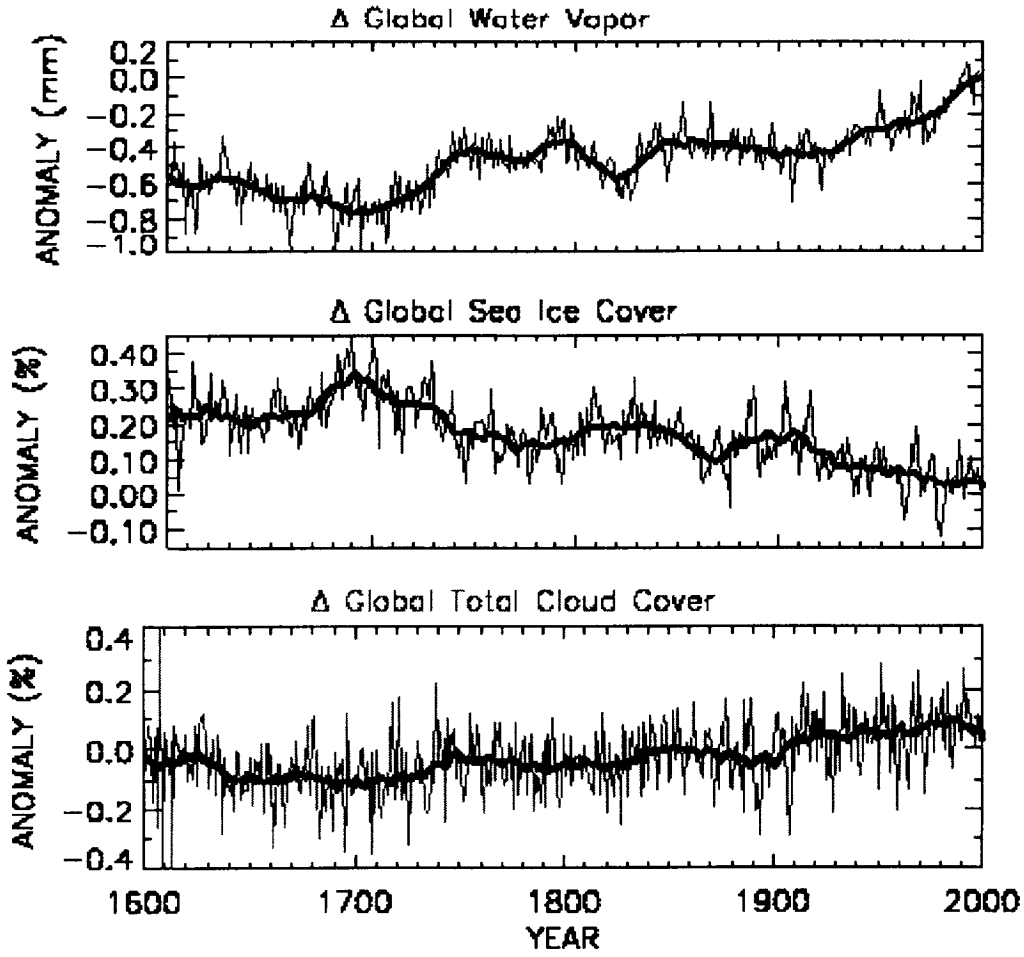

Figure 12: GCM simulated feedback time series

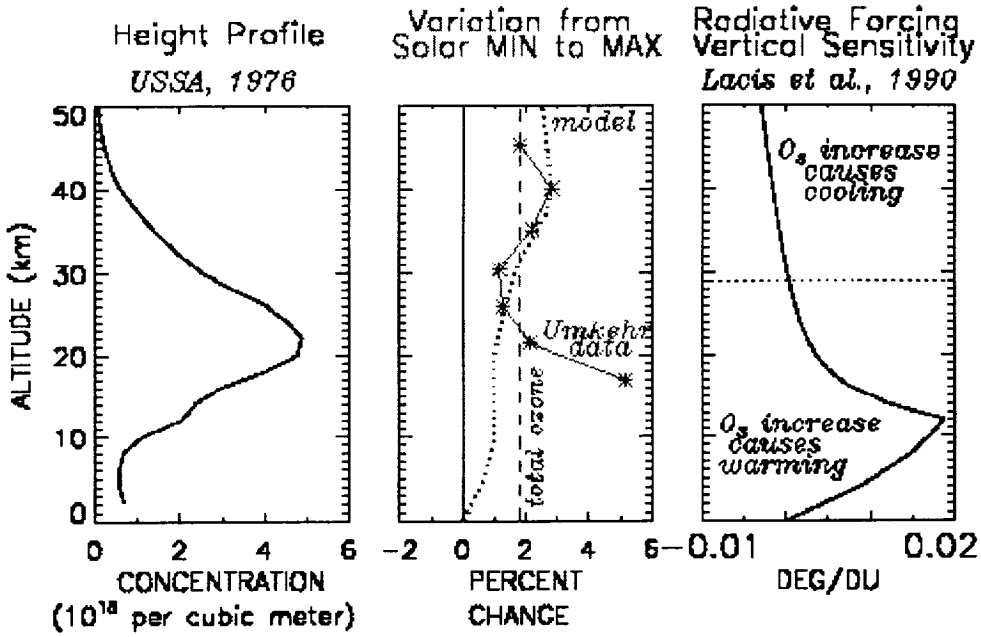

Figure 13: Ozone solar cycle

Climate Change Attribution?

Increasing greenhouse gas concentration is considered the most likely physical mechanism of surface warming during the past century because its climate forcing exceeds significantly that by any other individual process since 1850. But with this mechanism, alone, climate change attribution scenarios are irreconcilable in the pre- and post industrial epochs. Table 1 summarizes values of climate change, climate forcings and climate sensitivity that illustrate this, and that provide a simple basis for examining alternative scenarios that are consistent in these two epochs of quite different climate forcings.

The assumption in Case 1 of Table 1 that greenhouse gas forcing of 2.4 Wm^{-2} since 1850 is solely responsible for the observed 0.6°C warming implies a climate sensitivity of κ=0.25°C per Wm^{-2}, which is lower than the generally accepted range of 0.3 to 1°C per Wm^{-2}. Furthermore, were greenhouse gas forcing (of 0.13 Wm^{-2}) the only cause of the 0.3°C warming from 1650 to 1790 then the deduced pre-industrial climate sensitivity of κ=2.3°C per Wm^{-2} is inconsistent by a factor of ten with contemporary climate sensitivity. Allowing, in Case 2 of Table 1, for additional pre-industrial solar forcing of 0.35 Wm^{-2} from 1650 to 1790, together with greenhouse gas forcing, accounts for the 0.3°C warming with a more acceptable climate sensitivity of 0.6°C per Wm^{-2}. But with this climate sensitivity, greenhouse gas and solar forcing together produce far more warming since 1850 than the observed 0.6°C increase. Adopting, in Case 3, κ=0.7°C per Wm^{-2} as a reasonable estimate of climate sensitivity requires an additional cooling of 1.9 Wm^{-2} from 1850 to 1990, and of 0.05 Wm^{-2} from 1650 to 1790.

Surface cooling by industrial aerosols is indeed widely invoked as countering more than half of the warming expected from the greenhouse gas concentration increases since 1850. The detailed physical mechanisms, whether from direct or indirect aerosol forcing, are poorly known, but estimated to be in the range of 1 to 2 Wm^{-2} (see Figure 2). This is consistent with the forcing derived indirectly from the simplistic accounting in Table 1. Volcanism during the seventeenth century exceeded that during the twentieth century, and may have caused some cooling, of order 0.05 Wm^{-2}, required for consistency of the pre- and post industrial epochs in the case study in Table 1.

A plausible explanation for climate change in the past four hundred years is thus a combination of the natural processes that can account for pre-industrial climate change combined with anthropogenic influences that have become increasingly significant since 1850, and dominant in the past two decades.

	Epoch	Pre-industrial 1650-1790	Industrial 1850-1990
	ΔT	0.3°C	0.6°C
Case 1: Greenhouse gas forcing	ΔF_{GHG} $\kappa_{GHG} = \Delta T/\Delta F_{GHG}$	0.13 Wm^{-2} 2.3°C per Wm^{-2}	2.4 Wm^{-2} 0.25°C per Wm^{-2}
Case 2: Greenhouse gas and solar forcing	$\Delta F_{GHG}+\Delta F_{SUN}$ $\kappa_{GHG+SUN} = \Delta T/\Delta F_{GHG+SUN}$	0.13+0.35 Wm^{-2} 0.6°C per Wm^{-2}	2.4+0.38 Wm^{-2} 0.2°C per Wm^{-2}
Case 3: Greenhouse gas, solar and aerosol forcing	$\Delta F_{GHG}+\Delta F_{SUN}+\Delta_{Cooling}$ $\kappa_{ADOPTED}$	0.13+0.35-0.05 Wm^{-2} 0.7°C per Wm^{-2}	2.4+0.38-1.9 Wm^{-2} 0.7°C per Wm^{-2}

Table 1: Surface temperature changes, concurrent climate forcings and climate sensitivity estimates are listed during the pre-industrial epoch from 1650 to 1790, and in the industrial period from 1850 to 1990. The requirement for mutually consistent interpretations in these two epochs helps constrain the attribution of recent climate change.

Summary and Future Research

Changes in the Sun's radiation, clearly evident in 20 years of space based solar monitoring, are a plausible mechanism of climate change. Model simulations indicate that a Sun-climate connection can account for a significant fraction (0.45°C) of global surface warming since 1650 by adopting magnitudes of solar forcing (0.25%), climate sensitivity (0.8°C per Wm^{-2}) and surface temperature changes (0.7°C) that are all compatible with present understanding of these values. But the attribution of about 0.25°C of the observed 0.6°C surface temperature increases since 1900 to direct solar radiative forcing requires that other forcings of order 2 Wm^{-2} -- such as by direct and indirect aerosol cooling and albedo changes, for example -- be invoked to offset the warming by greenhouse gases.

Because the duration of space-based solar monitoring is only two decades, it is not yet known whether long term changes actually occur in solar forcing, such as the speculated increase since the seventeenth century. Detecting such changes, if they exist, is a future challenge requiring long term solar monitoring with exceedingly high radiometric precision and stability, by, for example, the programs identified in Figure 14. Since the processes by which solar forcing impacts terrestrial global change are highly wavelength dependent, equally challenging will be the determination of solar spectrum variability, which is essentially unknown because of the lack of monitoring at all but the shortest UV wavelengths.

Not known at all, yet, is the mutual impact of the various forcings on the ability of the climate to respond to each -- so that, for example, might solar forcing in the pre-industrial epoch have impacted climate differently than in the present era of large greenhouse gas and aerosol concentrations? Also lacking is adequate specification of indirect solar forcings via UV modulation of ozone and the middle atmosphere and by modulation of energetic particles in the atmosphere that affect cloud formation processes. Pathways that facilitate indirect solar UV radiative impacts on climate are known but sensitivities in existing models are smaller than empirical evidence suggests. In the third case, both the physical pathways and the sensitivities need better specification.

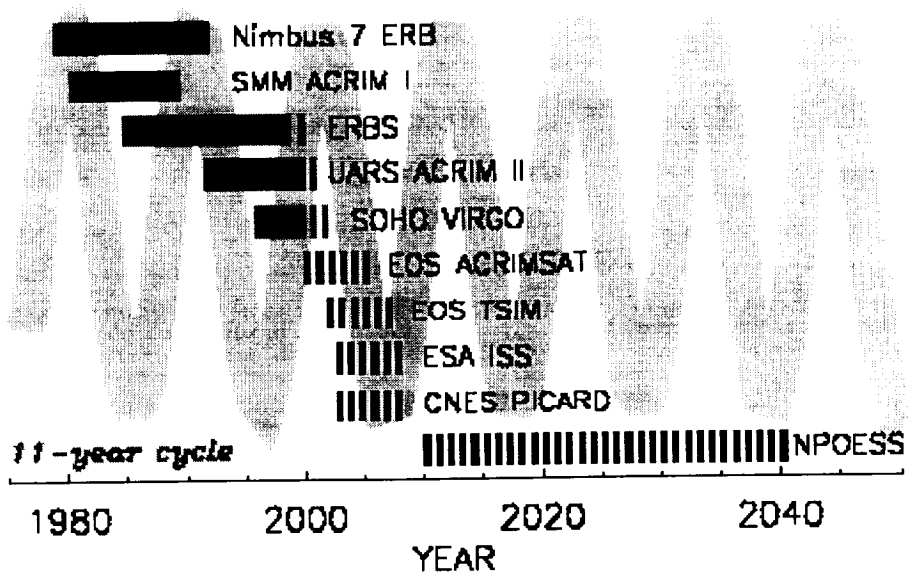

Figure 14: Future missions

Related Publications

Climate Change 1994. Radiative Forcing of Climate Change and An Evaluation of the IPCC IS92 Emission Scenarios, Intergovernmental Panel on Climate Change (IPCC), 1995, J.T. Houghton et al., Eds., Cambridge University Press.

The Sun's Variable Radiation and its Relevance for Earth, J. Lean, 1997, Annual Review of Astronomy and Astrophysics, 35, 33-67.

Climate Forcing by Changing Solar Radiation, J. Lean and D. Rind, 1998, Journal of Climate, 11, 3069-3094.

Evaluating Sun-Climate Relationships Since the Little Ice Age, J. Lean and D. Rind, 1999, Journal of Atmospheric and Terrestrial Physics, 61, 25-36.

Simulated Time-dependent Climate Response to Solar Radiative Forcing Since 1600, D. Rind, J. Lean and R. Healy, 1999, Journal of Geophysical Research, 104, 1973-1990.

The Role of the Sun in Climate Change, D. V. Hoyt and K. H. Schatten, 1997, Oxford University Press.

Simulations of the Influence of Solar Radiation Variations on the Global Climate with an Ocean-Atmosphere General Circulation Model, U.Cubasch et al.,1997, Climate Dynamics, 13, 757-767.

SEASONAL TO INTERANNUAL CLIMATE VARIABILITY AND PREDICTABILITY

Jagadish Shukla

George Mason University (GMU)
Center for Ocean-Land -Atmosphere Studies (COLA)
(shukla@cola.iges.org)

Introduction

It is well known that day-to-day changes of detailed weather can not be predicted beyond a few weeks because of chaotic dynamics which can amplify even small initial errors due to incorrect observations used for defining the initial state of the atmosphere, or imperfect governing equations used for making predictions. However it is now well established that although detailed day-to-day weather cannot be predicted, seasonal mean circulation and rainfall anomalies can be predicted through the influence of the boundary conditions at the Earth's surface (sea surface temperature (SST), soil wetness, snow etc.), if these boundary conditions can be predicted in advance. The causes of seasonal and interannual variability of the atmospheric circulation and rainfall can be explained by the following three mechanisms: internal dynamics of atmosphere, ocean-land interaction and ocean-atmosphere interaction. Although the three processes operate together, and the observed seasonal and interannual variability is a consequence of interactions among them, for conceptual simplicity, it is possible to design numerical experiments to determine what fraction of variability is caused by each of the three processes. Large number of such experiments have carried out during the past 25 years. Based on a very large number of observational and modeling studies, it is now well established that changes in the boundary conditions of SST, soil wetness, snow cover, etc. can produce large and systematic changes in atmospheric circulation.

This is particularly true for the tropical region where flow patterns are so strongly forced by SST that there is almost no sensitivity to changes in the initial conditions. This is a unique and fundamental property of the tropical atmosphere. Likewise the tropical oceans have a unique property that tropical sea surface temperature is almost completely determined by the overlying atmospheric forcing. A combination of these unique properties of atmosphere and ocean make it possible to predict tropical SST variations, and therefore, tropical circulation and rainfall at seasonal to interannual time scales. More recently it has also been found that if tropical SST changes are quite large, even the extratropical circulation over certain regions can be predicted at seasonal to interannual time seales.

In addition to major advances in our understanding of the predictability of seasonal to interannual variations, there is also an in-situ and space observing system which allows a near real time description of the three dimensional structures of the tropical Pacific ocean. Measurements of sea level, SST and surface wind from satellites combined with subsurface measurements from an array of moored buoys makes it possible to define dynamically consistent initial conditions for integration of coupled models.

In this paper we present two major results: 1. We show that the tropical atmosphere (and ocean) has unique property of showing no sensitivity to changes in the initial conditions (exception to chaos). 2. We show that by combining a hierarchy of models, it is possible to predict regional climate anomalies at seasonal to interannual time scales. We present a case study for January through March average conditions over North America region. First tropical Pacific sea surface temperature (SST) is predicted by coupled ocean-atmosphere model which is used to statistically specify global SST. The predicted SST is used to force a global atmospheric model. A high resolution limited area model (ETA model) for which lateral boundary conditions are prescribed from the output of the global atmospheric model is used to calculate regional climate anomalies over North America.

Results

In this paper, we show 6-9 month forecasts of surface air temperature and precipitation in North America for a three month average conditions during January through March, 1998, using a two-tiered approach. In the first tier, a coupled ocean-atmosphere model is used to predict the tropical pacific SST anomaly several seasons in advance. A higher resolution global atmospheric general circulation model (AGCM) is used to predict the seasonal mean circulation anomalies several months in advance in the second tier.

We provide evidence that the two-tiered approach can be extended, using nested regional climate models, to produce accurate regional climate predictions. The models used in the two-tiered approach and nested regional climate simulation have significantly improved in recent years to a level that makes seasonal prediction feasible.

The tropical Pacific SST pattern was predicted for up to 9 months in advance using a coupled ocean-atmosphere model with available input data at the time of the forecast (June, July, August, 1997). Multiple realizations of the coupled model forecast were averaged to produce an ensemble mean SST forecast that was then statistically extended to predict the global SST anomaly. The latter was added to an observed climatology for global SST and used as a lower boundary condition for an ensemble of integrations of the global atmospheric model. Each of the global integrations was used to provide the lateral boundary conditions for a companion integration of a regional climate model. The ensembles of global and regional model predictions were made at least 6-9 months prior to the verification time of the forecasts.

The Tropical Pacific SST Forecast

The SST forecast produced by the coupled model and subsequent statistical projections shown in Figure 1, called for an unprecedented, anomalously warm surface temperature in the tropical eastern and central Pacific. The predicted warmer than normal water in the Pacific was located east of the dateline along the equator and extended about 5°-10° north and south of the equator. The peak SST value forecast by this model was about 3°C above normal.

Up to the time that the forecast was made, during the ENSO (El-Niño Southern Oscillation) warm event the model had been quite accurate in predicting the onset and rapid increase of the SST anomaly, although its prediction of the magnitude of the maximum anomaly was substantially smaller than observed. The JFM98 forecast made six months in advance was quite accurate in terms of amplitude, phase relative to the annual cycle and spatial pattern. The predicted maximum anomaly was west of the observed maximum and fell short of the observed amplitude by about 1°C. Compared to similar predictions and simulations made prior to this one, the forecast was considered to be quite accurate and generally deemed successful.

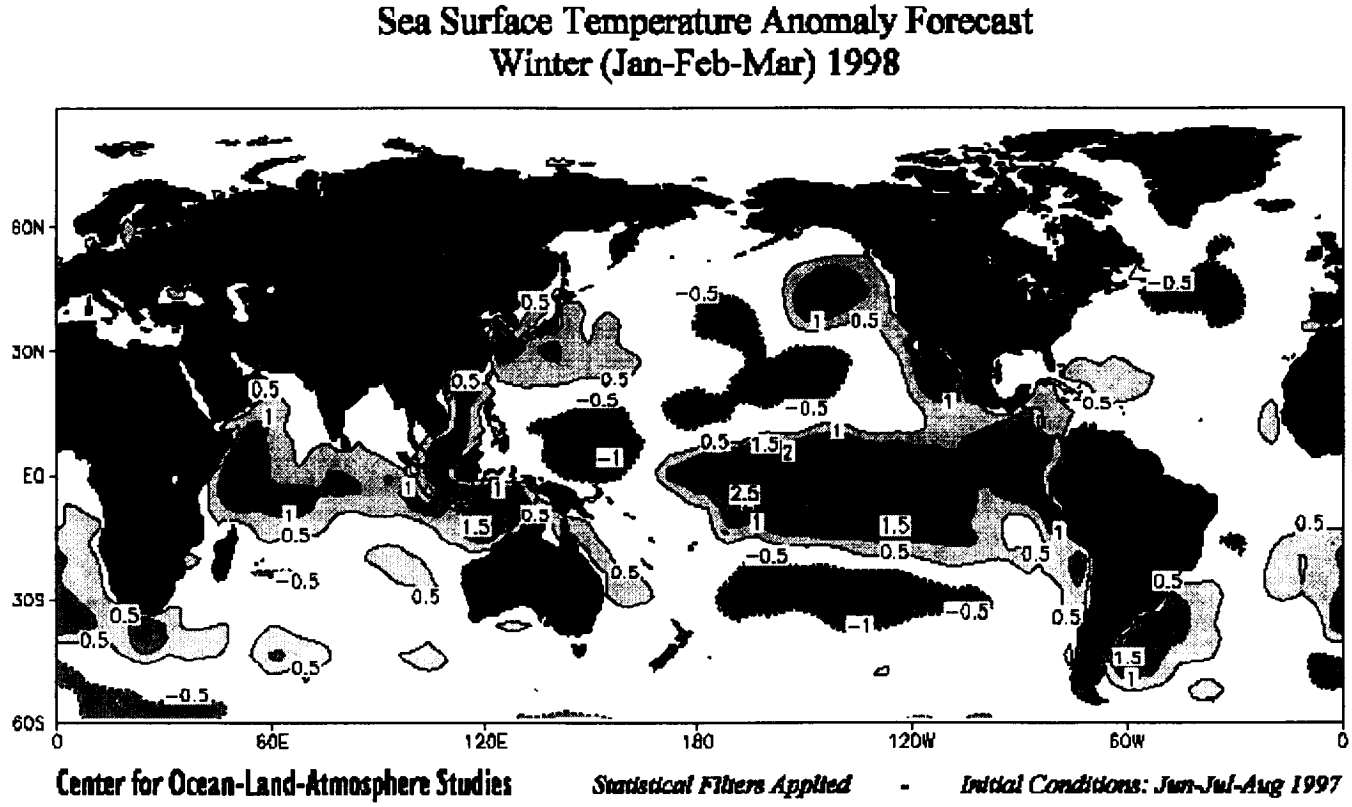

Figure 1: Forecast SSTA for January - March 1998 for the global (non-polar) oceans produced by the application of statistical projections to the tropical Pacific SSTA produced by the Tropical Pacific coupled model. The contour interval is 0.5°C with red shading for positive departures from normal and blue shading for negative departures.

The Surface Air Temperature over North America

The model-based SST forecast was applied as a lower boundary condition to the COLA atmospheric circulation model to produce an ensemble of nine forecasts. The ensemble members were generated by initializing the model with slightly different initial conditions to provide some measure of the uncertainty of the forecast. The model ensemble mean forecast for surface air temperature (Figure 2) had a generally warmer than normal winter

for most of northern North America. Positive departures form normal are shaded in red, and negative departures are shaded in blue. With the exception of the Atlantic coast, parts of the Gulf of Mexico coast, and the southern parts of the southwestern states of the U.S., the entire continental U.S. and most of Canada were forecast to have seasonal mean temperatures (January through March 1998) more than 1°C (2°F) above normal. The largest departures from normal in the U.S. were predicted to occur in the northern plains states (Minnesota, the Dakotas and Montana) with seasonal mean temperature more than 3°C (6°F) above normal. In Canada, anomalous temperatures more than 6°C (12°F) above normal were forecast for Manitoba and the Northwest Territories. For winters in central North America, the historical record of observations indicates that seasonal mean anomalies of more than 3°C occur less than 15% of the time, and 6°C above normal for entire season has been observed less 5% of the time, on average.

Precipitation over North America

Typically, predictions of precipitation are less reliable than temperature forecasts due to the fact that precipitation is more variable, has a smaller spatial correlation scale and is non-normally distributed. Nevertheless, the large-scale characteristics of precipitation anomalies are know to be correlated with those of other fields and some information may be obtained from predictions of seasonal mean precipitation. The seasonal mean predicted precipitation anomaly for January through March 1998 is shown in Figure 3. Positive departures form normal (more than usual precipitation) are shaded in green, and negative anomalies are shaded in yellow. The main features of the anomaly pattern are a swath of positive anomalies to the south and a band of negative anomalies to the north. The positive anomalies (more than 1 mm day^{-1} or 3.5 inches for the entire season above normal) extend form the Pacific northwest states of the U.S., through California and the southwest U.S. into Mexico, and along the Gulf of Mexico into the southeast U.S. The band of negative departures from normal extends from the Pacific coast of Canada through the norther plains of the Great Lakes states of the U.S. into the maritime provinces of Canada. The largest departures form normal are forecast for northern California and central Mexico, but a significant region of more than normal precipitation (1.5 mm day^{-1} or 5 inches above normal) extends through the southwest states (southern California, Arizona, New Mexico, and Texas) and the Gulf states (Louisiana, Mississippi, Alabama, Georgia, and Florida). Forecasts for Alaska and Hawaii (not shown) are near normal and below normal precipitations respectively. The forecast for California, Mexico and the southwest U.S. precipitation amount was nearly unprecedented compared to the historical record of observations, occurring less than 1% of the time or once per century.

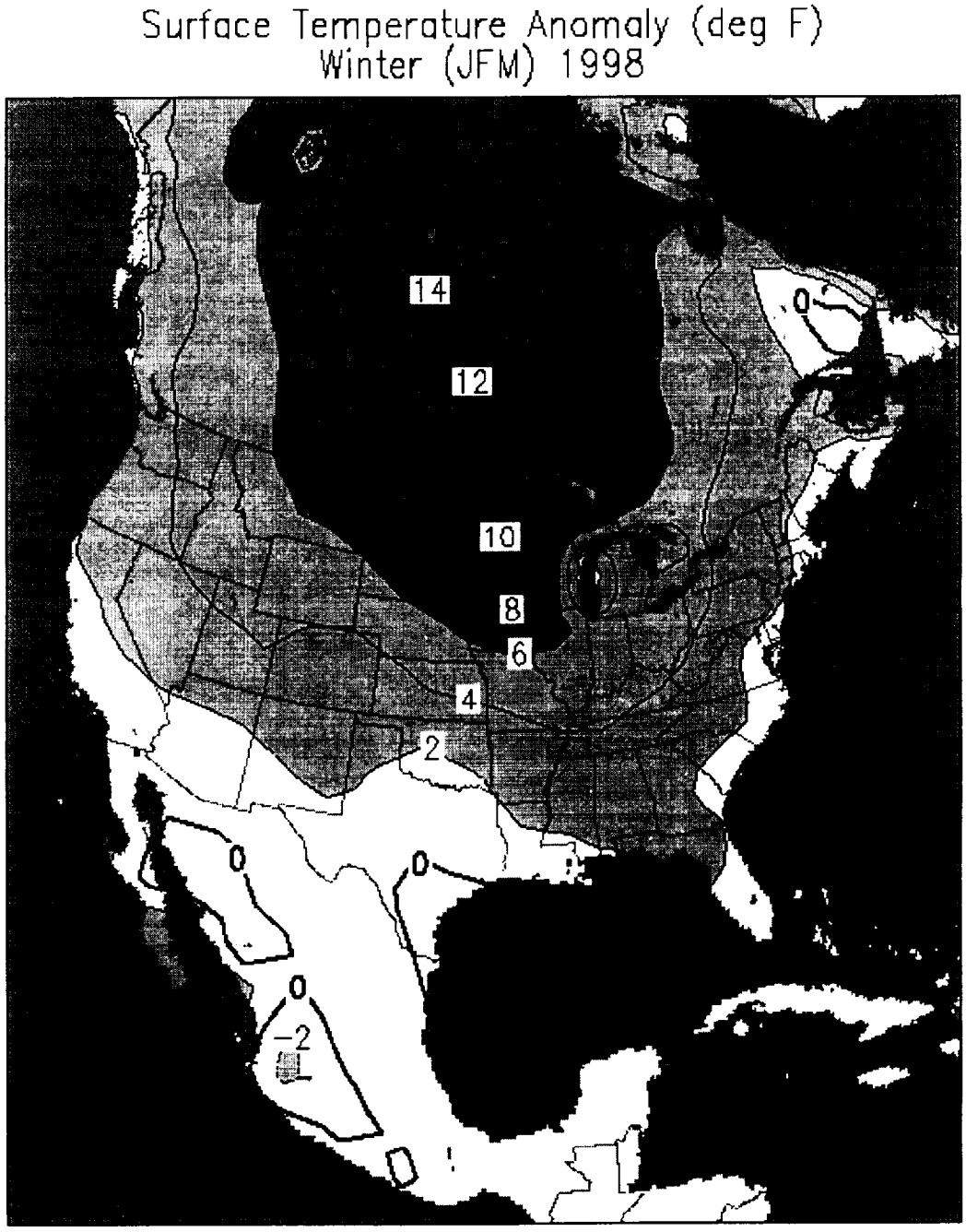

Figure 2: Forecast surface air temperature anomaly for January - March 1998 produced by the COLA atmospheric general circulation model. (AGCM) The lower boundary condition applied at oceanic gridpoints was the SST obtained by adding the SSTA shown Figure 1 to the observed climatological mean SST. The ensemble mean of nine forecasts with slightly perturbed initial conditions (based on atmospheric observations for mid-December) is shown. The anomaly is defined relative to the COLA AGCM climatological mean. The contour interval is 1°C with red shading for positive departures from normal and blue shading for negative departures.

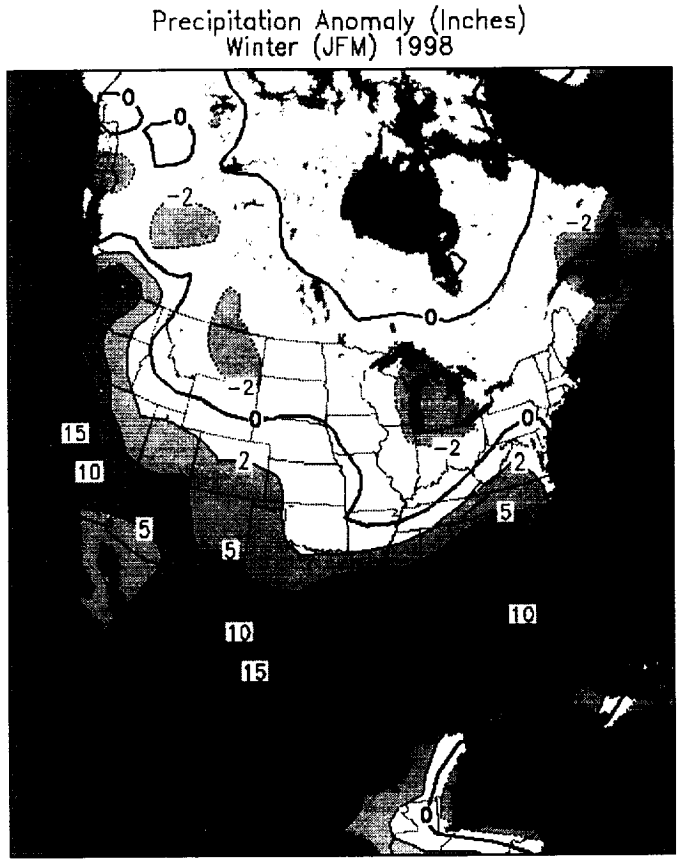

Figure 3: Forecast precipitation anomaly for January - March 1998 produced by the COLA atmospheric general circulation model. Contours are shown 0, q0.5, q1, q2, q3, q4, and q5 mm/day with green shading for positive departures from normal and yellow shading for negative departures.Regional Rainfall Forecasts

Figure 4 shows nine maps each showing the regional model prediction of continental U.S. precipitation for each of the members of the ensemble in the JFM98 case. It can be seen that in certain regions there is uncertainty in predicting the regional rainfall. It is therefore necessary to generate large ensembles so that a reliable probabilistic forecast can be produced. Figure 5 shows the observed seasonal mean (JFM98) precipitation over the continental U.S. Three boxes are shown on the map indicating where regional analysis was performed. Figure 6 shows the daily total rainfall for the southwest (SW) box as observed and as predicted by global and nested regional models for each day in JFM98. The regional model forecast is on top, and the global model forecast is on the bottom. The observed are in the middle for comparison. The figure demonstrates the advantage that the regional model has for simulating the storminess in that region. The nested regional model correctly captures the number and intensity of rain events.

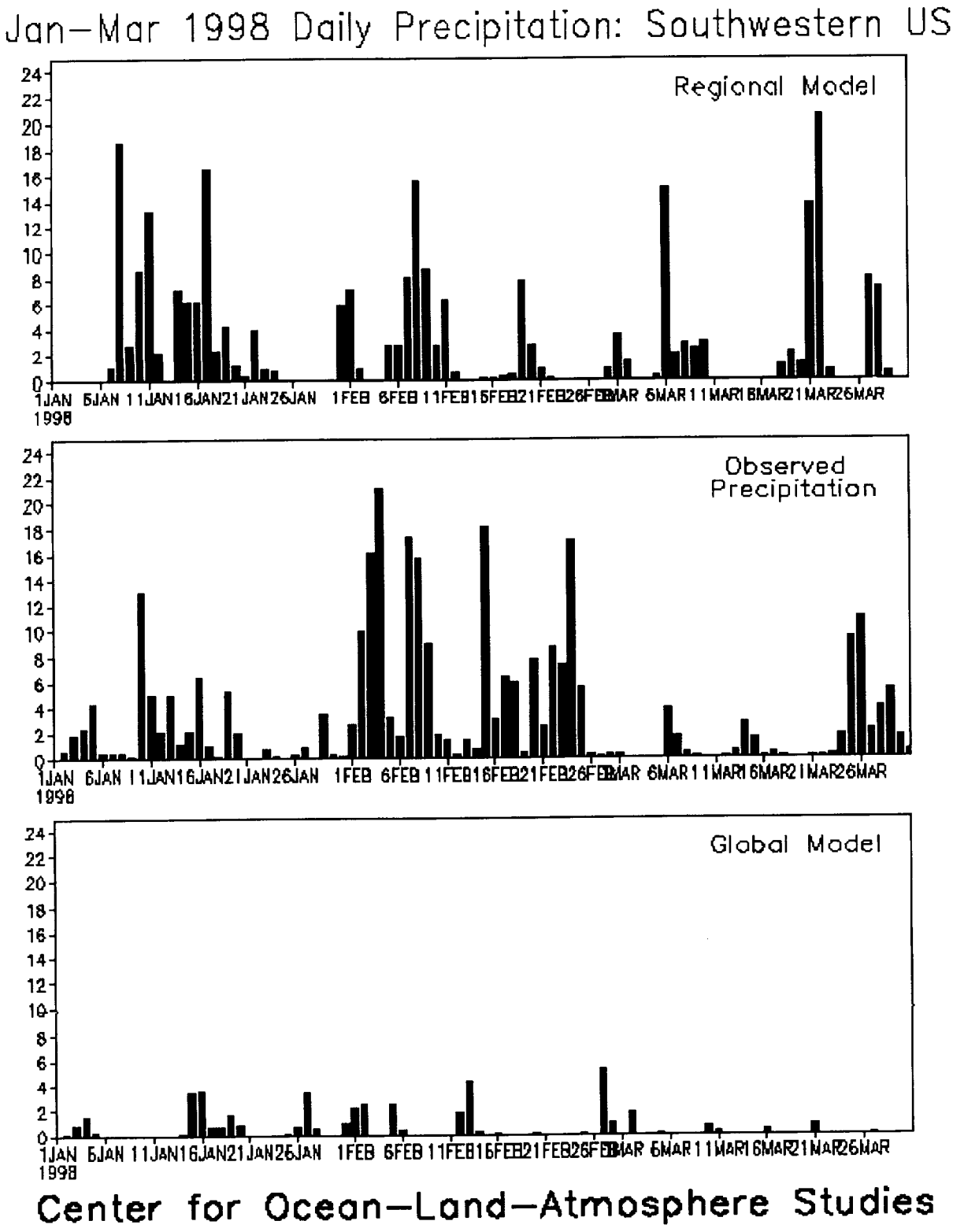

Figure 4: Continental U.S. Precipitation predicted by regional model for nine members of ensemble for JFM98.

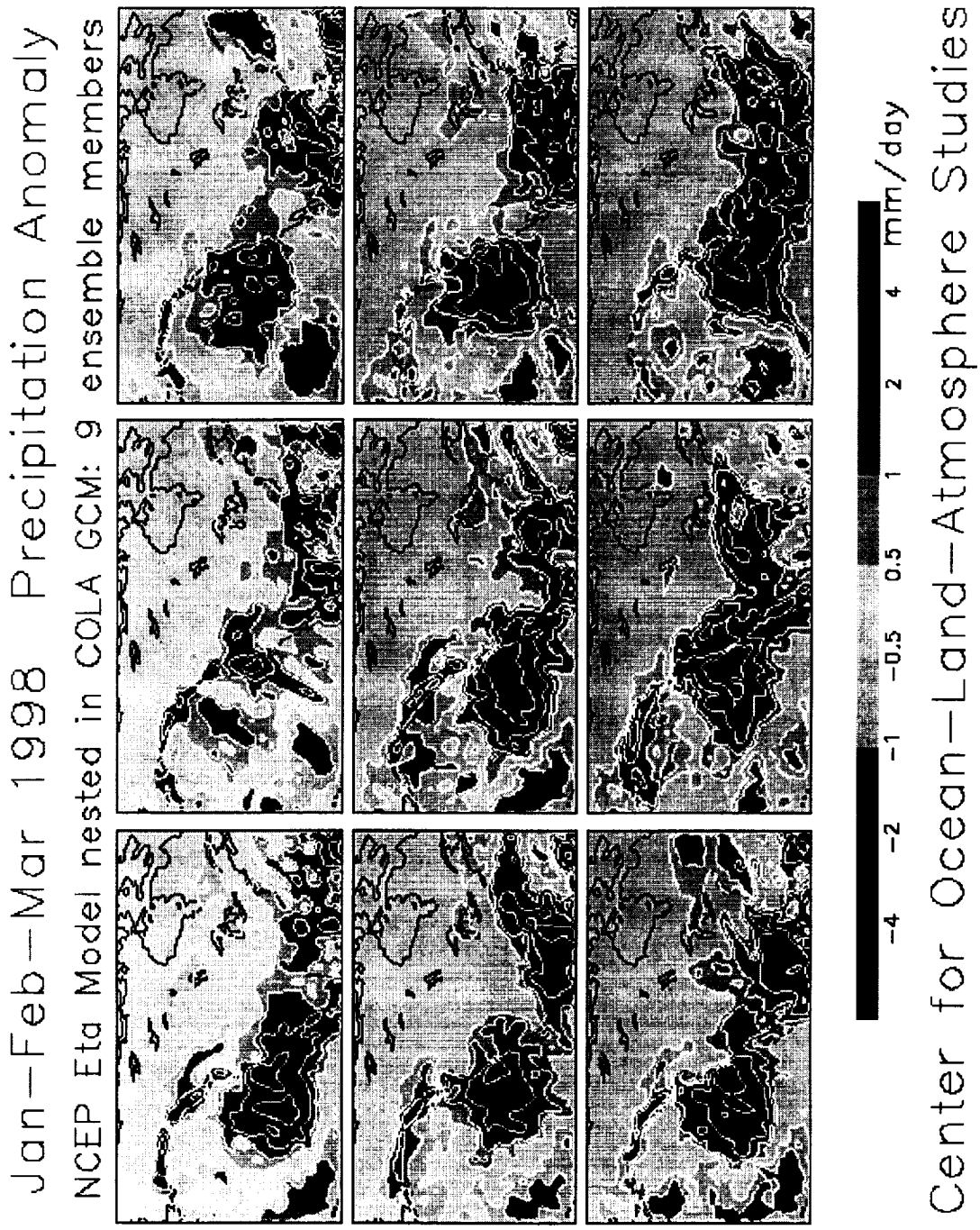

Figure 5: Observed seasonal mean (JFM98) precipitation (mm/day) over the continental US.

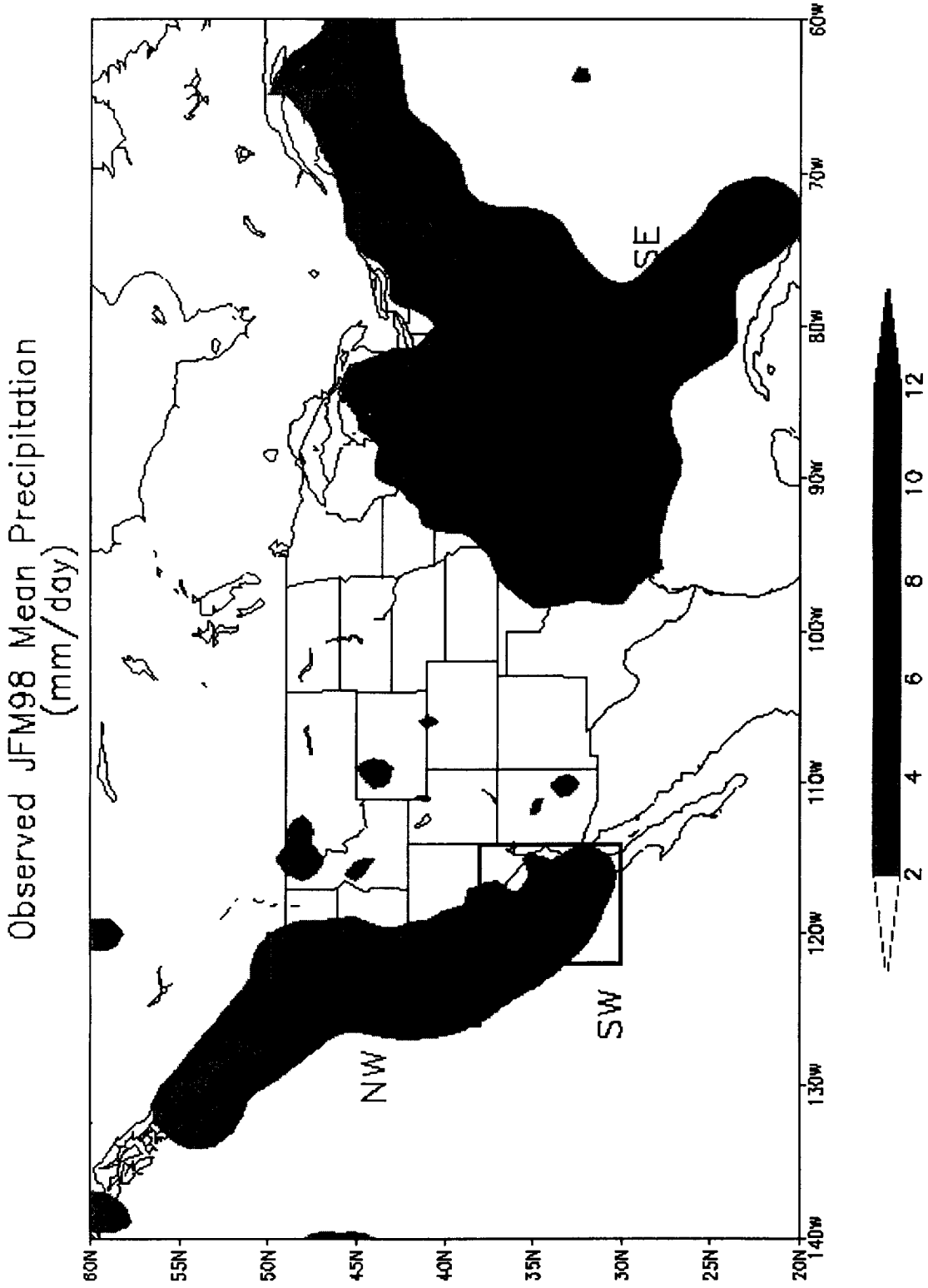

Figure 6: Daily total precipitation (mm/day) averaged for the box labeled SW in Fig. 4 for each day in JFM98 for the regional model forecast (top), observed (middle) and global model forecast (bottom).

It is difficult to say whether such accurate forecasts can be produced routinely. In this particular case the large scale flow pattern was predicted with remarkable degree of success six months in advance. Figure 7 shows three depictions of the 500 mb height anomaly-observed, predicted at six months lead and hindcast. The latter two were produced using exactly the same model and initial conditions, but the lower boundary conditions was the six-month lead SST forecast from the coupled model and the observed SST (hindcast). The forecast was very good, and the hindcast was even better, showing the potential for predicting the height anomaly had we predicted the SST perfectly.

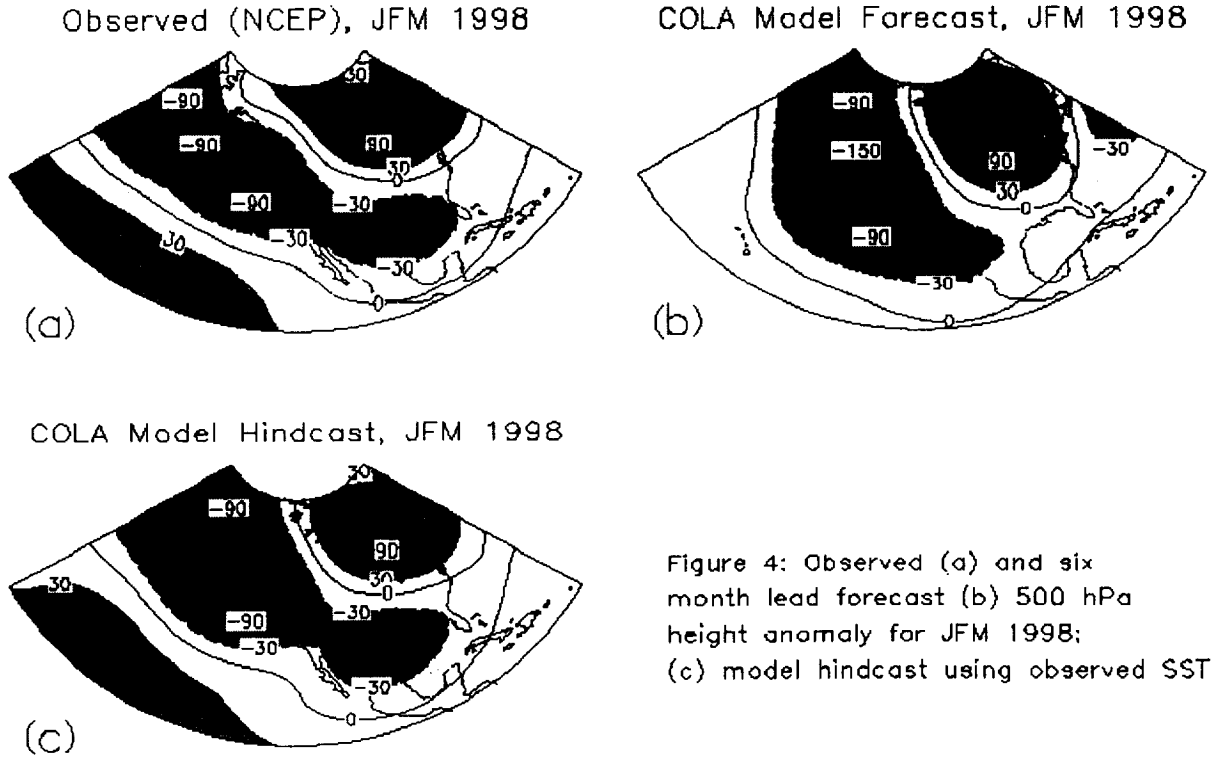

Figure 4: Observed (a) and six month lead forecast (b) 500 hPa height anomaly for JFM 1998; (c) model hindcast using observed SST

Figure 7: JFM98 mean 500 mb height anomaly: observed (top left); six month forecast (top right); hindcast (bottom).

Discussion of Uncertainty in Climate Forecasts

In discussion of any climate forecast produced by a numerical model, it must be stressed that there is a substantial element of uncertainty in any such product. The Earth's climate is highly variable, and the current stat of the science of climate variations indicates that only certain regions on the globe and only certain seasons of the year are appreciably predictable. One of the major advances of climate dynamics is the establishment of a scientific basis for the predictability of seasonal average climate anomalies. Therefore, while weather fluctuations are known to be predictable beyond about two weeks lead time, climate variations in the tropics and select regions outside the tropics are predictable on seasonal to interannual time scales. The extratropical climate is highly variable, and the

influence of tropical SST anomalies is responsible for only a portion of the observed variation. Recent research has shown, however, that, in the presence of large tropical SST anomalies, the seasonal climate over the Pacific-North American region is highly predictable. Despite elements of uncertainty, the numerical model can produce a forecast for each point on the globe for each moment in the future. It is a matter of current scientific inquiry to interpret the numerical model output in the context of climate uncertainty. In discussing the results of this study, we emphasize that the results are the products of a numerical model for which a detailed quantitative analysis of the uncertainty has yet to be made.

It should also be noted that the prediction methodology employed in this study involves two distinct numerical model products. The first step of the forecast procedure involves a coupled ocean-atmosphere model. The inclusion of observational information and the high degree of predictability of tropical Pacific SST provide a measure of confidence for the SST anomaly forecast. The final step of the forecast procedure (after the intervening steps that effectively project the output of the coupled model form tropical Pacific SST to global SST using statistical techniques based on historical observations) involves a model of the global atmosphere only. The final step assumes that the SST anomlay forecast produced in the first four steps is "perfect". We emphasize the differences between the first step and the final step, because it is important to keep in mind that forecasting tropical Pacific SST anomalies and forecasting the global effects of those anomalies are distinct. The two parts of the forecast procedure have different levels of uncertainty and, hence, different levels of reliability.

The memory required for predicting SST changes reside in the upper ocean. To exploit the theoretical predictability of the climate system for the benefit of society, it is essential that in-situ and global observations be combined to define the initial state of the global atmosphere and upper ocean. Both, the improved models and extensive global observations are required to produce useful climate forecasts.

EL NIÑO: MONITORING, PREDICTION, AND IMPACTS

Chester F. Ropelewski and Antonio D. Moura

International Research Institute for climate prediction
Lamont-Doherty Earth Observatory of Columbia University
chet@iri.ldeo.columbia.edu, amoura@iri.ldeo.columbia.edu

Introduction

Interannual variability over the most recent three to four years has provided an unprecedented opportunity for the climate community. The recent sequence of La Niña and El Niño episodes have allowed us to: a) reap the benefits of relatively new ocean observational systems, b) exercise a new generation of coupled ocean/atmosphere models for operational seasonal climate predictions and c) initiate development, testing and implementation of seasonal forecast applications tools. This paper briefly describes some of the related activities in these areas at the newly formed International Research Institute for climate prediction.

Monitoring

Over the past two decades significant improvements in real-time monitoring of the climate have been achieved through collaborative efforts of the international climate community. Among the most significant of the enhancements to observations was the initiation and implementation of the Tropical Atmosphere Ocean (TAO) Array of buoys for in situ measurements of the equatorial Pacific Ocean. These measurements have been invaluable for providing data for analysis and prediction of the Pacific Ocean surface temperature as well as the thermal substructure. Not only does the TAO array allow climate scientists to monitor the state of the equatorial Pacific but it also provides observational input for data assimilation systems of coupled numerical ocean/atmosphere models.

The success of the TAO array has led the Global Ocean Observing System (GOOS) to plan expansions of in situ monitoring into the other ocean basins. The initial deployment of several buoys as part of the PIRATA array in the equatorial Atlantic is a successful example of this expansion.

The value of the TAO measurements has been dramatically enhanced through their use in conjunction with a number of satellite observations. Among these are the NOAA AVHRR estimates of sea surface temperatures and the TOPEX/POSEIDON estimates of sea level, Figure 1. Sea level is proportional to the ocean heat content and a proxy for sea surface temperature, both key variables for monitoring the equatorial oceans. Thus the satellite measurements allow climate scientists access to independent, continuous, high-resolution measurements of the ocean with global coverage.

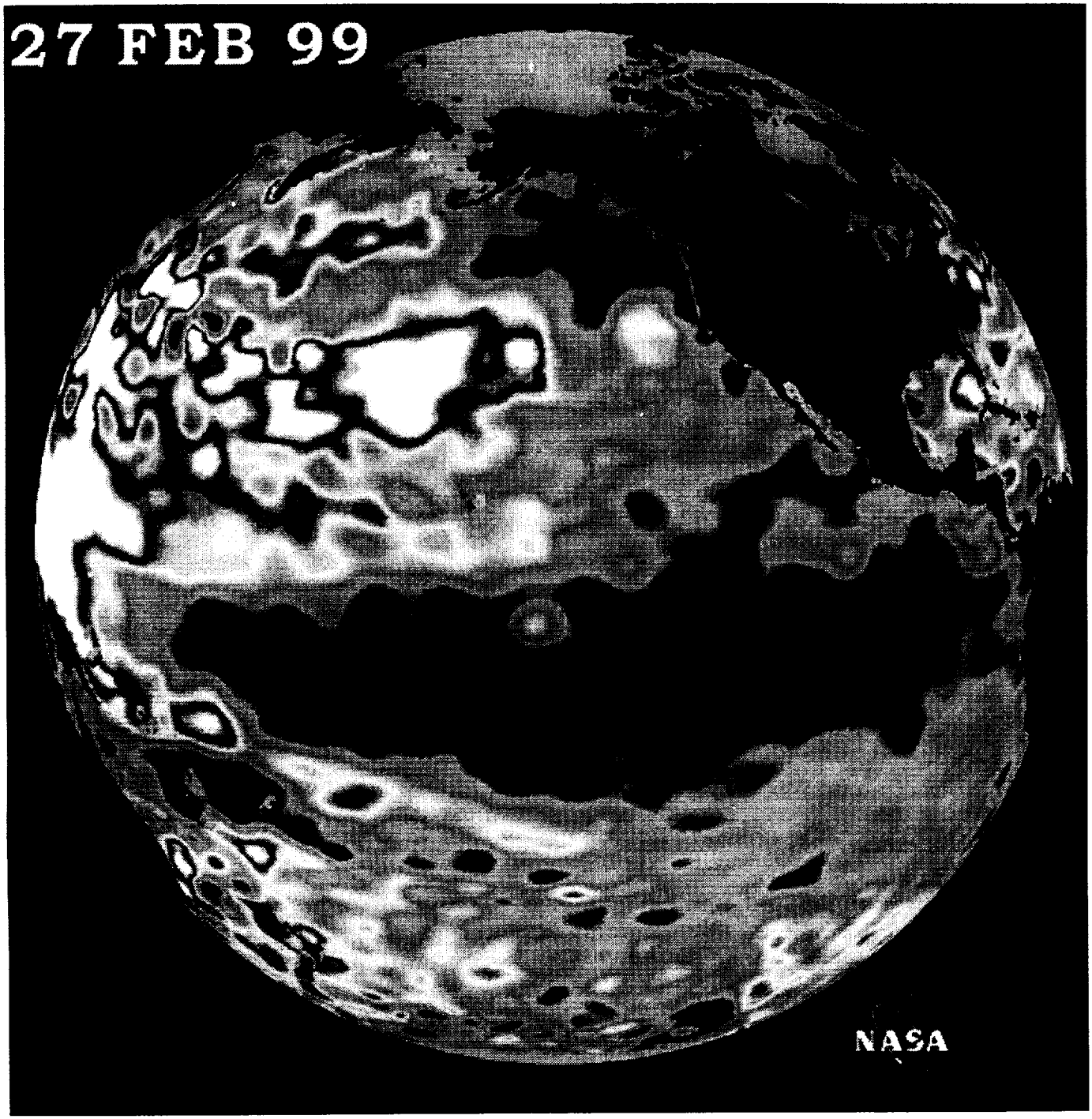

Figure 1: Sea surface height anomaly estimated by TOPEX/POSEIDON. Negative (positive) height anomalies are in blue (red). Source: JPL/NASA

The El Niño/Southern Oscillation (ENSO) has been extremely active since the early 1980's. In particular, an alternating sequence of La Niña and El Niño conditions starting in 1996 has been accompanied by an extraordinary sequence of rainfall and temperature extremes over many regions of the globe. Much of the ENSO-related activity has been described in detail elsewhere. Below, we briefly summarize the evolution of the ENSO episodes over this remarkable period.

After a nearly continuous period of El Niño episodes and El Niño-like conditions for the first half of the 1990's La Niña conditions appeared late in 1995. La Niña conditions had peaked in 1996 and climate forecasters were already turning their attention to the possibility yet another El Niño episode forming in 1997. By early in the year (1997) most models and empirical forecasts were indicating the inception and evolution of a major El Niño episode. The forecasts were realized with the appearance of extremely strong El Niño conditions that dominated the global climate throughout 1997 in into early 1998. This "El Niño of the century" grew to surpass the great 1982/83 El Niño in magnitude and then gave way to moderate La Niña, cold episode conditions, by mid-1998. The sequence of events starting in early 1996 is well documented by the alternating cold (La Niña) sea surface temperature and warm (El Niño) sea surface temperature in the equatorial Pacific, Figure 2.

For the most part the rainfall and surface temperature patterns followed those expected during warm and cold episodes e.g., Figure 3. In particular, a series of extremely wet and dry years in the far western Pacific, including Indonesia, were mirrored by a series of extremely dry and wet years from just east of the dateline eastward across the Pacific. These rainfall extremes were associated with a number of significant disruptions to the economy and well being of several Pacific nations.

Prediction

The highly active period of ENSO variability starting in the mid-1990s has provided a challenging test bed for the developing coupled ocean-atmosphere numerical models. For the first time, these models were being exercised for real-time climate prediction. Much to their credit this generation of models did very well in forecasting the continued evolution of equatorial Pacific sea surface temperatures. Numerical forecasts of seasonal patterns of temperature and precipitation anomalies based on predicted sea surface temperature, while far from perfect, also provided useful climate information to a wide range of users.

Not all of the rainfall and temperature anomaly patterns typically experienced during ENSO warm episodes occurred with the 1997/98 ENSO. In particular, the 1997 monsoon seasons in Australia and India averaged near the long term mean rainfall amount despite fears that this strong El Niño would bring disastrous droughts as they did in Australia during the 1982/1983 warm episode.

On the other hand some of the ENSO signals were much stronger than had been expected. Eastern equatorial Africa, Kenya, southern Somalia, the Ethiopian Highlands and northeastern Tanzania experienced extremely heavy rainfall in late 1997 into early 1998. While

excess rainfall is expected in much of eastern equatorial Africa area during El Niño years the rainfall during the episode exceeded previous records at several stations and was associated with widespread flooding.

One of the lessons learned for seasonal climate forecasting is that regional i.e., ocean basin-scale, sea surface temperature anomalies can have a strong influence on local and regional atmospheric circulation and rainfall patterns. One example of this was an area of strong positive sea surface temperature anomalies in the Indian Ocean. The strong Indian Ocean temperature anomalies are thought to have been partially responsible not only for the near average summer monsoon rainfall in India and Australia but also for the extremely heavy rainfall in eastern equatorial Africa. The IRI Net Assessment forecast for Africa for the October through December period 1997, Fig.4, captured most of the major rainfall anomalies, in part, because strong positive Indian Ocean temperature anomalies were included in the numerical model runs that formed the basis for the Net Assessment.

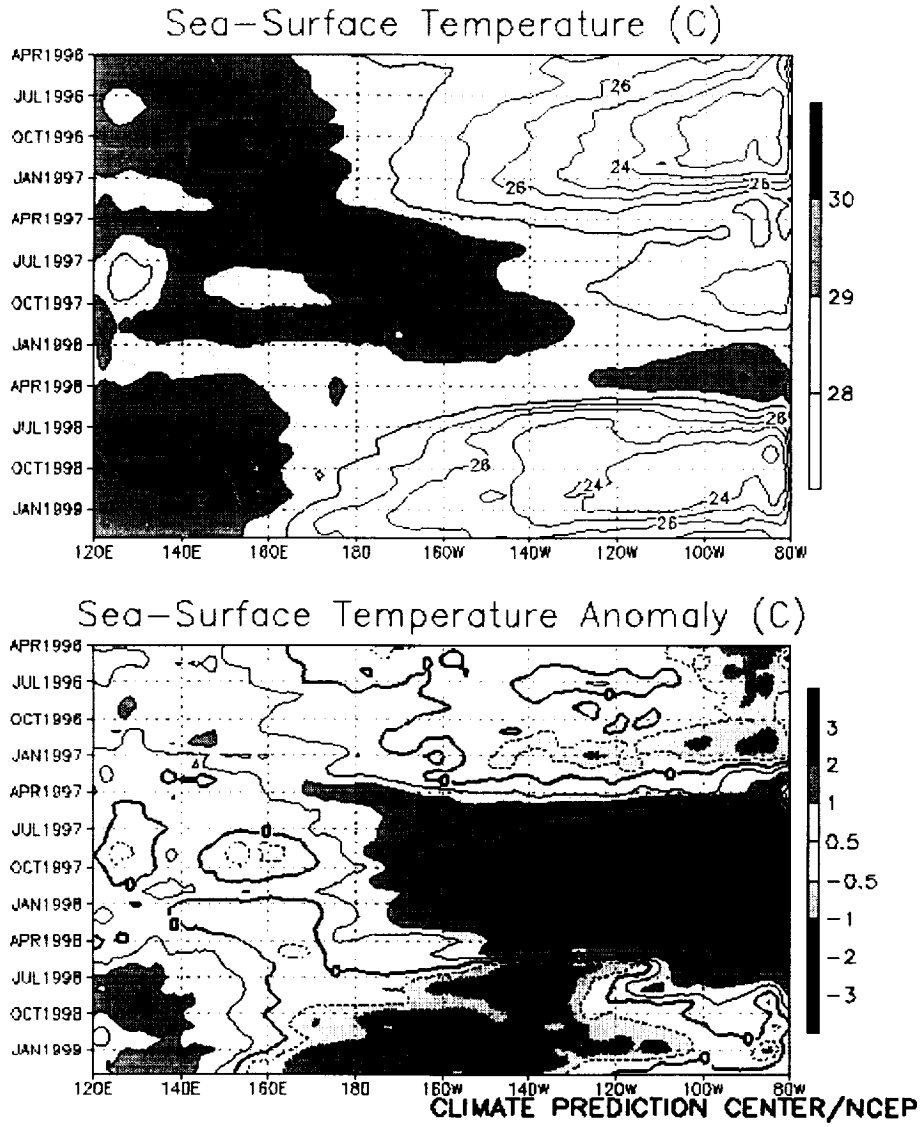

Figure 2: Time-longitude cross section of monthly mean (top) and anomalous (bottom) sea surface temperatures averaged over a band 5 degrees on either side of the equator. Dashed lines indicate negative anomalies. (Original analysis from CPC Climate Diagnostics Bulletin).

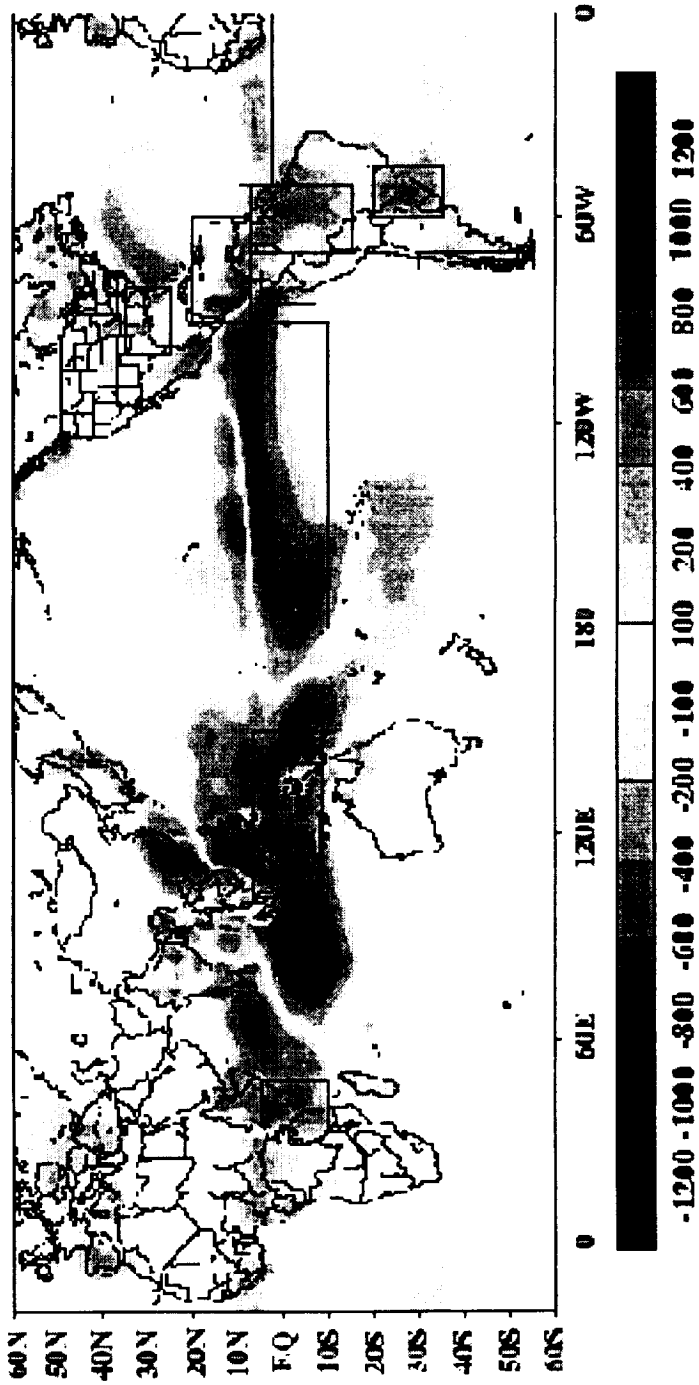

Figure 3: Accumulated precipitation anomalies (mm) for June through December 1997. (Adapted from Bell and Halpert, 1998). Based on a merged analysis of rain gauge and satellite-derived precipitation estimates (Xie and Arkin, 1998).

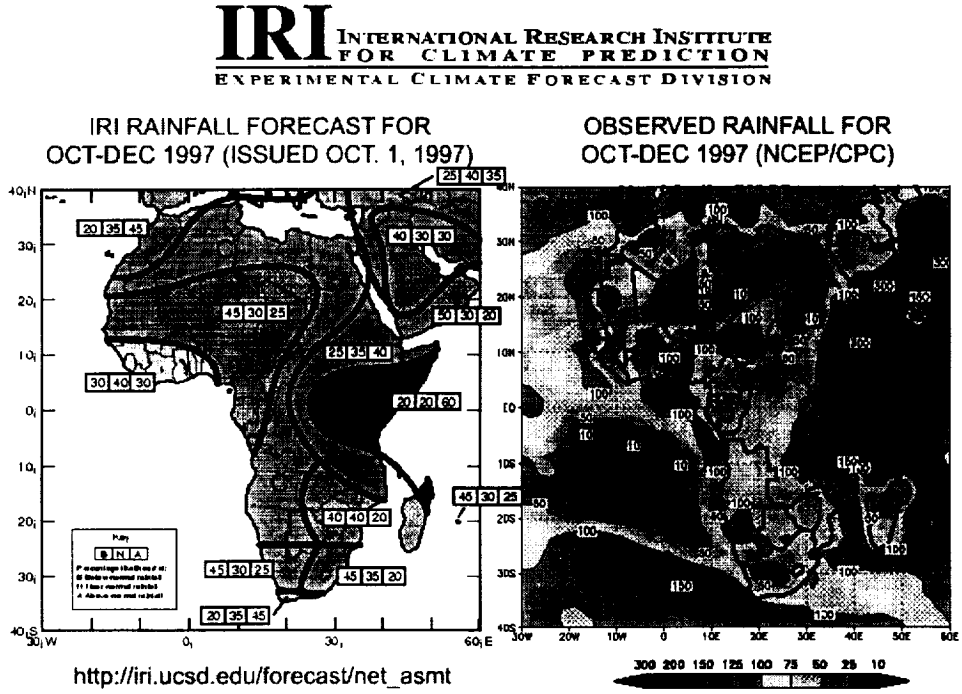

Figure 4: The IRI Net Assessment Forecast for Africa during the October through December 1997 season (left) and analysis of observed rainfall (right) for the same season.

During 1998 the equatorial Pacific sea surface temperatures fell rapidly as El Niño conditions gave way to La Niña. However, the far eastern Pacific sea surface temperatures remained above average through the year. During late February and early March of 1999 these lingering warmer than average coastal ocean temperatures gave some concern that El Niño was back despite continuing La Niña conditions in the central equatorial Pacific. Concern was heightened by reports of rainfall in Piura and other locations that generally received no rain during this of year. These concerns were alleviated by the end of March when the unusual rainfall ceased and the positive temperature anomalies declined along the South American Coast.

Applications

The application of climate data, information, and predictions spans a very broad range of disciplines at the interfaces between climate forecasting and climate-related economic and social issues. The application of climate information, including forecasts and assessments, can have an influence on policy and decision-making. Climate-applications areas include agronomy, hydrology, public health, emergency management, fisheries, economics, public policy, and anthropology, and cut across public and private sectors. The initial efforts of the IRI's Applications Research Division include the identification of several pilot applications activities. Among the goals of these pilot applications are the development, utilization and assessment of experimental end-to-end prediction systems i.e., from

modeling research and experimental climate forecasts to development and implementation of applications with feed back from the users. The pilot applications projects necessarily involve active participation of researchers, technical experts, and decision-makers from the relevant target regions.

In one pilot project the IRI Applications Research Division has been working with various components of the South American fisheries. This project, begun in 1997, was sparked by the initiative of the end-users for better and more relevant climate information. Early results have identified the potential for increased use of climate forecasts by the fisheries sector. Work is continuing on several aspects of the problem including studies of the quantitative link between the biology and the climate variability.

The negative consequences of El Niño on small pelagic fisheries in Peru have been well documented in previous episodes. However, the IRI pilot project has already revealed some subtle and complex variations in the relationship between catch, climate and subsequent re-actions by the fisheries. For example, during the relatively favorable 1996 La Niña season a fairly substantial catch of anchovy was documented, Figure 5. (Note: There is usually a "ban" on fishing during the February to March and July to September period, accounting for the low catch values during those months.) During April and May of 1997 the evolving El Niño forced the anchovy stocks to concentrate closer to shore in ever shrinking areas of relatively cold nutrient-rich water. This made fishing more efficient and resulted in an even larger overall catch in April and May of 1997 than in the previous year. The May 1997 catch was down from the April catch primarily because of a short lived (7 day) fishing ban that the government was not able to sustain due to pressure from the industry. Environmental conditions then led to vertical and horizontal migration of the small pelagics. Nonetheless, during the first year of the 1997/98 El Niño there was an overall increase in catch. Despite this increase in catch the quality of the catch, particularly in 1998, was much less, since it contained a mixture of fish species whose fat and oil content were well below average. More importantly it led to an over-fishing of commercial species which had survived the harsh conditions of the El Niño, reducing the capability of the stock to recover. This period of over-fishing was followed by a much reduced catch for the remainder of 1997 and 1998. The overall, long-term, effect of the 1997/98 El Niño remains to be seen but it has already put severe pressures on the fisheries industry of the area.

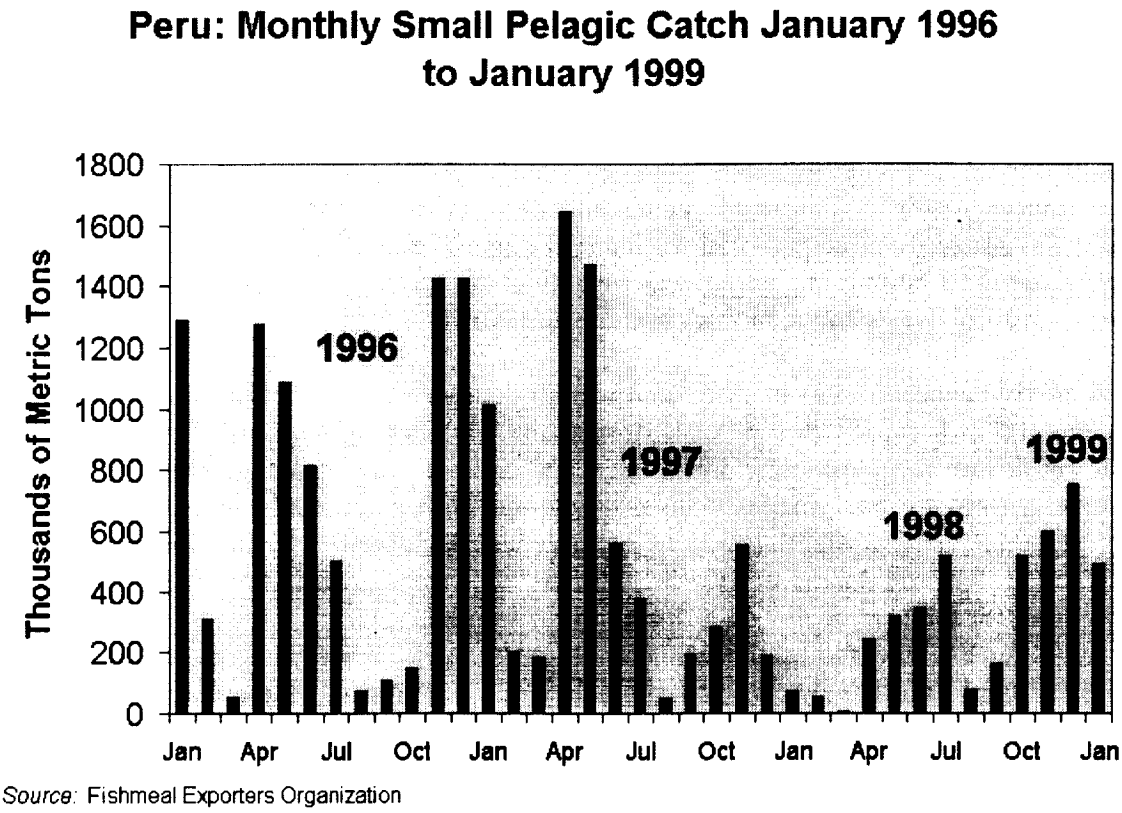

Source: Fishmeal Exporters Organization

Figure 5: Time series of small pelagics catch in the eastern Pacific. (Data source: Fishmeal Exporters Organization)

Summary

During the past two decades seasonal climate prediction has moved from the research laboratory into the realm of operations. Global climate forecasts are being issued regularly at the IRI and other institutions. The success of this enterprise has depended on the synergy between improved global observations of the climate system, improved theoretical understanding and the emergence of numerical models that predict interannual climate variability. A formidable challenge remains in developing and implementing the scientific and social tools for the efficient and equitable application of climate forecasts to a varied using community.

Acknowledgments

We wish to acknowledge our IRI colleagues Nick Graham, Simon Mason and Lisa Goddard for their invaluable input to the prediction discussion and to Kenny Broad for his vital contribution to the applications discussion. Finally, we thank Brendon Hoch, also at the IRI, for assistance with the graphics.

CO-OPERATION BETWEEN SPACE AGENCIES AND THE WORLD CLIMATE RESEARCH PROGRAMME

Hartmut Grassl

World Climate Research Programme (WCRP)
c/o World Meteorological Organization
(grassl_h@gateway.wmo.ch)

Global Climate Variability and change as well as many climate processes cannot be understood without earth observation from space by dedicated satellites. Therefore, a close and long-term co-operation between space agencies and WCRP is a prerequisite in order to achieve the central goal of WCRP:

To understand and predict – to the extent possible – climate variability and climate change including human influences.

Numerous success stories can already be named involving many space agencies (including the operational meteorological satellite services), large groups of scientists, in situ data providers and the co-ordination of the infrastructure of WCRP. These success stories are of a different kind: Firstly, WCRP as a stimulator of dedicated satellite sensors to understand climate processes, secondly, sub-projects mainly of GEWEX (Global Energy and Water Cycle Experiment of WCRP) delivering *global* time series of several climate parameters, thirdly, improvement of general circulation models for atmosphere and ocean through validation with satellite data sets, fourthly, trend analyses in the stratosphere and fifthly, attribution of climate change to causes. I will give an example for each type.

Stimulation of New Sensors for Climate Research

In June 1996, I was writing to the major space agencies on behalf of WCRP's Joint Scientific Committee in order to point to gaps that would remain even after the launch of the new generation of earth observation satellites (EOS-AM, EOS-PM, ENVISAT, ADEOS II). In addition, climate research would need:

1. Three-dimensional observations of cloud-water and cloud-ice and aerosols in the atmosphere in order to determine the feedback of clouds to changed temperature distribution, a prerequisite for the reduction of the uncertainty range of climate sensitivity to external forcing (mainly due to cloud feedback);

2. Upper soil wetness measurements needed for the starting fields of forecast models trying to exploit the soils' memory for longer-term predictions up to seasonal timescales. These starting fields would help in better water resource management;

3. Vertical profiles of wind velocity, especially for the tropics, which are needed for better weather forecasts but also for better water vapour convergence estimates, a prerequisite to improve parameterizations of precipitation formation in climate models.

To all three requests all major space agencies have responded favorably. Not only plans have emerged but already approved missions like the combination of PICASSO (a joint NASA/CNES aerosol lidar mission) and CLOUDSAT (a NASA cloud radar mission) but also the Earth Radiation Mission (ERM), studied by ESA, should be named here, since its combination of radar, lidar and radiometer on the same satellite would facilitate synergies between the different sensors. Hopefully, negotiations between ESA and NASDA will lead to the proper burden sharing for easier approval of the mission.

In this context, it is worth mentioning that WCRP will always advocate for the continuation of successful missions, for example, the radar altimeters onboard TOPEX/POSEIDON and ERS 1/2). The World Ocean Circulation Experiment (WOCE) has, since its inception in the early eighties, tried hard to get ocean topography measurements during its field phase. In the nineties, with the sensors mentioned and their high quality data, it got even more than anticipated. This was the reason that I also asked, in the letter mentioned, for a gravity mission in order to fully take advantage of the precise ocean topography measurements for ocean circulation studies, which would need more precise geoid information. Again the missions GOCE and GRACE on both sides of the Atlantic will help to get this information.

Global Climate Parameter Data Sets

The close relationship between GEWEX and many space agencies has led to many joint successes in this field, High up on such a list is the International Satellite Cloud Climatology Project (ISCCP) which processes data from all operational meteorological satellites having a free and open exchange of data policy. Started as an independent scientific activity in 1982, it soon became the first formal project of WCRP and is now one of several GEWEX data projects. However, it is the one with the most diverse satellite data assemblage and the largest infrastructure. Every six hours since July 1983, a global set of many cloud parameters is available on a 2.5x2.5 degree grid and several higher resolution subsets exist, for example, for the Baltic Sea catchment, one of the five continental scale experiments of GEWEX. Input comes from 4 geostationary and two polar orbiting satellites and the algorithms taken have been validated by field experiments, e.g., FIRE (First ISCCP Regional Experiment). As Figure 1 shows that there is an annual course of cumulus cloud amount and interannual variability in the amount of cloudiness. However a trend analysis over the time period since 1983 is still not possible, since it had to be assumed that the mean backscattering of solar radiation by the entire earth has not changed in this period. The reason being the inadequate in-flight calibration of many satellite sensors.

Other parameters, for which satellite information is essential and for which we have first global data sets from GEWEX sub-projects are: Precipitation (monthly means over 10 years for a 2.5x2.5 degree grid), water vapour (only in a five year pilot project for 1998-192) and surface radiation fluxes. Soon we will have aerosol optical depth, mainly over oceans, as another importance climate parameter set. This list is not exhaustive and other global data sets are assembled by other WCRP projects as well, always in close co-operation with space agencies to the benefit of both partners.

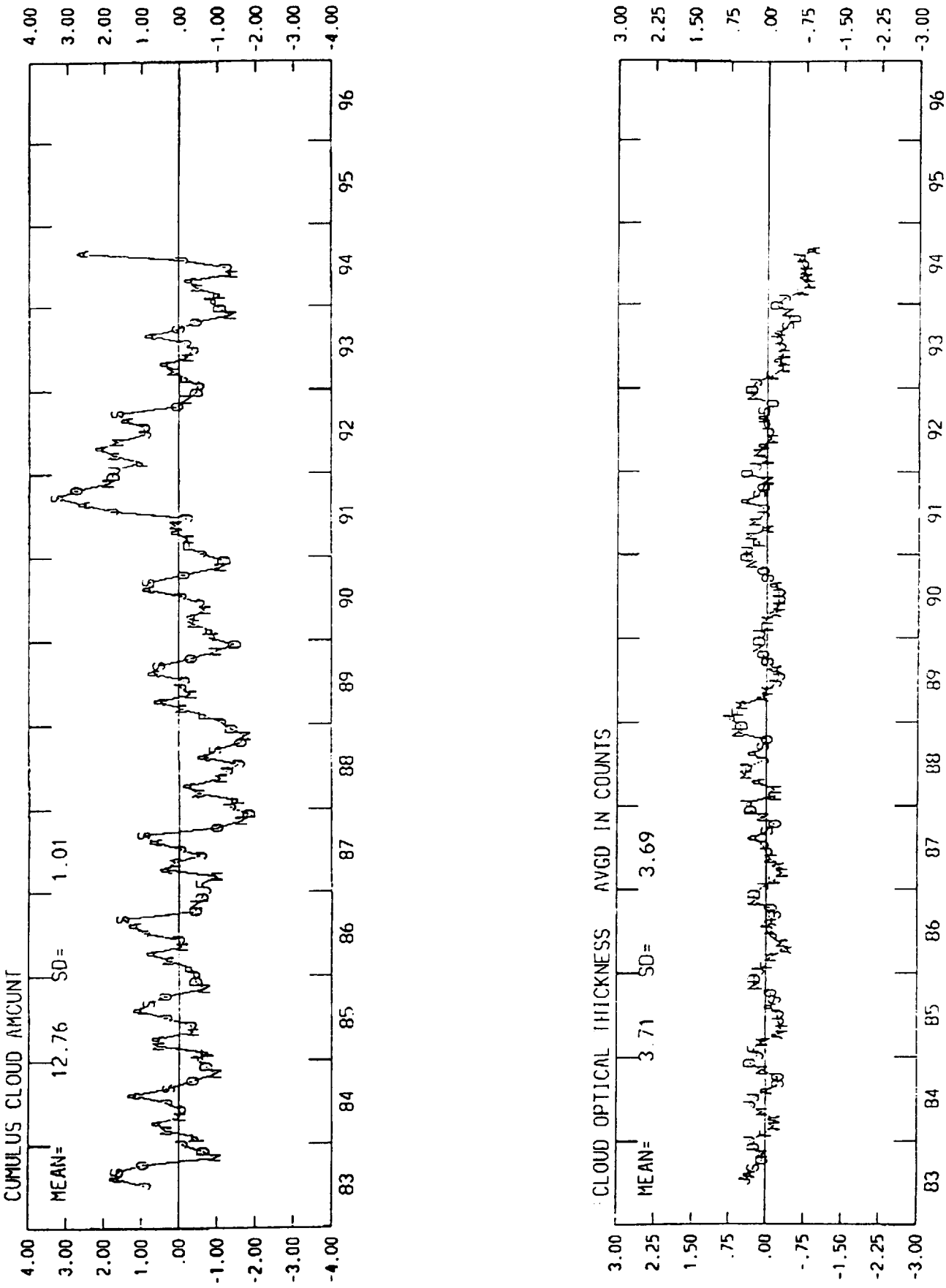

Figure 1: Global mean monthly cumulus cloud amount and mean monthly cloud optical thickness anomalies (over a 2.5x2.5 degree grid) as derived by ISCCP from satellite data for the period July 1983 to August 1994, data provided by Dr. W. Rossow, NASA-GISS, New York.

Validation of Circulation Models

Major progress in modeling of the general circulation in atmosphere and ocean is only achievable with new observations, both for global as well as regional models. There have been many steps forward in the validation of models by satellite data or by merged satellite and in situ data.

A major step was the availability of the data from the Earth Radiation Budget Experiment (ERBE), which has led to the validation of the models' radiation budget at the top of the atmosphere that is a basic capability to be reached by any climate model.

Agreement with the measured radiation budget at the top of the atmosphere is only a necessary, but not sufficient model test and the much more stringent test is a comparison with the observed surface radiation budget. However, the data set available from the GEWEX sub-project on Surface Radiation Budget (SRB) is still not precise enough for a really stringent model test that would, for example, mean the solution of the question on the amount of solar radiation absorption in a cloudy atmosphere. In addition, precipitation data sets over oceans are still not advanced enough to be used for a thorough model test. In other areas, for example the ocean circulation model tests, the satellite-derived ocean topography has led to major improvements of models since the accuracy was high enough to detect systematic model errors.

A recent, very promising example of model validation is the comparison between ISCCP cloudiness information and the vertical and horizontal cloud distribution in the circulation model of the European Centre for Medium Range Weather Forecasts (ECMWF), showing that the circulation model realistically develops clouds in the correct height with appropriate optical depth.

Trend Analysis in the Stratosphere

It is well known that the strong ozone depletion in the stratosphere has been followed by several satellite sensors after it had been detected from ground-based spectral UV-radiation measurements. The less obvious longer-term cooling trend in the lower stratosphere (larger than the warming trend at the surface, interrupted for a few yeas in 1963, 1982 and 1991 by strong volcanic eruptions) has only recently been established on global scale by a group in SPARC (Stratospheric Processes and their Role in Climate) through the merging of all available data sets from radiosondes and satellite sensors. The combination of ozone trend, greenhouse gas trends, and temperature trend in the lower stratosphere has allowed for the fist time, with the help of model calculations, to *attribute* the temperature trend to certain causes:

The significant cooling trend in the lower stratosphere in mid- and high latitudes during the recent decades is largely due to ozone depletion and to a lesser extent to the increase in long-lived greenhouse gas concentrations.

Integrated Observing Strategy (IGOS)

The office of the World Climate Research Programme in Geneva is a partner in IGOS. IGOS was started by the space agencies through the Committee on Earth Observing Satellites (CEOS), but is now a joint undertaking by space agencies, several UN agencies and the global change research programmes, IGBP and WCRP. In this respect, it should:

- formulate requirements to be met for certain climate parameters;
- help to identify the gaps in observing systems related to climate parameters through contributions to the IGOS pilot projects;
- contribute to measures to fill the gaps identified.

At present, WCRP is involved in three of the six IGOS pilot projects, namely GODAE (Global Ocean Data Assimilation Experiment), the Ozone Project and the Disaster Management Support Project. While WCRP was setting the stage through its projects TOGA and WOCE for GODAE and will systematically contribute through the Ocean Observing Panel for Climate (OOPC) to its implementation, it is contributing to the Ozone Project mainly by formulation of requirements to be met for a sufficient ozone monitoring and an attribution of causes to observed changes. Concerning the Disaster Management Support Project, WCRP has again set the stage through the breakthrough to seasonal climate anomaly predictions (in the project TOGA) which help to prevent disaster following droughts, still the most important natural disaster affecting mankind. Improvement of seasonal to interannual predictions of climate variability, a major goal of CLIVAR (Climate Variability and Predictability study of WCRP) is – maybe – the strongest contribution to disaster prevention.

In view of all these joint and successful activities, we should not only look forward to continued co-operation between space agencies and the World Climate Research Programme, but we must co-operate in even more fields.

REPORT DOCUMENTATION PAGE

Form Approved
OMB No. 0704-0188

1. AGENCY USE ONLY *(Leave blank)*

2. REPORT DATE
July 1999

3. REPORT TYPE AND DATES COVERED
Conference Publication

4. TITLE AND SUBTITLE
NASA Scientific Forum on Climate Variability and Global Change
UNISPACE III

5. FUNDING NUMBERS
Code 930.5

6. AUTHOR(S)
Robert A. Schiffer and Sushel Unninayar

7. PERFORMING ORGANIZATION NAME(S) AND ADDRESS (ES)
Earth and Space Data Computing Division
Goddard Space Flight Center
Greenbelt, Maryland 20771

8. PEFORMING ORGANIZATION REPORT NUMBER
99A01344

9. SPONSORING / MONITORING AGENCY NAME(S) AND ADDRESS (ES)
National Aeronautics and Space Administration
Washington, DC 20546-0001

10. SPONSORING / MONITORING AGENCY REPORT NUMBER
CP–1999–209240

11. SUPPLEMENTARY NOTES
Third United Nations Conference on the Exploration and Peaceful Uses of Outer Space, July 19–30, 1999.
Published by NASA as a contribution to United Nations Office of Outer Space Affairs for UNISPACE III.

12a. DISTRIBUTION / AVAILABILITY STATEMENT
Unclassified–Unlimited
Subject Category: 47
Report available from the NASA Center for AeroSpace Information,
7121 Standard Drive, Hanover, MD 21076-1320. (301) 621-0390.

12b. DISTRIBUTION CODE

13. ABSTRACT *(Maximum 200 words)*

The Forum on Climate Variability and Global Change is intended to provide a glimpse into some of the advances made in our understanding of key scientific and environmental issues resulting primarily from improved observations and modeling on a global basis. This publication contains the papers presented at the forum.

14. SUBJECT TERMS
Climate variability, Global change, El-Nino, Southern Oscillation, La Nina

15. NUMBER OF PAGES
84

16. PRICE CODE

17. SECURITY CLASSIFICATION OF REPORT	18. SECURITY CLASSIFICATION OF THIS PAGE	19. SECURITY CLASSIFICATION OF ABSTRACT	20. LIMITATION OF ABSTRACT
Unclassified	Unclassified	Unclassified	UL

Unispace-III/NASA Scientific Forum on Climate Variability and Global Change (20 July 99, Vienna, Austria

Program Plan

9.00-9.15 am: Introduction(Chair/Co-Chair/Rapporteur): Climate and Global Change Issues. [Dr. Robert Schiffer (NASA/HQ), Dr. Sushel Unninayar (NASA/GSFC)]

9.15-9.55 am: Ozone Depletion, UVB and Atmospheric Chemistry. [Dr. Richard Stolarski (NASA/GSFC)]

9.55-10.35 am: Global Climate System Change and Observations. [Dr. Kevin Trenberth (NCAR)]

10.35-11.15 am: Predicting Decade-to-Century Climate Change: Prospects for Improving Models. [Dr. Richard Somerville (SIO)]

11.15-11.55 am: Sun-Climate Connections. [Dr. Judith Lean (NRL)]

12.00-2.30 pm----------LUNCH----------

2.30-3.10 pm: Seasonal to Interannual Climate Variability and Predictability. [Dr. Jagadish Shukla (COLA)]

3.10-3.50 pm: El-Nino: Monitoring, Prediction, Applications, Impacts. [Dr. Chester Ropelewski & Dr. Antonio Moura (IRI)]

3.50-4.30 pm: Understanding/Predicting Changes in Terrestrial and Marine Ecosystems; Links with the Global Carbon Cycle. [Dr. Tony Janetos (WRI)]

4.30-4.45 pm: Cooperation Between Space Agencies and the World Climate Programme (WCRP). [Dr. Hartmut Grassl (WMO/WCRP)]

4.45-5.00 pm: Closing Remarks: Contemporary Global Change Science. [Dr. Ghassem Asrar, Associate Administrator for Earth Science, NASA/HQ]

5.00-5.30 pm: Panel Discussions: All Keynote Speakers and All Participants
[Development of recommendations to be submitted to UN/COPUOS/Agenda Item 7]

5.30-6.30 pm: RECEPTION (Astronauts and Cosmonauts Event)

++

For more details on UNISPACE-III see UN/OOSA Website: [http://www.un.or.at/OOSA/unisp-3/]

Acronyms:

COLA: Center for Ocean-Land--Atmosphere Studies
GSFC: Goddard Space Flight Center
IRI: International Research Institute for Climate Prediction
NASA: National Aeronautics and Space Administration
NCAR: National Center for Atmospheric Science
NRL: Naval Research Laboratory
SIO: Scripps Institute for Oceanography
WCRP: World Climate Research Programme
WMO: World Meteorological Organization

National Aeronautics and
Space Administration
July 1999